

Developmental and Pathological Effects of Psychosine on Oligodendrocytes of the Twitcher Mouse

BY

Hongling Zhu

B.S., University of Science &
Technology of China, 2004

THESIS

Submitted as partial fulfillment of the requirements
for the degree of Doctor of Philosophy in Anatomy and Cell Biology
in the Graduate College of the
University of Illinois at Chicago, 2012
Chicago, Illinois

Defense Committee:

Orly Lazarov, Chair
Ernesto R. Bongarzone, Advisor
Maria I. Givogri, Co-Advisor
Douglas Feinstein, Anesthesiology
Lawrence Wrabetz, University at Buffalo
Margot Mayer-Proschel, University of Rochester

ACKNOWLEDGEMENTS

First of all, I would like to devote my deepest appreciation to my dear parents: they have given me all what they have and made me who I am now. With their unconditional and endless love, support and understanding, no matter where I am and what I am doing, I can always feel their hearts accompanying throughout every step in my life. Without their assurance, I can never imagine if I could have done all those alone on the other side of the earth. It is their warm voices and thoughts that give me the strength and motivation to go through this long journey to accomplish my Ph.D. degree.

Here, I would like to thank Dr. Scott Brady, the head of the Anatomy and Cell Biology program for recruiting me from China and providing this precious opportunity to pursue my Ph.D. in such a welcoming academic environment of our department. I would also thank Dr. Conwell Anderson, the previous Director of Graduate Studies and Dr. Jonathan Art, the Associate Dean of Graduate College, both of who are great help for me to settle down at the Medical School of UIC.

During all those years, I have been very grateful for having Dr. Ernesto Bongarzone as my advisor and Dr. Maria Givogri as my co-advisor. Both of them are such caring people not only for my scientific development but also personality perfection, which really make me feel it is a second big family here for me. I'm especially thankful for Dr. Bongarzone for his generous advices and guidance for my progresses in this dissertation. I would thank him for his patience to me as an international student. Dr. Givogri is always so encouraging and helpful during my way of accomplishing the work.

Their persistence and enthusiasm for science and their success in academic pursuit all set them as wonderful examples for me to learn for now and forever.

I feel lucky having been part of Bongarzone Lab, which provides me with excellent scientific approaches, great collaborations, and terrific team work. I have to thank Mrs. Aurora Lopez-Rosas, who has been taking good care of the lab businesses as well as us from the very moment when we joined the lab. I would also thank all my lab mates Adam White, Benjamin Smith, Ludovico Cantuti, Amy Hebert, Agnieszka Kaminska, Marta Santos, Ariel Finkielsztejn, and Tuba Sural, as well as Dr. Givogri's group: Kasia Pituch, Ana Lis Moyano, and Felecia Marottoli. I also need to thank Shuo Huang, Angie Green and Alicia Rizzo for their help in some of my experiments. They are all smart students and great persons to get along with. I must thank my collaborators Guanlan Li and Xi Qiu from Dr. Richard van Breemen's lab and Francesca Ornaghi from Dr. Lawrence Wrabetz's lab, without them some of my work might not have been accomplished. I also thank Jenifer Hu, Paul Polak, and Sergey Kalinin for their great discussions along my work.

I like to give my great appreciation to my thesis committee: Dr. Orly Lazarov (chair), Dr. Ernesto Bongarzone, Dr. Maria Givogri, Dr. Douglas Feinstein, Dr. Lawrence Wrabetz from University at Buffalo and Dr. Margot Mayer-Proschel from University of Rochester, as well as Dr. Howard Lipton who had to withdraw from my committee due to time confliction for my dissertation. All of their help and guidance have been a great

stimulus for my progresses. It's great honor for me to have them involved in my work. I am grateful for their time and energy.

Last but not least, I would like to thank Bin Wang, who has been a respectable big sister for me, helping me finding the right way to go through the ups and downs of my life in Chicago. I also would like to thank Chang You and her family, Lingling Chen and her family, their friendships and encouragement have been the solid ground for me to move forward.

I must thank all the people at Department of Anatomy & Cell Biology, especially staff at our main office; without their help and coordination, I might not successfully finish my school here.

The work has been done by financial contributions from the board of Trustees of the University of Illinois, and NIH (R01 NS065808A) and Morton Cure Paralysis Foundation Awards to ERB.

TABLE OF CONTENTS

CHAPTER	PAGE
CHAPTER ONE	1
INTRODUCTION	1
1.1 KRABBE DISEASE	1
1.1.1. CLINICAL DEFINITION	1
1.1.2. MOLECULAR BASES OF GALC DEFICIENCY	2
1.1.3. PSYCHOSINE TOXICITY HYPOTHESIS	4
1.1.4. TWITCHER MOUSE MODEL	7
1.2 APOPTOTIC MACHINERY	8
1.2.1. GENERAL DEFINITION	8
1.2.2. APOPTOSIS IN KD	9
1.3 OLIGODENDROGENESIS	10
1.3.1. GENERAL INFORMATION	10
1.3.2. CONTROL CELL PROLIFERATION VS. CELL DEATH IN OLIGODENDROGENESIS	11
1.3.3. SHH PATHWAY IN OLIGODENDROGENESIS	12
CHAPTER 2	15
SPECIFIC AIMS	15
CHAPTER 3	17
EXPERIMENTAL DESIGN	17
CHAPTER 4	21
MATERIALS AND METHODS	21
4.1. ANIMALS.	21
4.2. CELL CULTURES.	22
4.3. IMMUNOCYTOCHEMISTRY.	23
4.4. CG4 CELLS PROLIFERATION ASSAY.	24
4.5. MTT ASSAY.	24
4.6. SHH STIMULATION ASSAY.	25
4.7. TISSUE COLLECTION AND β-GALACTOSIDASE HISTOCHEMISTRY.	25
4.8. IMMUNOHISTOCHEMISTRY.	26
4.9. BRD_U ASSAY.	27
4.10. TUNEL ASSAY	27
4.11. STEREOLOGY.	28
4.12. B-GALACTOSIDASE ENZYME ASSAY	28
4.13. REVERSE-TRANSCRIPTASE PCR ANALYSIS	29
4.14. EMBRYO COLLECTION.	29
4.15. WESTERN BLOTTING	30
4.16. MYELIN ISOLATION	30
4.17. PSYCHOSINE EXTRACTION AND QUANTIFICATION.	31
4.18. STATISTICAL ANALYSIS.	32

CHAPTER 5	33
EXPERIMENTAL RESULTS	33
RESULTS PERTINENT TO SPECIFIC AIM 1	33
RESULTS PERTINENT TO SPECIFIC AIM 2	66
CHAPTER 6	77
DISCUSSION	77
CHAPTER 7	92
CONCLUSIONS	92
CHAPTER 8	94
FUTURE DIRECTIONS	94
REFERENCES	96
VITA	111

LIST OF TABLES

<u>TABLE</u>	<u>PAGE</u>
I. QUANTITATIVE PROFILE OF CELL DEATH AND CORRELATION WITH PSYCHOSINE STORAGE IN THE TWI LUMBAR SPINAL CORD.....	49
II. QUANTITATIVE PROFILE OF OG AND OL CELL DEATH IN THE TWI LUMBAR SPINAL CORD	53
III. QUANTITATIVE PROFILE OF ASTROGLIAL CELL DEATH IN THE TWI LUMBAR SPINAL CORD	54
IV. QUANTITATIVE PROFILE OF MICROGLIAL/MACROPHAGE CELL DEATH IN THE TWI LUMBAR SPINAL CORD	55

LIST OF FIGURES

<u>FIGURE</u>	<u>PAGE</u>
1. Progressive accumulation of psychosine in the postnatal TWI spinal cord	34
2. MBP-LacZ expression in oligodendrocytes isolated from the MBP-LacZ/TWI mouse	35
3. The MBP-LacZ/TWI mouse as a model to study changes in numbers of oligodendrocytes bearing the TWI mutation	36
4. Distribution of LacZ+ OLs in the P7 TWI spinal cord	39
5. Distribution of LacZ+ OLs in the P15 TWI spinal cord.....	40
6. Distribution of LacZ+ OLs in the P30 TWI spinal cord.....	41
7. Distribution of Olig2+ OPCs in the P7 TWI spinal cord.....	42
8. Distribution of ASPA+ OLs in the P7 TWI spinal cord.....	43
9. Increase of PDGFR- α , Olig2 and PLP protein levels in cervical segments of P7 TWI cords.....	47
10. Proliferating OPCs increase in the spinal cord of sick TWI mice.....	48
11. Increased levels of cleaved caspase 9 in the TWI spinal cord.....	50
12. TUNEL and caspase 3 co-label dying cells in the spinal cord.....	51
13. Olig2+/TUNEL+ cells are found in the TWI spinal cords.....	56
14. LacZ+/TUNEL+ cells are found in the TWI spinal cords.....	57
15. GFAP+/TUNEL+ cells are found in the TWI spinal cords.....	58
16. IB4+/TUNEL+ cells are found in the TWI spinal cords.....	59
17. Effects of psychosine on proliferation and survival of CG4 cells.....	63
18. Psychosine promotes cell process retraction in oligodendrocytes.....	64
19. Enrichment of psychosine in myelin.....	65
20. Psychosine is present in the CNS of the mouse embryo.....	68

21. Subtle changes in oligodendrogenesis in embryonic TWI spinal cords.....	69
22. Distribution of Olig2+ OPCs in embryonic mutant spinal cords.....	70
23. More Olig2+ cells within the mantle region of the E12.5 TWI cord....	71
24. Sonic Hedgehog (SHH) ligand and receptor seem unaffected in TWI embryos.....	74
25. The floor plate SHH domain is enlarged in TWI cords at E10.5.....	75
26. Analysis of SHH effector Gli1 and downstream target genes PDGFR- α and Nkx2.2.....	76
27. Mechanistic model of demyelination in the TWI spinal cord.....	87

LIST OF ABBREVIATIONS

KD	Krabbe Disease
GALC	β -Galactosylceramidase
GalCer	Galactosylceramide
CGT	Ceramide Galactosyltransferase
b-gal	b-galactosidase
MBP	Myelin Basic Protein
PLP	Proteolipid Protein
ASPA	Aspartoacylase
SHH	Sonic Hedgehog
SMO	Smoothened
PTC	Patched
PDGF-AA	Platelet-derived Growth Factor-AA
PDGF α	Platelet-derived Growth Factor Receptor α
GFAP	Glial Fibrillary Acidic Protein
WT	Wild Type
TWI	Twitchee
PSY	Psychosine
OLs	Oligodendrocytes
OGs	Oligodendroglia
OPCs	Oligodendrocyte Progenitor Cells
CNS	Central Nervous System
PNS	Peripheral Nervous System

DWM	Dorsal White Matter
VWM	Ventral White Matter
pMN	Motor Neuron Progenitor Domain
TUNEL	Terminal deoxynucleotidyl transferase dUTP nick end labeling
TdT	Terminal deoxynucleotidyl transferase
HPLC	High-Performance Liquid Chromatography
PKC	Protein Kinase C

SUMMARY

Studies in this dissertation have provided new insights of the pathology of Krabbe disease (KD). KD is an autosomal recessive demyelination disorder caused by genetic defect on the lysosomal enzyme β -Galactosylceramidase (GALC). The accumulation of galactosylsphingosine (psychosine) was hypothesized to kill oligodendrocytes (OLs) and lead to myelin loss. The work presented here will provide new evidence that psychosine may contribute to the demyelination through blockage in the myelinogenesis instead of causing the direct killing of OLs.

In 1973, Kunhiko Suzuki proposed that high levels of psychosine kill myelin-forming cells. He also proposed that psychosine was just a non-functional byproduct during galactosylceramide (GalCer) synthesis since it presented at merely traceable amounts at normal conditions. The ‘psychosine hypothesis’ has stood out for almost 40 years; however, all clinical therapies designed on this basis have provided very limited protection against the disease. Progresses in this lipid metabolic disease have revealed new mechanisms to better understand KD. In 2009, our laboratory demonstrated that psychosine was enriched in membrane lipid rafts, where it may affect raft-associated signaling via modification of the raft architecture. While there are several well-known raft-associated signaling pathways are critical for oligodendrogenesis, we proposed that the genetic defect on psychosine metabolism would affect oligodendrogenesis during embryonic CNS development and disrupt the homeostasis of oligodendrocyte proliferation and survival. An extrapolation of this hypothesis also applies to our model

to explain demyelination. We have examined whether SHH pathway, which is fundamental for the correct formation of OLs, was altered during embryonic formation of OLs in the Twitcher (TWI) mouse, an animal model for KD. We have also measured for the changes OL cell death and abundance in postnatal life of the TWI mouse, attempting to correlate our findings with demyelination and psychosine accumulation.

Our studies show a transient increase in OL progenitors during embryonic life of the TWI mouse, without major changes in SHH abundance or that of its receptors, PTC and SMO. However, evidence that a higher SHH-dependent activity behind this cellular response was evident. Cell death analysis in combination with cell lineage analysis showed that unexpectedly, the period of demyelination in this mutant was characterized by lower levels of OL cell death but higher levels of microglia/macrophages cell death. These results suggest that OL cell death and myelin loss are two separate events in the disease. While studies in our Bongarzone group has shown that psychosine affect cellular transport such as endocytosis, exocytosis and axonal transport, it is very likely that myelinogenesis is compromised via disruption in myelin lipid trafficking of OLs and mature OLs may undergo a dying-back program similar to that seen in neurons. Altogether, the findings in this dissertation will contribute to the field of KD by providing quantitative parameters of oligodendrogenesis in the context of psychosine accumulation. These in turn may contribute to devise more effective therapeutic approaches for the treatment of this disease.

CHAPTER ONE

INTRODUCTION

1.1 Krabbe Disease

1.1.1. Clinical Definition

Krabbe disease (KD), also known as Globoid cell leukodystrophy is an autosomal-recessive inherited demyelinating disease that affects both peripheral and central nervous systems (Lloyd 1996). The disease is named after Danish neurologist Knud H. Krabbe as he described the first five infantile cases in 1916 (Krabbe 1916). Histologically, KD has been described by its diffuse myelin loss, severe gliosis and the presence of multinucleated globoid cells (Andrews et al. 1971; D'Agostino et al. 1963; Yunis and Lee 1969). Mutations in β -galactosylceramidase (GALC) lead to the deficiency of this enzymatic activity in the disease (Suzuki and Suzuki 1970). GALC is a lysosomal enzyme that hydrolyzes galactosyl-sphingolipids (Suzuki and Suzuki 1971). Consequently, psychosine (galactosylsphingosine), one of GALC substrates, progressively accumulates in the affected brain (Igisu and Suzuki 1984a; Igisu and Suzuki 1984b).

KD is an orphan disease with an incidence of ~1:100,000 (Aicardi 1993; Duffner et al. 2009). Based on the onset of disease symptoms, KD is classified in 4 clinical subtypes: early infantile (3-6 months) accounting for ~85-90% of affected patients, late infantile (6 months-3 years), juvenile (3-10 years) and adult (>10 years) (Wenger DA 2001). After first few months of apparently normal life, affected infants suffer of hyperirritability, hyperesthesia, stiffness of the limbs, and along with episodic attacks of

fever. Soon the symptoms develop into muscular hypertonia, optic atrophy, seizures and severe motor retardation (Dunn et al. 1969; Hagberg et al. 1969; Korn-Lubetzki et al. 2003). Death occurs within the first 3 years of age. Postmortem studies revealed infiltration of macrophages, astrogliosis and microgliosis, myelin loss, axonal and neuronal degeneration. Juvenile and adult variants show a milder disease progression: usually start with disturbance in walking due to poor coordination and balance; then progressively develop asymmetric limb weakness, tremors; visual failure and slow intellectual decline (Crome et al. 1973; Duffner et al. 2012; Lyon et al. 1991). Abnormalities in nerve conduction velocities are consistent with the demyelinating neuropathy, which occurs early and affect both sensory and motor nerve uniformly in KD (Marks et al. 1997; Siddiqi et al. 2006).

So far, nearly 100 mutations including single nucleotide polymorphisms in the GALC gene have been identified (Tappino et al. 2010). Certain mutations, such as the most common 30 kd large deletion, have been found to account for the classic infantile form (Kleijer et al. 1997; Wenger et al. 1997). However, there is no clear connection between most genetic mutations and specific clinical symptoms.

1.1.2. Molecular Bases of GALC Deficiency

KD is caused by loss-of-function mutations in the GALC gene (Chen et al. 1993; Suzuki 1985). In humans, GALC gene is located on chromosome 14q31 (Cannizzaro et al. 1994; Chen et al. 1993). This 60 kb gene comprises 17 exons, encoding a 3.8 kb mRNA (Luzi et al. 1995; Sakai et al. 1994). Two in-frame translational GALC isoforms are produced, giving rise to ~80 kd precursor proteins with a 42-amino acid (a.a.) or 26-

a.a. leader sequence respectively. Both precursors are proteolytically processed into ~50 kd and ~30 kd subunits, yielding the final 669-amino acid mature enzyme (Nagano et al. 1998). After synthesis and glycosylation in ER-Golgi complex, GALC is targeted into the lysosome mainly through the mannose-6-phosphate (M6P) sorting pathway. At the lysosome, GALC exerts its catabolic function of degrading galactosylsphingolipid, such as galactosylceramide (GalCer), galactosylsphingosine (psychosine), monogalactosylceramide and lactosylceramide.

Disease-associated mutations spread over the entire GALC gene without any preferential clustering (Tappino et al. 2010), and affect gene splicing, mRNA stability, protein folding and targeting of GALC (De Gasperi et al. 1996; Fu et al. 1999; Lee et al. 2010; Rafi et al. 1996). Interestingly, analysis on the relative frequency of GALC mutations reveals different mutation profiles for specific populations. For example, the large 30 kb deletion (c.1161+6532_polyA+9kdel) is the most common mutation in the Italian population associated with classic infantile KD (Wenger et al. 1997). Instead in Japan, the majority of infantile patients carry either c.683_694del12insCTC or c.2002A>C mutations (Xu et al. 2006). In the Druze and Moslem Arab populations of Israel, two separate inbred communities with extremely high incidence of KD (1:100 to 150 live birth), c.1796>G and c.1630G>A are most frequent (Rafi et al. 1996). The mutations described here use the HGVS (Human Genome Variance Society) nomenclature (Tappino et al. 2010). Previously, the 30 kd subunit of GALC enzyme was thought to be responsible for its catalytic activity (Rafi et al. 1995). However, the crystal structure of mouse GALC (83% identity with human GALC) shows all three protein domains (beta-sandwich, a.a. 25-41 and a.a. 338-452; TIM barrel, a.a. 42-337; and lectin

domain, a.a. 472-668) are contributing to the substrate binding (Deane et al. 2011). GALC needs the activity of saposins, which appear to associate to the surface of the enzyme close to the substrate-binding pocket (Harzer et al. 1997; Morimoto et al. 1989; Zschoche et al. 1994). Residue R380, which binds directly to galactose, is contributed by the loop region of a β -sandwich domain and mutations at this site lead to severe infantile KD (Selleri et al. 2000; Wenger et al. 1997). Seventy percent of missense mutations affected residues are buried within the structure of GALC, which are associated with misfolding or instability of the protein but without blocking the residential enzymatic activity, making the design of pharmacological chaperones a feasible therapeutic application to help stabilize the enzyme structure and correct the folding and trafficking defect associated with certain KD cases (Harzer et al. 2002; Kornfeld 1986).

1.1.3. Psychosine Toxicity Hypothesis

Since the identification of genetic cause to be GALC in 1970 (Suzuki and Suzuki 1970; Suzuki et al. 1970), KD is defined as one of the classic genetic leukodystrophies. GALC is a hydrolytic enzyme with optimal catalytic preference in the lysosome. In vivo, the major natural substrate of GALC is galactosylceramide (GalCer), which is the most abundant sphingolipid in myelin membrane, accounting for 2% dry weight in gray matter and 12% in white matter (Merrill 2008). However, unlike other lysosomal enzyme-deficiencies, GalCer does not accumulate significantly in KD (Eto and Suzuki 1970). Instead, psychosine, which presents only at trace levels in normal tissue, increases to very high levels (Taketomi and Nishimura 1964). To explain the paradoxical phenomenon, Miyatake and Suzuki initially proposed a hypothesis for the pathogenesis of KD, known

as the psychosine hypothesis (Miyatake and Suzuki 1972). In this hypothesis, they considered that: psychosine is an accident of nature without any definitive functions in vivo, coincidentally synthesized in myelinating cells during the active myelination period due to the large amount of sphingosine and GalCer synthesis. In normal circumstances, psychosine is rapidly degraded by GALC; however, in KD, psychosine cannot be degraded and consequently its abnormal accumulation kills myelin-forming cells, leading to demyelination and the consequent reduced accumulation of GalCer in KD. Psychosine accumulation has been confirmed in affected humans, dogs, monkeys and mice (Baskin et al. 1998; Igisu and Suzuki 1984b; Svennerholm et al. 1980).

A large number of in-vitro studies favor a psychosine-induced cell death to explain demyelination in KD (Giri et al. 2006; Haq et al. 2003; Taniike et al. 1999). Of relevance, most in vitro experiments, where exogenous administration of psychosine was applied, used concentrations above 10 μ M, which are extremely high enough and cause almost immediate cell death in most cell cultures (Formichi et al. 2007; Smith et al. 2011). Even though some studies showed that oligodendrocytes (OLs) might be more sensitive to psychosine treatment than astrocytes and neurons (Sugama et al. 1990), it is still inconclusive if those in vitro psychosine conditions are comparable to psychosine levels observed in vivo.

While psychosine hypothesis appears to suffice to explain demyelination in KD, there are still some paradoxes. According to the hypothesis, psychosine is mainly synthesized in myelin-forming cells during myelination. While both GalCer and psychosine are synthesized by UDP-galactose ceramide galactosyltransferase (CGT) and

degraded by GALC (Suzuki 2003), only psychosine but not GalCer is continuously accumulated during the disease.

The lack of GalCer accumulation in CNS can be easily explained by the death of OLs during demyelination. However, an evident caveat of this hypothesis is that if psychosine is synthesized as a byproduct of GalCer by myelinating glia and at the same time it kills these cells, its accumulation should at least arrest and reach a platform at late stages, because the cell sources for its synthesis would be eventually depleted. However, this is not the case. This begs the question: where is psychosine coming from? Either there are alternative synthetic cell sources and/or there is not so much cell death of myelinating glia. Recent studies in our lab have found that psychosine is also produced in some mutant neurons (Castelvetri et al. 2011). This finding is suggesting that psychosine can be synthesized in nervous system independent from myelination. A systematic analysis of OL cell death in the context of psychosine accumulation has not been done so far. Thus, we have no available quantitative data to answer the question about levels of cell death.

While psychosine has been posted as an error of nature, studies by White and Bongarzone have demonstrated that psychosine indeed may be a plasma membrane relevant molecule. Psychosine was found enriched in raft-like membrane microdomains, where it affects raft-associated signaling pathways by modifying the raft architecture (White et al. 2009). Maybe, psychosine has a function after all and that is to work as a modulator of raft biology. Several well-known raft-associated signaling pathways are critical for oligodendrogenesis (such as those mediated by SHH and PDGF-AA), and myelin is also known to have lipid rafts. How OLs respond to different levels of

psychosine has not really been studied. Furthermore, whether demyelination is caused by the selective accumulation of psychosine in myelin is also unclear. This dissertation will attempt to find answers to some of these questions.

1.1.4. Twitcher Mouse Model

The twitcher mouse (TWI) is a natural occurred mutant discovered at the Jackson Memorial Laboratory in 1976. TWI mice were identified as an enzymatically authentic model of KD due to the defective GALC activity (Kobayashi et al. 1980). TWI carries a premature stop codon mutation (W339X) in the GALC gene leading to mRNA decay (Lee et al. 2006; Sakai et al. 1996). The mutant mice are born asymptomatic for the first 3 weeks, but develop demyelination symptoms around postnatal day 20-22 (P20-22), and die between P40-P45 (Duchen et al. 1980). Its clinical and histopathological hallmarks share great similarity with human KD: rapid degeneration of myelin, infiltration and formation of multinucleated macrophage (globoid cells), and extensive astrogliosis and microgliosis. As disease progresses, demyelination is accompanied with progressive psychosine accumulation (Igisu and Suzuki 1984b; Shinoda et al. 1987; Suzuki and Taniike 1995). However, unlike human KD affecting primarily CNS, demyelination in TWI is more pronounced in PNS (Jacobs et al. 1982; Nagara et al. 1982).

Characterization of defects in OLs in TWI mice focused only in the very late stages of the disease (Takahashi et al. 1983; Takahashi and Suzuki 1984; Taniike et al. 1999; Taniike and Suzuki 1994). There are not studies that attempted to correlate OLs reduction with the accumulation of psychosine in a temporal manner. Furthermore, how is the proliferation of OL progenitors (OPCs), their migration, differentiation, and

maturation into myelinating OLs affected in the disease? Those very relevant questions have remained unanswered. To start addressing these questions, we took advantage of a transgenic line generated by Dr Wrabetz (Wrabetz et al. 1998). The MBP-LacZ transgene uses a minimal 750 bp promoter region of the human myelin basic protein (MBP) gene to drive the expression of the reporter gene LacZ specifically in myelinating OLs in the developmental CNS (Wrabetz et al. 1998). Dr. Wrabetz, Bongarzone and Givogri crossed this transgenic line with the TWI line and generated a new transgenic MBP-LacZ/TWI mouse, which has been used for the development of this thesis. This new line has proven to be a very sensitive model to study the changes in oligodendrogenesis. It will be discussed in details in following chapters.

1.2 Apoptotic Machinery

1.2.1. General Definition

“Programmed Cell Death” was first proposed by Lockshin and Williams in 1964 to describe the ability of cells to commit suicide via tightly regulated intrinsic machinery (Lockshin and Williams 1964). Unique morphological changes are described for apoptotic cells, including cell size shrinkage, condensation of cytoplasm and nucleus, cell membrane blebbing, and cell body breakdown (Kanduc et al. 2002; Majno and Joris 1995).

Apoptosis plays a very important role in both physiological and pathological processes to eliminate unwanted cells or dangerous cells (Hurle et al. 1996; Munoz-Pinedo 2012; Saunders 1966). Caspases-mediated apoptosis is critical for the nervous

system maturation in both health and disease (Hyman and Yuan 2012). Genetic knockout of caspases 3/9 leads to severe brain malformation (Leonard et al. 2002; Oppenheim et al. 2001; Zaidi et al. 2001). However, hyperactive apoptosis would lead to degenerative diseases, such as loss of neuronal cells in Alzheimer's disease (Muller et al. 2008; Shimohama 2000).

1.2.2. Apoptosis in KD

Several studies showed that apoptosis plays an important role in the pathogenesis of psychosine-induced cytotoxicity. For example, apoptotic nuclei were detected in postmortem KD brains (Jatana et al. 2002). Apoptotic profiles were also detected in some OLs in TWI mice (Taniike et al. 1999). In vitro experiments on OL cell lines or primary cultures showed that psychosine is sufficient to elicit caspases activation in OLs (Zaka and Wenger 2004). Further studies demonstrated that psychosine would induce AP1 via the c-jun/c-jun N-terminal kinase pathway and down regulate NF-kB mediated anti-apoptotic signals (Haq et al. 2003), activate secretory phospholipase A2 (Giri et al. 2006), down regulate peroxisome proliferator-activated receptor-alpha (PPAR-alpha) (Haq et al. 2006), all of which would contribute to cell death in OLs. Caspase-mediated apoptosis is also involved in the preferential killing of periphery immune cells of KD patients (Formichi et al. 2007). Recent studies in the Bongarzone lab showed the involvement of active caspase 3 in axonal damage in TWI mouse, consistent with a model of dying back neuropathy (Castelvetri et al. 2011; Smith et al. 2011).

While the death of OLs has been proposed as the major cause for demyelination in KD (Miyatake and Suzuki 1972), a quantitative analysis of this process in the context

of demyelination and psychosine accumulation is not available. In this dissertation, we have addressed this aspect and characterized apoptosis in OLs, astrocytes and microglia in the postnatal spinal cord of the TWI mouse.

1.3 Oligodendrogenesis

1.3.1. General Information

In vertebrates, oligodendrogenesis is programmed and mostly executed during embryonic development. After formation of the notochord, dorso-ventral patterning signals (e.g. BMP, SHH, and Wnt) are secreted by organizer structures and work synchronously to direct a sequential spatiotemporal neurogliogenesis (Levine and Brivanlou 2007; Liem et al. 2000). Neurons are generated first from neuroepithelial cells in the neuroectoderm, a process that is completed by the first half of gestation. A switch to astrocyte and OL genesis is then established. In the mouse spinal cord, oligodendrocyte progenitor cells (OPCs) are initially generated from specialized ventral ventricular regions known as pMN (motor neuron-OLs progenitor zone) at around E9 (Bongarzone 2002; Ligon et al. 2006). Those OPCs migrate laterally and dorsally into the mantle area of the spinal cord, contributing vastly to the population of OLs in the mature spinal cord (Ligon et al. 2006). Later around E15, a second dorsal wave of OPC is established from radial glia cells to supplement the dorsal OLs pool (Cai et al. 2005; Vallstedt et al. 2005). The maturation of OPCs to form myelin sheath mainly takes place during early postnatal days, and last till early adulthood to complete (Gao et al. 2009; Jakovcevski et al. 2009).

Oligodendrogenesis involves morphological, signaling, physiological and survival changes of OPCs as they undergo a well-defined default differentiation program (Jackman et al. 2009). The undifferentiated OPCs start with a simple bipolar morphology. In the absence or with very low amounts of mitogens such as PDGF-AA, OPCs will exit the cell cycle, grow more cellular processes to form the stereotypical spider shape (Hall et al. 1996). Eventually, these cells contact nude axons and will start the process of myelination (Baumann and Pham-Dinh 2001). In parallel, synthesis of specific myelin components including myelin lipids, proteins, receptors and transcription factors is developmentally coordinated (Jackman et al. 2009; Li et al. 2009; Tekki-Kessaris et al. 2001).

1.3.2. Control Cell Proliferation vs. Cell Death in Oligodendrogenesis

A tight regulation of cell division and cell death ensures enough numbers of neural cells are generated to meet the need of growing nervous system. This balance between proliferation and apoptosis has been documented for the oligodendroglia lineage in the developing rodent optical nerve (Raff et al. 1998). During early postnatal days, proliferation and differentiation of OPCs are two parallel events happening in CNS (Miller et al. 1985). Since myelinating OLs are post-mitotic cells, the final number of surviving OLs depends on the number of dividing OPCs and the number of apoptotic OPCs and OLs as well as the number of axons to be myelinated. Proliferation of OPCs is mainly regulated by mitogenic signals, especially PDGF-AA (Gard and Pfeiffer 1990). However, OPCs themselves have an intrinsic timer that controls when they turn into quiescent adult OPCs (Kondo 2001; Raff et al. 2001). Studies by Barres et al found that

~50% OLs generated in developing optic nerve would undergo apoptosis, which suggests that OPCs are generated in great excess (Barres et al. 1992). While multiple cytokines such as PDGF, insulin-like growth factor-1, ciliary neurotrophic factor, and neurotrophin-3 are required for long-term survival of OLs in vitro (Vos et al. 1996), in vivo the number of OLs greatly depends on the interaction with axons (Barres et al. 1993; Greenwood and Butt 2003). Furthermore, even after genetic manipulation to over-express PDGF and to induce excessive OPCs, the final number of myelinating OLs remains unaltered because there is compensatory apoptotic cell death of immature OLs (Calver et al. 1998b). Those studies underline the importance for a proper balance between cell proliferation and cell death during development of the nervous system.

1.3.3. SHH Pathway in Oligodendrogenesis

Multiple signaling pathways control the induction, proliferation and survival of OPCs, including a wide range of growth factors (e.g., PDGF-AA, FGF2, neuregulin-1), chemokines (e.g., CXCL1), as well as inhibitory signals such as BMP2/4 (Aberg 2010; Miller 2002; Qi et al. 2002). Among those, two signaling pathways are most critical for the oligodendrocyte lineage: that mediated by sonic hedgehog (SHH) and platelet-derived growth factor-AA (PDGF-AA). Whereas SHH is necessary and sufficient for the commitment of undifferentiated precursors into OPCs (Hu et al. 2009; Nery et al. 2001; Orentas et al. 1999), PDGF-AA is essential for OPC proliferation, migration and cell survival (Baron et al. 2002; Calver et al. 1998a; Noble et al. 1988).

During the embryonic neural development, SHH is synthesized and secreted by notochord and the floor plate of neural tube, creating a gradient of concentration along

the dorso-ventral neuroaxis (Briscoe and Novitch 2008). SHH gene encodes a 45 kd preprotein, which is processed to produce a 20 kd N-terminal signaling domain (SHH-N) (Lee et al. 1994). SHH-N is post-transcriptionally modified by the addition of a cholesterol molecule to its C-terminus and a palmitate to its N-terminal cysteine (Farzan et al. 2008). Palmitoylation appears to regulate the tethering of protein to membrane, which is required for efficient signaling (30- folds increase compared with non-palmitated form). SHH binds to its heterodimer receptor patched/smoothened (PTC/SMO) in the plasma membrane (Singh S 2006). Interaction of SHH-N with PTC leads to translocation of SMO, a G-protein coupled receptor. Activated SMO triggers downstream signal cascades for the induction of different cell identities, mediated by the Gli family of Zinc-finger containing transcription factor (Huangfu and Anderson 2006). Three Gli proteins have been identified in vertebrates, with transcriptional activator and/or repressor properties. Two classes of transcript factors are regulated through them: SHH-repressed (e.g., Pax6/7, Dbx2, Irx3), and SHH-induced, including Nkx2.2/6.1, Olig1/2. Expression of Nkx2.2/6.1 and Olig1/2 plays a key role in OPC commitment and precedes the expression of other OPC markers such as PDGF receptor -alpha (PDGFR- α) and myelin genes (Guillemot 2007). SHH is found to be associated with caveolin-1 in Golgi apparatus and transported to lipid raft microdomain (Mao et al. 2009). Its receptor PTC directly interacts with caveolin-1 in raft. Depletion of membrane cholesterol disrupts the distribution of PTC/SMO complex in the membrane altering their ligand-receptor binding properties (Karpen et al. 2001).

As an inherited infantile demyelination disease, developmental oligodendrogenesis apparently is the major target for the pathogenesis in KD. Given the

fact that psychosine is a lipid raft-enriched sphingolipid and its accumulation in rafts modifies raft architecture and associated signaling (White et al. 2009), it is of importance to test whether this modification is also contributing to the pathology of oligodendrogenesis in the disease.

CHAPTER 2

SPECIFIC AIMS

RATIONALE: Krabbe disease (KD) is characterized by the progressive accumulation of psychosine and demyelination, due to the deficiency in GALC. Most studies focused on the severe demyelination stages in the TWI mouse, a naturally occurred loss-of-function model for KD. While the psychosine toxicity hypothesis has been widely accepted, the underlying mechanisms for myelin loss in vivo have remained elusive. Emerging new studies are revealing other pathologic roles of psychosine as a lipid raft-associated sphingolipid, indicating possible raft-associated signaling changes. My dissertation has focused on determining the temporal and anatomic pattern of myelinating OLs in the TWI spinal cord and its correlation cell death and with psychosine accumulation. My work has also attempted to challenge the idea that psychosine alters oligodendrogenesis in the embryo by altering raft-associated SHH pathways.

HYPOTHESIS:

In this study we hypothesized that psychosine is a lipid raft-associated sphingolipid with dose-dependent effects on oligodendrogenesis in developing CNS: at low concentrations, psychosine provides a permissive platform for raft-associated SHH signaling facilitating the formation of OPCs. At high concentrations, psychosine disturbs membrane homeostasis of OLs, triggers demyelination first and eventually, kills OLs.

The hypothesis was tested by the following aims:

***Aim 1-** To measure for psychosine effects on proliferation, maturation and death of postnatal TWI OLs.*

***Aim 2-** To measure for changes in oligodendrogenesis in the embryonic TWI mouse.*

CHAPTER 3

EXPERIMENTAL DESIGN

To challenge our hypothesis and test our specific aims, the following experiments were proposed:

To characterize the spatiotemporal accumulation pattern of psychosine in the TWI spinal cords. This study allows us to co-relate the psychosine accumulation with the disease progression course and the anatomic pathologic phenotypes. Psychosine is extracted using a standardized chloroform/methanol-based protocol and quantified by liquid chromatography tandem mass spectrometry (LC-MS/MS). The TWI spinal cords are dissected into dorsal and ventral halves at three anatomic levels: cervical, thoracic, lumbar. Increase of psychosine during the lifespan of the TWI mouse is compared to aged match wild type (WT) controls at postnatal days 7, 15, 30 and 40.

To characterize the reporter gene expression pattern in the new transgenic MBP-LacZ/TWI mouse model. The transgenic MBP-LacZ/TWI provides an approach to follow the pathological changes on OLs during disease. The activation of LacZ reporter gene is examined in MBP-LacZ/TWI primary glia cultures to identify its expression period. β -galactosidase activity assay and quantitative PCR of MBP transcripts are performed with MBP-LacZ/TWI tissues to further verify whether the transgenic system properly follows the demyelination changes from P7 to P40.

To characterize the spatiotemporal distribution of myelinating OLs in MBP-LacZ/TWI spinal cords. This experiment systematically analyzes how the myelin-forming OLs are affected during the disease course. OLs are revealed by X-gal histochemical reaction for

β -galactosidase expressed in the transgenic mice. OL population in white matter of mutant spinal cords is estimated under stereological microscopy and compared with age-matched WT at P7, P15 and P30. LacZ⁺ OLs are examined in both dorsal and ventral white matters (DWM and VWM) of all three levels of spinal cord as described in Goal 1.

To examine the pathogenic effects on the generation or the maturation of OLs in TWI spinal cord. Defect in myelination can be caused either by compromised generation of OLs or by blockage in OL maturation. To address those two aspects, oligodendroglia cells labeled with Olig2 (a transcriptional factor expressed in all OLs) and mature OLs labeled with ASPA (an enzyme expressed in mature OLs) are quantified using stereological microscopy in P7 TWI spinal cords. Protein levels of PDGFR- α (marker for OPC), Olig2 and PLP (myelin protein) are analyzed by western blotting.

To examine the proliferative capability of TWI OPCs during demyelination. Defect in the OPCs may act as a compound pathological factor for demyelination. To examine this possibility in KD, BrdU incorporation assay is performed in P29 TWI and WT. BrdU labeled spinal cords are dissected out at P30. Proliferative OPCs are identified by BrdU+Olig2⁺ double labeling and quantified by stereology as described above.

To determine the role of apoptosis in the demyelination pathology of KD. This study is to systematically assess the appearance and distribution of apoptotic cells in TWI and to determine the relation between OLs cell death and demyelination. Apoptotic cells are identified by TUNEL assay within the 10 μ m spinal cord cross sections of TWI and WT from P7 to P30. Cell identities are determined with cell lineage markers: Olig2/b-gal/PLP (oligodendrocytes), NeuN (neurons), GFAP (astrocytes), and Isolectin-IB4 (microglia/macrophages). The apoptotic cell populations are analyzed under fluorescence

microscopy and quantified with ImageJ software. Active caspase 9 level is examined by western blotting as for overall apoptosis in TWI spinal cord.

To determine effects of psychosine on proliferation and survival of oligodendroglial cells in vivo. In vitro psychosine treatment is performed on CG4 (a rodent OPC cell line) and primary OL cultures. Proliferation of CG4 affected by psychosine is estimated by live cell counting with trypan blue staining. Mature OLs obtained by shaking-off from primary glia cultures are treated with psychosine and their survival is examined by MTT staining.

To determine if psychosine is preferentially accumulated in myelin. Psychosine is a lipid raft-enriched sphingosine. Since myelin is a type of raft-like membrane, psychosine is very likely to be selectively accumulated in myelin. This possibility may partially explain why myelin-forming cells become specific target in KD. To test this hypothesis, myelin membrane is isolated from whole brains of TWI and WT of P7, p15, P30 and P40. Psychosine is extracted and quantified by mass spectrometry as described in Goal 1.

To determine if psychosine is accumulated in TWI embryos. As a genetic disease, the mutation in the GALC gene is very likely to cause lipid metabolic abnormality even at embryonic stage. This experiment aims to examine this possibility, which may contribute to the pathology of KD. TWI and WT embryonic spinal cords are collected at E10.5, E12.5 and E15.5. Psychosine is extracted and quantified as described in Goal 1.

To characterize the spatiotemporal distribution of OPCs in embryonic TWI spinal cords. OPCs generated in E10.5, E12.5 and E15.5 spinal cords are identified by immunohistochemical staining for Olig2. Unbiased stereology is performed on the both

cervical and lumbar regions of TWI and WT to determine the abundance and distribution of OPCs.

To characterize how SHH signaling pathway is affected in embryonic TWI spinal cords. This experiment is to determine changes in raft-associated signaling pathways in mutant embryos. SHH signaling is first tested, which is critical for the generation of OPCs from embryonic neuroepithelium cells. The protein levels of SHH ligand, receptors (PTC/SMO), and downstream effectors (Gli1, Nkx2.2, PDGFR- α), are examined by western blotting and analyzed by ImageJ software. Both TWI and WT spinal cord samples are run by triplicates from E10.5, E12.5 and E15.5.

To determine if psychosine directly affects SHH pathway in vitro. This in vitro experiment is to testify the possibility the psychosine is responsible for the observations found in vivo. NSC cultures are obtained from E12.5 TWI and WT spinal cord and stimulated with SHH-N ligand with or without low-dose of psychosine for 72 hours. SHH signaling pathway is then examined by western blotting as described in experiment 11.

CHAPTER 4

MATERIALS AND METHODS

4.1. Animals.

Twitcheer colony: breeder Twitcheer heterozygous mice (C57BL/6J, *twi*^{+/+}; Jackson Laboratories, Bar Harbor, ME) were maintained under standard housing conditions with approval of the Animal Care and Use Committee at the University of Illinois Chicago. The mutant TWI mice were allowed to survive as long as humanely possible. When a mouse reached a moribund condition, it was killed.

MBP-LacZ/TWI double mutant colony: This thesis used MBP-LacZ/TWI mice, generated previously by Dr. Wrabetz and Bongarzone. Heterozygous Twitcheer females were crossed with 18.2MBP-LacZ transgenic males (B6SJLF1, Wrabetz et al. 1998). The double heterozygotes (carrying the Twitcheer mutation and the MBP-LacZ reporter gene) were selected and performed 10 backcrosses with C57BL/6J as for breeding parents.

For genotyping, DNA was extracted from clipped tails of newborn mice at postnatal day 1 (P1) to P3. TWI mutation was detected with primer pairs TWF 5'-CACTTAATTTTCTCCAGTCAT and TWR 5'-TAGATGGCCCACTGTCTTCAGGTG and followed by an EcoRV DNA digestion to discriminate mutant from WT gene as described previously (Dolcetta et al. 2006; Sakai et al. 1996). Transgenic MBP-LacZ was detected with primer pairs MBLZF 5'-CCGCCTCTTTTCCCGAGATG and MBLZR 5'-GGCGGATTGACCGTAATGGG.

4.2. Cell Cultures.

Primary Glia Cultures: MBP-LacZ positive newborn mice from 18.2MBP-LacZ transgenic colony were selected for mixed glia cell primary cultures, following the standard culture protocol as described previously (Bongarzone et al. 1996). Newborn (0-3-day-old) mouse brain cortices were used for the establishment of glial cultures. After dissection of the brains in a sterile hood, the cerebral hemispheres were placed in a 60 mm petri dish containing cell medium (DMEM/F12, 10% fetal calf serum, FCS). Tissue was dissociated through a nylon mesh, and cells were collected in 50 ml of cell medium. The cell suspension was poured through two collector tissue sieves (first a 230 μ m then a 140 μ m pore size sieve). The filtered cell suspension was added to 50 ml conical tubes and centrifuged for 5 min at 1,000 rpm in a clinical centrifuge. The cell pellet was re-suspended in cell medium (5×10^5 cells/ml), and plated on poly-L-lysine coated coverslips or tissue culture flasks. Cells were incubated at 37°C in 5% CO₂, with changes of medium every 4 days.

As for OLs enrichment, glia cells were cultured in flask for 14 days in vitro (div) and were first shaken at 200 rpm for 1 hour in 37°C incubator to get off the microglia cells. The remaining cells in flask were washed twice with medium and continued with shaking at 280 rpm for 20 hours. OLs, shaken off from the bottom astrocyte layer, were collected and incubated in 10cm tissue culture dish at 37°C for 20 minutes to get rid of contaminating astrocytes. OLs remaining in the suspension were transferred into poly-L-lysine coated plates for further analysis.

CG4 cell culture: CG4 is a rat immortal OPC cell line that can be maintained as OPCs and also induced to OLs. CG4 cells are cultured as OPCs, in 70% BS medium

(DMEM/F12 with 2.2g/L NaHCO₃, 5mg/L insulin, 16.1mg/L putrescine, 50mg/L transferrin, 4g/L glucose, 8ng sodium selenite) plus 30% B104 conditioned media (BCM: DMEM/F12 with B27 supplement to culture B104 cell for 4 days, and then collected). Differentiated CG4 cells are induced by withdrawing BCM, using BS medium along with 2% FCS.

eNSCs cell cultures: Embryonic neural stem cell (eNSC) cultures were established according to standard eNSC culture protocol (Chojnacki and Weiss 2008). In brief, embryos of E12.5 were dissected out from pregnant WT female mice. The embryonic spinal cords were isolated under dissection microscope. Cells were dissociated by 200- μ l plastic tip with a micropipette to achieve single-cell suspension and then plated in a density of 200,000 cells/ml in complete medium containing 1 \times DMEM/F12 (1:1), glucose (0.66% wt/vol), glutamine (2mM), NaHCO₃ (14.6mM), HEPES buffer (5 mM), insulin (23 mg ml⁻¹), transferrin (93 mg ml⁻¹), progesterone (19 nM), putrescine (56 nM) and sodium selenite (21 nM), plus 20 ng/ml EGF and 10ng/ml bFGF. Cultures were incubated at 37°C/5% CO₂ for 5 to 7 days (100 μ m spheres will form in medium). They can be passaged into secondary cultures at a density of 50,000/ml or be processed for further analysis.

4.3. Immunocytochemistry.

Primary cultures were grown on coverslips for 14 days in vitro (DIV). Detection of β -Galactosidase expression in oligodendrocyte lineage cells was performed by a modification of technique by Feltri et al. (Feltri et al. 1992). Briefly, cells were fixed with 0.05% glutaraldehyde in PBS for 5 min at room temperature. After 2 washes (5 min

each), cells were incubated with X-Gal to a final concentration of 0.8 mg/ml in X-Gal developer (35 mM $K_3Fe(CN)_6$ /35 mM $K_4Fe(CN)_6$ /2 mM $MgCl_2$ in PBS) at 37°C for 2 hours. Cells were then washed twice in PBS and stained with following primary antibodies: anti-A2B5, anti-O4, anti-O1 (mouse IgM, 1:20). Those antibodies were visualized with fluorescein-conjugated anti-mouse IgM secondary antibody (1:600, Jackson ImmunoResearch). Double stained cells were photographed on Zeiss stereoscope (AX10) in bright-field illumination for the blue color of X-Gal staining, and in fluorescence field for the florescent labeling.

4.4. CG4 cells Proliferation Assay.

CG4 cells are plated at a density of 20,000/ml into poly-D-lysine coated 24-well plates. 0.5nM, 1nM, 5nM, 50nM, 100 nM, 1 μ M, 2.5 μ M, 5 μ M psychosine (Matreya) were dissolved in DMEM medium and added onto the cells for 72 hours. Then cells were trypsinized and the final numbers were counted in each well using hemocytometer. D-sphingosine (Sigma) was used as lipid control of psychosine.

4.5. MTT Assay.

OL cells were obtained by shaking-off from mixed primary glia cultures and were plated at a density of 2,000 cells /well in poly-L-lysine coated 96-well plate. Cells were allowed to differentiate for 3 days and then treated with 1 μ M, 2 μ M psychosine (Matreya) and 1 μ M D-sphingosine (Sigma). Cells treated for 24 hours or 36 hours were incubated with

MTT reagent (R&D) at 37°C for 20 minutes and picture of stained live cells were taken under inverted bright-field microscope.

4.6. SHH Stimulation Assay.

Newly passaged eNSCs in single-cell suspension were plated at 50,000 cells /ml in 6 well plates. Cells were stimulated with 200 ng/ml SHH ligand (Peprotech) plus or not plus 20 nM psychosine in NSC complete medium (20 ng/ml EGF and 10 ng/ml bFGF added).

After 3 days growth in culture, new-formed neurospheres were collected and SHH signaling pathway was examined by western blotting.

4.7. Tissue collection and β -Galactosidase histochemistry.

Postnatal mice genotyped for MBP-LacZ/TWI, and MBP-lacZ/WT were anesthetized with 2-bromo-2-chloro-1,1,1-trifluoroethane (Sigma, St. Louis, MO) and transcardially perfused with PBS followed by 4% paraformaldehyde (PFA)/PBS. Spinal cord were postfixed for 2 hours, and rinsed 3 times in PBS, cryoprotected in 30% sucrose overnight, embedded in OCT (Tissue-Tek, Sakura Finetek USA, inc., Torrance, CA, USA) and cross sectioned on a cryotome at 50 μ m thickness.

For X-Gal histochemistry, spinal cord sections from cervical, thoracic and lumbar segments were air-dried and rinsed three times in PBS to remove OCT. Sections were stained in 0.8mg/ml X-Gal at 37°C for 2 hours. Sections were then washed 3 times in PBS, dehydrated with serial graded ethanol, clarified in xylenes, and coverslipped with Permount.

4.8. Immunohistochemistry.

Immunoperoxidase assay: Tissue sections were first quenched for endogenous peroxidase activity by incubating the sections in 3% H₂O₂ in PBS for 30 min. Tissue was then blocked in 4% bovine serum albumin (BSA) in PBS for 1 hr at room temperature. Sections were incubated with rabbit anti-Olig2 antibody (1:500, abcam), rabbit anti-aspartoacylase serum (ASPA, 1:5000, a kind gift of Dr. James Garbern), in 1% BSA/0.3% triton X-100/PBS for 72 hr at 4°C. Bound primary antibody was detected using the avidin-biotin-peroxidase system as recommended by the manufacturer (Vector Laboratories, Burlingame, CA). After development with diaminobenzidine, and H₂O₂, sections were air-dried, dehydrated with serial graded ethanol, clarified in xylenes, and coverslipped with Permount.

Immunofluorescence labeling: Tissue sections were blocked in 4% BSA/ PBS for 1 hour at room temperature and incubated with primary antibodies in 1% BSA/0.1% triton X-100/PBS overnight at 4°C. After three washes with PBS, Alexa-488, Alexa-555 or Alexa-649 conjugated-secondary antibodies (Jackson ImmunoResearch Inc.) were added for 2 hours at room temperature. Sections were mounted with anti-fade mounting medium (vectashield, vector, Burlingame, CA), and then were examined under fluorescence microscope. The primary antibodies used were: olig2 (Millipore), beta-galactosidase (Promega), proteolipid protein (PLP, monoclonal antibody AA3), active caspase 3 (cell signaling), NeuN (Millipore), GFAP (Millipore), SHH (Santa Cruz). Isolectin IB4-Alexa488 was from Invitrogen.

4.9. BrdU Assay.

A solution of 20 mg/ml 5'-bromo-2'-deoxyuridine (BrdU, Sigma-Aldrich, St. Louis, MO, USA) was prepared in sterile saline solution. Postnatal mice were intraperitoneally injected at a dose of 100mg/kg every 8 hours. After 24 hours, mice were sacrificed and spinal cord was collected and crossly sectioned at 50 μ m as described above. For BrdU labeling, sections were treated with 2 M HCl for 15 min at 37 °C to denature DNA and then rinsed in 0.1 M sodium borate, pH 8.5, for 10 min. Sections were incubated with antibodies: mouse monoclonal anti-BrdU (Becton Dickinson, San Jose, CA) diluted 1:200 and alexa 555-conjugated goat anti-mouse secondary antibodies. Sections were mounted with anti-fade mounting medium (vectashield, vector, Burlingame, CA).

4.10. TUNEL Assay

Apoptotic cells in TWI and WT spinal cords were detected by TUNEL assay (DeadEndTM Fluorometric TUNEL Kit from Promega). Briefly, 10 μ m frozen sections were permeabilized with 20ng/ml protease K for 10 minutes at room temperature. After PBS washes, the sections were fixed with 4% PFA for 5 minutes. Sections were washed with PBS again and equilibrated with Equilibration Buffer for 10 minutes. Then sections were incubated with TdT reaction mix at 37 °C for 1 hour. The reaction was stopped with 2X SSC buffer and processed further for other immunohistochemical staining.

4.11. Stereology.

For unbiased stereological studies, 50- μm -thick spinal cord cross-sections were selected in an interval 1 every 10 (for postnatal tissue) or every 5 (for embryonic tissue) and stained accordingly. Quantification of positive cell markers was performed with design-based stereology system (StereoInvestigator version 8, MBF Bioscience, Williston, VT, USA). Briefly, interested regions in the spinal cord were traced under a10X objective and all cell markers were counted under a 63X objective (Zeiss AX10 microscope, Carl Zeiss Ltd., Hertfordshire, England). The sampling parameters were set up according to the software guide to achieve the coefficient of error ranged between 0.09 and 0.15 using the Gundersen test, normally a counting frame size 100X100 μm , optical dissector height 20 μm , and an average of 10 sampling sites per section were chosen.

4.12. β -Galactosidase Enzyme Assay

Brainstem and spinal cord tissues from MBP-LacZ/TWI or WT were collected at P7, P15, P30 and P40. Tissues were homogenized in 250 mM Tris buffer (pH 7.8) and centrifuged at 15,000 rpm for 15 min at 4 °C. As described before, β -galactosidase assay was performed using a modified o-nitrophenyl- β -D-galactopyranoside (ONPG) substrate technique (Wrabetz et al.1998). 50 μl protein supernatant were incubated with a 1.75 ml reaction solution (3.5 mg/ml ONPG, 100 mM Na_2HPO_3 , 2 mM MgCl_2 , 50 mM β -mercaptoethanol) for 1-3 hours at 37 °C. The reaction was terminated by 1M Na_2CO_3 and measured absorbance at 420 nm. Standard curves were prepared from commercially synthesized β -galactosidase (Sigma).

4.13. Reverse-Transcriptase PCR Analysis

RNA was isolated from tissues using CsCl₂ gradient centrifugation as described (Chirgwin et al. 1979). cDNA was synthesized using Superscript cDNA synthesis kit (Invitrogen). cDNA product was treated with RNase to remove remaining RNA and amplified using Taqman one step real-time PCR master mix (Invitrogen). The following primers were used for MBP: 5'-CACAGAAGAGACCCTCACAGCGACA-3' and 5'-CCGCTAAAGAAGCGCCCGATGGA-3'; GAPDH: 5'-GTATGACTCTACCCACGG-3' and 5'-GTTTCAGCTCTGGGATGAC-3'; 94 °C for 30 s, 50 °C for 60 s, and 72 °C for 60 s.

4.14. Embryo Collection.

Standard housed heterozygous $GALC^{+/-}$ female mice were set up for time-traced mating with the heterozygous $GALC^{+/-}$ males. Vaginal plugs were checked everyday to determine the exact copulation date for the female mice. Embryos at E10.5, E12.5 and E15.5 days were obtained by sacrificing the pregnant female. Uteri were dissected out and embryos collected. Tail clips from each embryo were obtained and used for genotyping. For western blotting, spinal cords were dissected out using micro-surgical tools under a stereomicroscope and frozen down on dry ice immediately; for immunohistology studies, whole embryos were fixed with 4% PFA/PBS overnight at 4°C and then cryo-protected and sectioned as described above.

4.15. Western Blotting

Spinal cord samples dissected from TWI and WT mice or embryos were homogenized in lysis buffer: 1% triton, protease inhibitor cocktail (PIC), 4mM PMSF, 100pM Okadaic Acid in PBS. Samples were sonicated on ice and were quantified for protein content using the BCA Bradford assay (Bio-Rad). Equal amount of protein were loaded (20 μ g/lane) on a 4-12% 10 well 1.5mm precast Nupage gels (Invitrogen). Gel electrophoresis was performed using the XCell Sure-lock vertical electrophoresis system (Invitrogen). After transferring to PVDF membrane, blots were blocked with milk/BSA solution and then treated with primary antibodies. Antibodies used in this study were the following: anti-olig2 (abcam), PLP (monoclonal antibody AA3), GAPDH (Millipore), SHH (Santa Cruz), SMO (Santa Cruz), PTC1(Santa Cruz), Gli1(Santa Cruz), PDGFR- α (Santa Cruz), Nkx2.2 (mouse monoclonal antibody), and Actin (Chemicon). Antibody-reactive products were detected using peroxidase-labeled secondary antibodies and ECL chemiluminescent substrate (Pierce, Rockford, IL). Wild type and twitcher protein blots were exposed for the same amount of time on the same film to allow for comparison of protein abundance. Protein levels were semi-quantified using ImageJ software (NIH).

4.16. Myelin Isolation

Brain tissues were homogenized in 0.3 M sucrose solution containing 20mM Tris-Cl buffer (pH 7.45), 1mMEDTA, 1mMDTT, 100 μ M phenylmethylsulfonyl fluoride (PMSF). The homogenate was centrifuged over 0.83 M sucrose at 75,000g for 35 min. The crude myelin band was collected at the 0.3 M /0.83 M sucrose interface and further

purified by osmotic shock in 20mM Tris-Cl buffer. Myelin fraction was pelleted down by centrifuging at 12,000g for 15 min and stored at -20 °C for further analysis.

4.17. Psychosine Extraction and Quantification.

Psychosine Extraction: Spinal cords samples dissected from TWI and WT mice or embryos were homogenized in water and extracted for psychosine as described (Galbiati et al. 2007a). Briefly, 500 μ l tissue lysate was mixed with 5ml of Folch phase (chloroform and methanol mixture 2:1 v/v) and filtered to remove debris. Then 1ml 0.9% NaCl was added. After centrifugation, lipids in lower phase were evaporated and re-suspended in 2ml methanol. Extracts were then partially purified on a strong cation exchanger column, SupelcleanTM LC-SCX (Sigma, cat # 57018) pre-conditioned by 2 ml methanol. Columns were washed several times with Folch phase and methanol, and samples were released from the column with 1.7 ml methanol: 0.4 M CaCl₂ (3:1 v/v). Eight pmole internal standard (lyso-lactosylceramide) were added to each sample, and further passed through Bond Elut-C18 solid phase extraction columns (Varian, Part # 12102052) previously activated by 5ml methanol and 5ml H₂O. After several washes with water, the remaining lipid residues were released with 7.5ml of chloroform: methanol (1:2 v/v). After evaporation to dryness, each residue was dissolved in 200 μ l methanol containing 5 mM ammonium formate and used for mass spectrometry analysis.

Mass Spectrometry: Psychosine samples extracted from spinal cord tissue were quantified by liquid chromatography tandem mass spectrometry (LC-MS/MS). The HPLC system consists of Shimadzu (Columbia, MD) LC-10Advp pumps with a Leap (Carrboro, NC) HTS PAL autosampler. Psychosine was measured using a Waters XTerra

3.5 μm , MS C18, 2.1 x 100 mm analytical column. Positive ion electrospray tandem mass spectrometry was performed using an Applied Biosystems (Foster City, CA) API 4000 triple quadrupole mass spectrometer with a collision energy of 29 eV for psychosine and 37 eV for the internal standard, lyso-lactosylceramide. The dwell time is 1.0 s/ion during multiple reaction monitoring.

4.18. Statistical Analysis.

Results are the average from three to five different experiments and are expressed as mean \pm standard error (SE). Data were analyzed by the Student's *t* test. *p* values <0.05 were considered statistically significant.

CHAPTER 5

EXPERIMENTAL RESULTS

RESULTS PERTINENT TO SPECIFIC AIM 1

5.1. Psychosine accumulates since early postnatal days in TWI spinal cord. A direct correlation between psychosine accumulation in different regions of the spinal cord and the disease progress (measured by the loss of OLs) is not available for the TWI mutant. In order to clarify this question, we carried out a systematic and temporal quantification of psychosine levels in 6 regions of TWI spinal cords from P7 to P40. Figure 1 shows the corresponding results for psychosine levels in dorsal and ventral hemihalves isolated from cervical, thoracic and lumbar segments of TWI and WT spinal cords. In normal tissue (WT), psychosine content was consistently low in all spinal cord regions within the range of 2-6 pmol/mg from all studies time points (P7, P15, P30, and P40). As expected, psychosine was progressively accumulated in TWI spinal cords, and goes up to 300-400 pmol/mg in P40 tissue. At the asymptomatic P15, psychosine was already increased to ~60 pmol/mg in dorsal spinal cords and ~110 pmol/mg in ventral spinal cords. Furthermore, even at P7, psychosine was modestly but significantly increased to ~7 pmol/mg in dorsal regions (3 fold respect WT) and ~12 pmol/mg in ventral regions (6 fold respect WT).

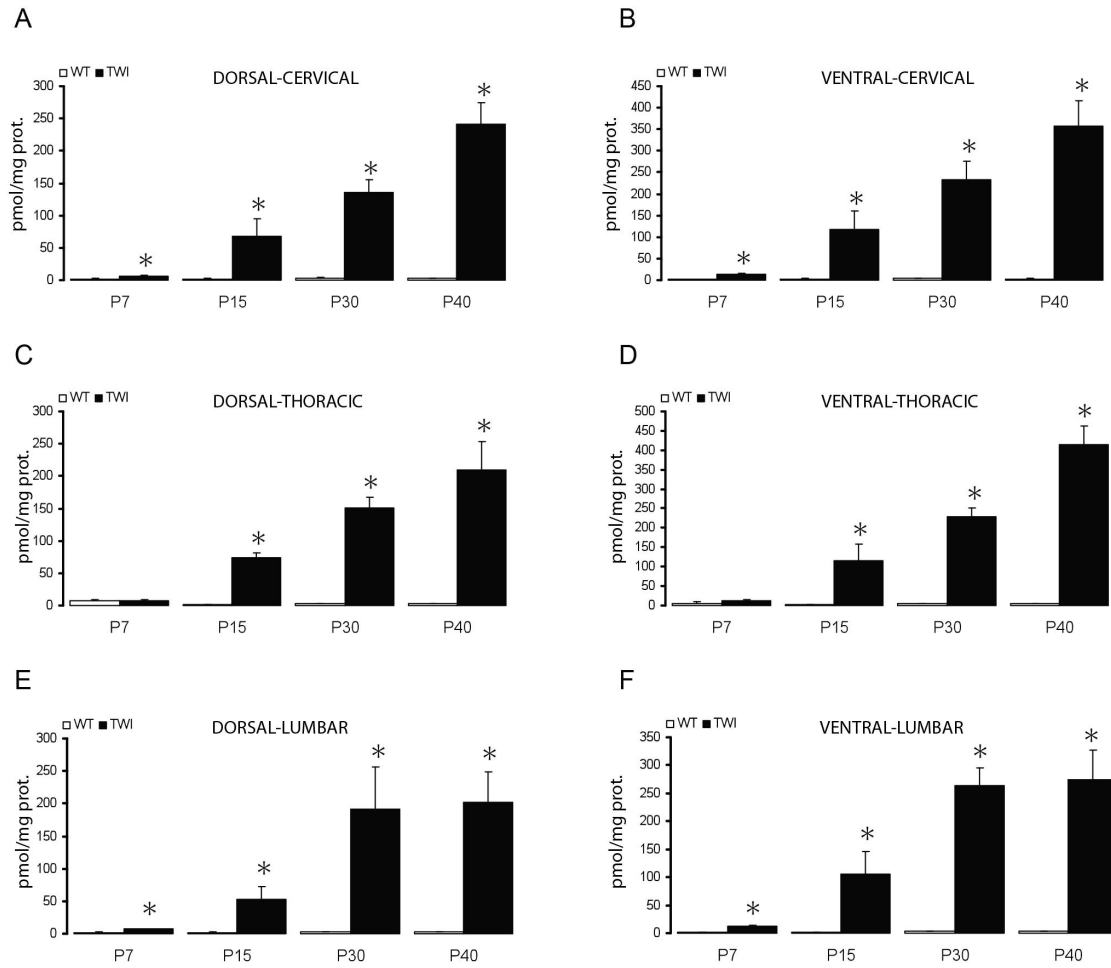


Figure 1. Progressive accumulation of psychosine in the postnatal TWI spinal cord. A-F) P7, P15, P30 and P40 TWI and time-matched WT spinal cords were dissected into dorsal and ventral halves at the cervical, thoracic and lumbar segments. Psychosine was purified and quantified by mass spectrometry. Psychosine progressively accumulated in TWI spinal cords. Psychosine accumulated more in ventral regions along the cord. N=3 animals per genotype per time point. *p<0.05.

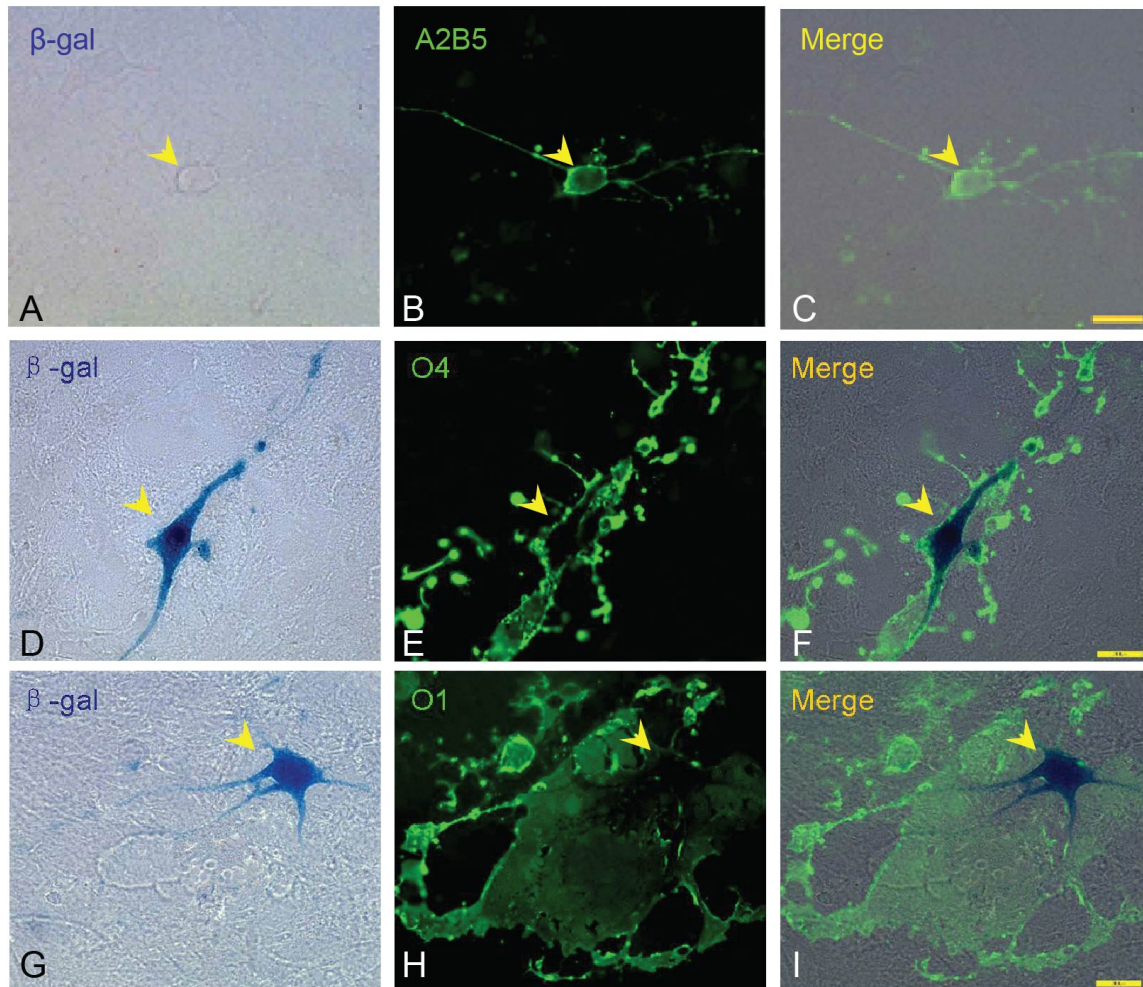


Figure 2. MBP-LacZ expression in oligodendrocytes isolated from the MBP-LacZ/TWI mouse. A-I) Mouse glial primary cultures were prepared from WT and TWI postnatal day P2-4 cortices and cultured on coverslips for 7, 14 and 21 days. After fixation, cultures were stained for b-galactosidase and the oligodendrocytes markers A2B5, O4 and O1. LacZ was expressed only in the cell bodies (arrowheads) of intermediate and more mature oligodendrocytes. Bar 20 micron.

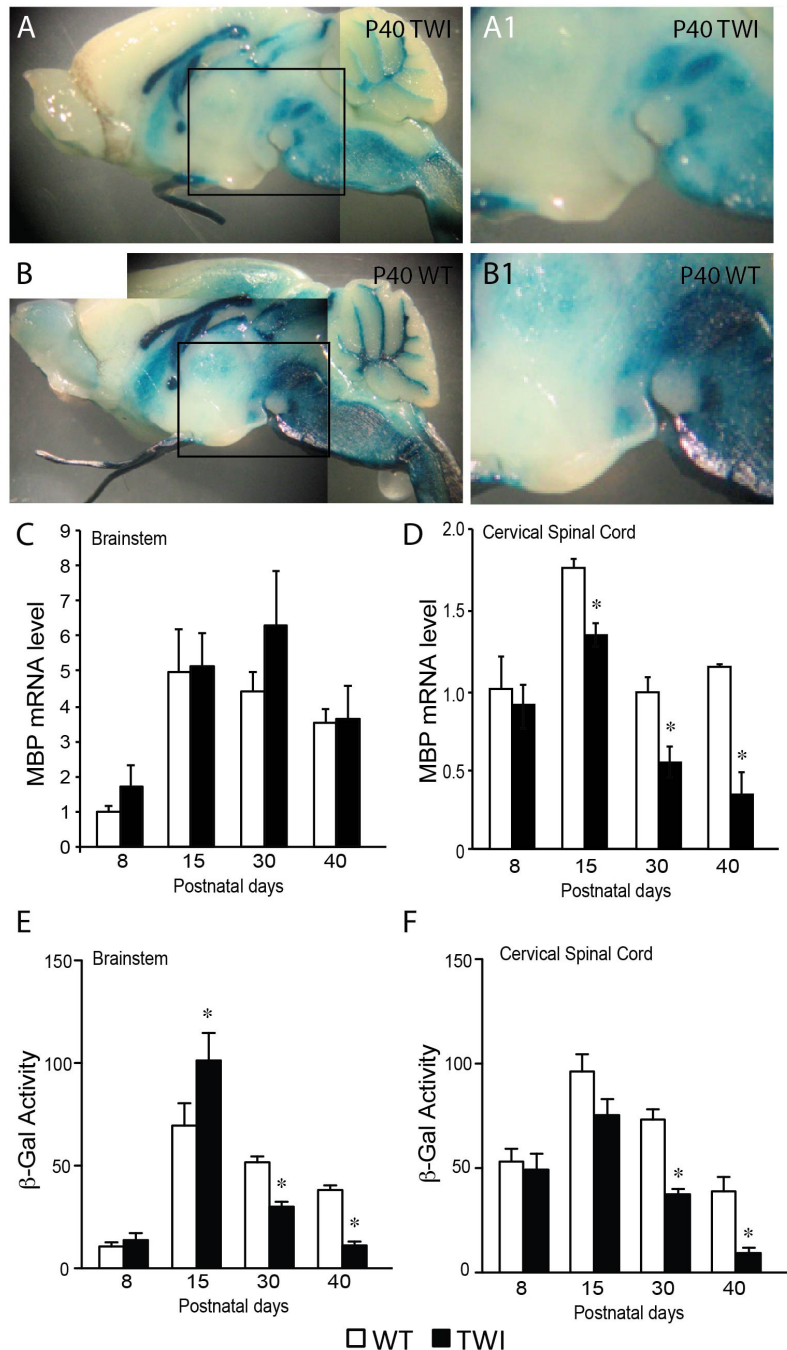


Figure 3. The MBP-LacZ/TWI mouse as a model to study changes in numbers of oligodendrocytes bearing the TWI mutation. A-B) P40 brains from MBP-LacZ/TWI and age-matched MBP-LacZ controls were sagittally sectioned and stained for LacZ. A noticeable reduction of LacZ+ expression was observed in the mutant brain (A, A1). C, D) Expression levels of MBP transcripts in the brainstem (C) and spinal cord (D) were quantified by Taqman PCR. E, F) Lysates from brainstems (E) and spinal cord (F) were prepared from MBP-LacZ/TWI and MBP-LacZ spanning postnatal days 8 to 40 and assayed for b-galactosidase activity (b-gal.) N=4-6 animals per genotype. *p<0.05.

5.2 The new MBP-lacZ/TWI double mutant expresses LacZ in myelinating OLs.

Using in vitro glia primary cultures obtained from the MBP-LacZ/TWI mouse, we demonstrated that the LacZ transgene was active only in O4+ and O1+ OLs (Figure 2D-I), but not in A2B5+ OPCs (Figure 2A-C). The reporter gene was expressed throughout the cell body of OLs and much less on cellular processes or myelin-like membranes, making it a simple and clear labeling system for quantitative studies of myelinating OLs.

5.3 Quantitative analysis of LacZ+OLs in developing TWI spinal cords of P7-P30.

TWI mice are born asymptomatic and remain as such for the first 2-3 weeks of life (Duchen, Eicher et al. 1980). Available studies on TWI OLs focused on symptomatic but not on pre-symptomatic stages. To obtain a more complete understanding of pathological changes in TWI OLs previous to the demyelinating phase (which starts between 20-25 days in the cord), we decided to take advantage of a new MBP-LacZ/TWI transgenic mouse generated by a previous collaboration between our lab and Larry Wrabetz's lab. Before starting the analysis, in collaboration with Dr. Wrabetz lab, we conducted a characterization of the transgene expression during postnatal life by measurement of β -galactosidase activity and quantitative PCR of MBP transcripts. Expression of the 18.2 MBP-LacZ transgene is neuronal dependent and it has been shown to shut off after myelination is complete (Wrabetz et al. 1998). Figure 3A-B shows that expression of LacZ in myelinated regions of P40 TWI brains was greatly reduced when compared with time-matched WT brain, suggesting that the new 18.2 MBP-LacZ/TWI may allow monitoring for changes in myelinating OLs during disease. β -galactosidase activity and PCR analysis of MBP transcripts (Figure 3C-F) in brainstem and spinal cord showed

good correlation between MBP promoter transcription and LacZ activities from P7 to P30 but not at P40, where the transcription of the transgene is severely reduced in the mutant. In view of these results, further analysis of quantification of LacZ⁺ OLs in the mutant environment were conducted in all three anatomical regions (cervical (C1-C4), thoracic (C1-C6), and lumbar (L1-L3) between P7 to P30 by unbiased stereology.

At P7, the anatomic distribution pattern of LacZ⁺ OLs showed no obvious difference in the mutant spinal cord (Figure 4A). However, using unbiased stereology, an average of 15% decrease in cell numbers was measured in dorsal and ventral white matter (DWM, VWM) in lumbar mutant segments (Figure 4B,C). Interestingly, a ~25% increase of LacZ⁺OLs was measured in the cervical mutant segment (Figure 4B,C). While there was no significant difference in the distribution of LacZ⁺ OLs along the length of the P7 WT cord ($p_{wt} \text{ (cervical: lumbar)} >0.1$), mutant LacZ⁺ OLs were significantly different in the P7 TWI cord, with more OLs in cervical than in lumbar regions ($p_{twi} \text{ (cervical: lumbar)} <0.05$), suggesting an abnormal synchronization of myelination along the mutant cord.

At P15, LacZ⁺ OLs were further reduced (30%-40%) in mutant DWM and VWM respect WT (Figure 5A-C). Figure 6A shows show pictures of the P30 MBP-LacZ/TWI and MBP-LacZ/WT sections stained for LacZ. At this time point, previous studies have shown definite demyelination in TWI mice (Bourque, Bornstein et al. 1983; Ida and Eto 1990; Suzuki and Taniike 1995) and a reduction OLs was expected. Our quantitative analysis confirmed a general 30-40% reduction of LacZ⁺ OLs in TWI in all cord regions except in VWM of lumbar mutant cord (Figure 5C).

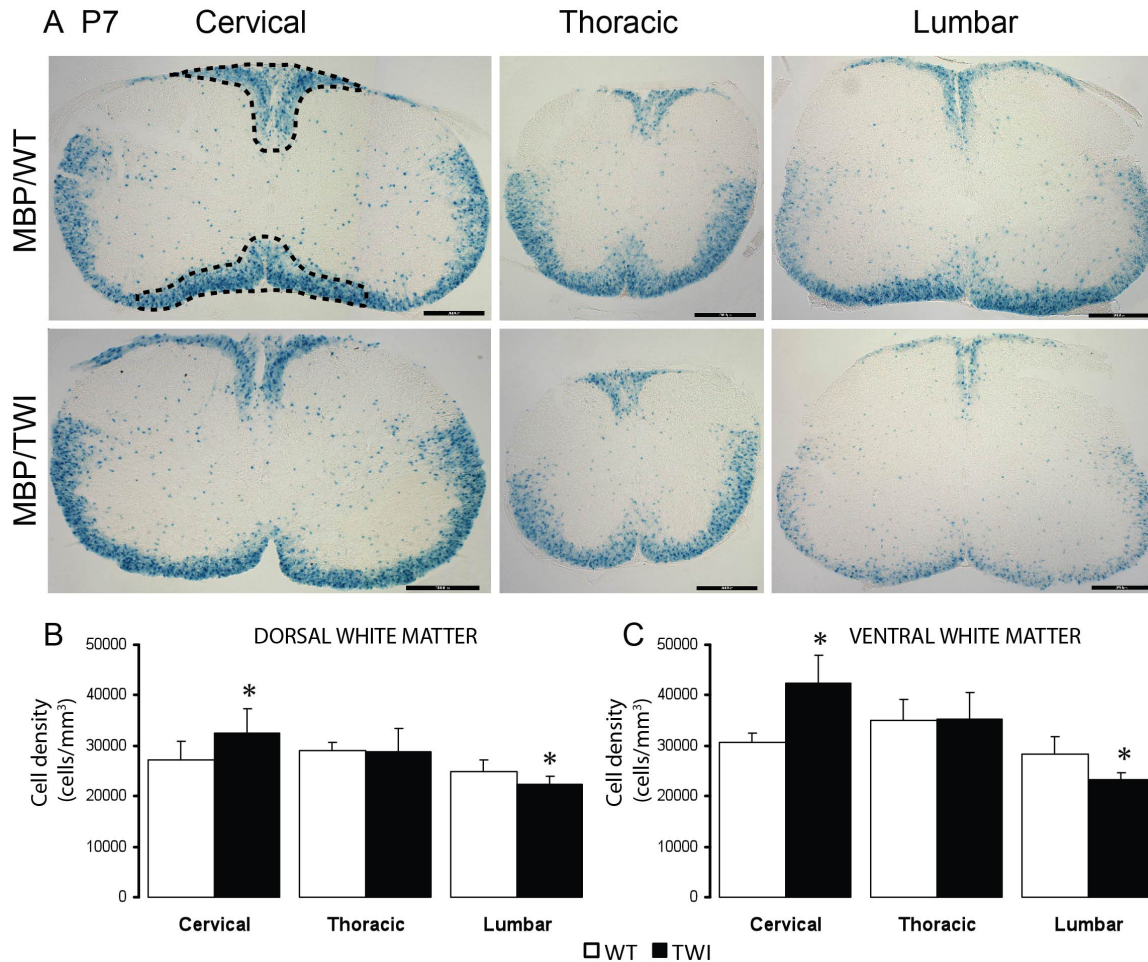


Figure 4. Distribution of LacZ+ OLs in the P7 TWI spinal cord. A) Spinal cords from time-matched TWI and WT were dissected into cervical, thoracic and lumbar segments and cut into 50 μ m sections. OLs were stained for β -galactosidase activity. B, C) LacZ+ OLs located in both dorsal (B) and ventral (C) white matter were quantified using stereology. TWI dorsal and ventral white matter cervical cords showed a significant increase in LacZ+ cells density. In contrast, TWI dorsal and ventral white matter lumbar cords showed a significant decrease in LacZ+ cells density. N=3 animals per genotype. *p<0.05.

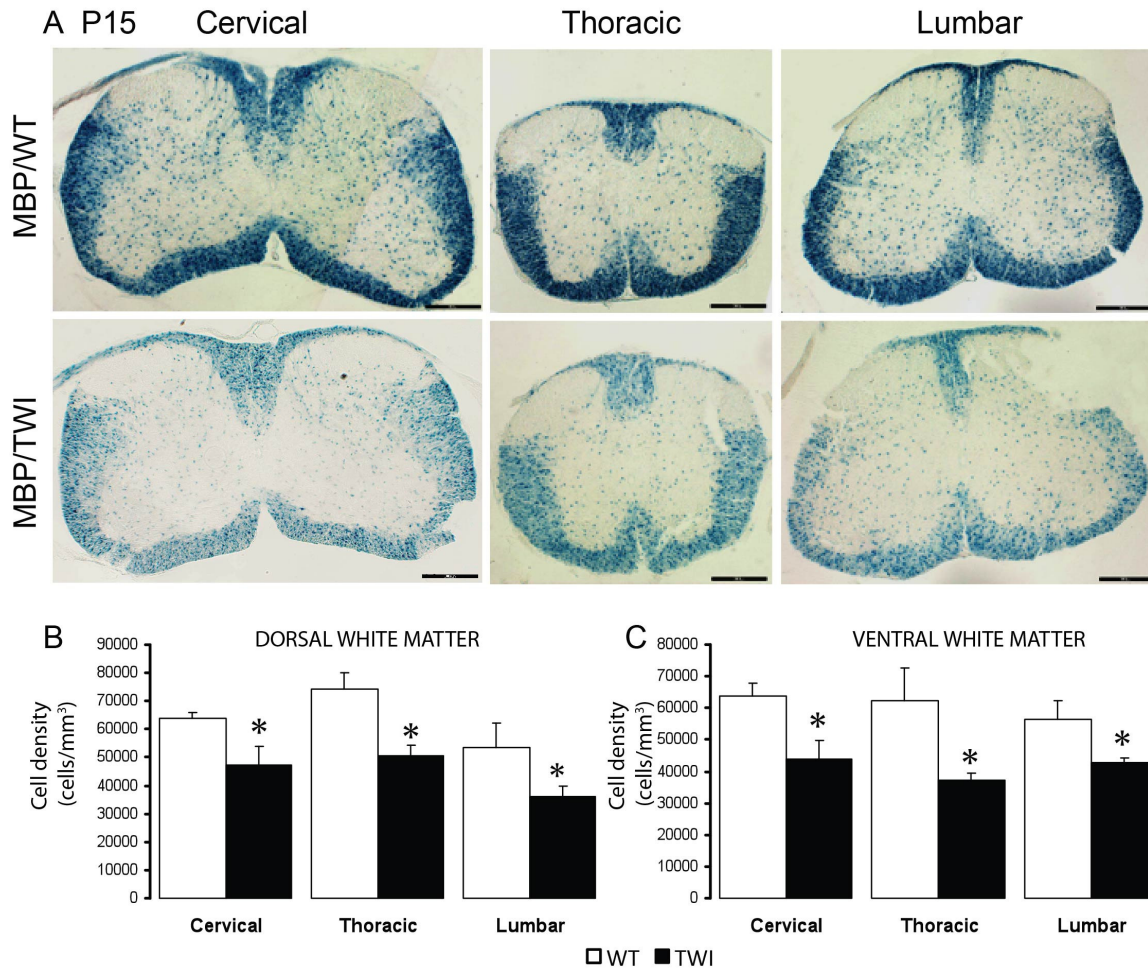


Figure 5. Distribution of LacZ+ OLs in the P15 TWI spinal cord. A) Spinal cords from age-matched TWI and WT were dissected into cervical, thoracic and lumbar segments and cut into 50 μ m sections. OLs were stained for β -galactosidase activity. LacZ+ OLs located in both dorsal (B) and ventral (C) white matter were quantified using stereology. LacZ+ cells density was significantly reduced in the TWI dorsal and ventral white matter of every segment at this age. N=3 animals per genotype. *p<0.05.

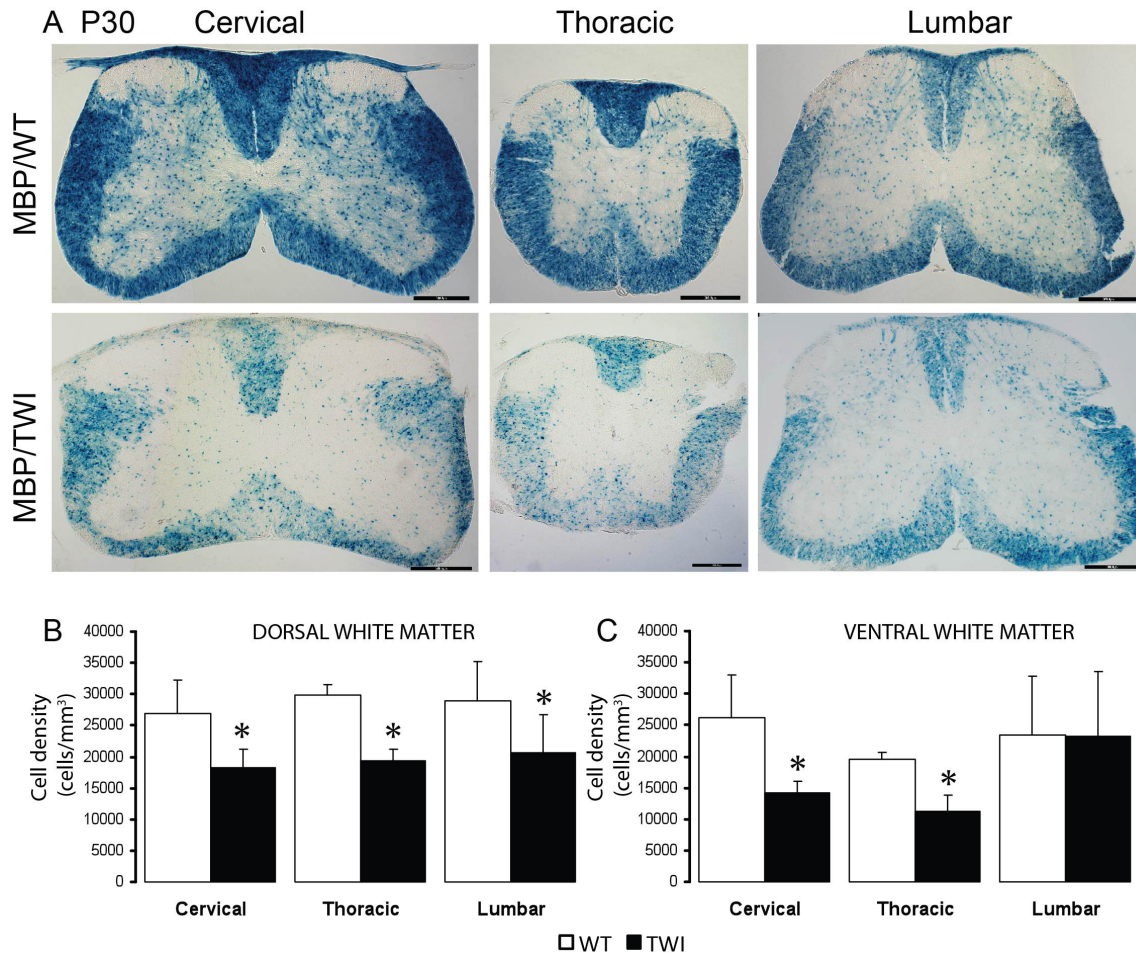


Figure 6. Distribution of LacZ+ OLs in the P30 TWI spinal cord. A) Spinal cords from age-matched TWI and WT were dissected into cervical, thoracic and lumbar segments and cut into 50 μ m sections. OLs were stained for β -galactosidase activity. LacZ+ OLs located in both dorsal (B) and ventral (C) white matter were quantified using stereology. LacZ+ cells density was significantly reduced in the TWI dorsal and ventral white matter of every segment at this age. N=3 animals per genotype. *p<0.05.

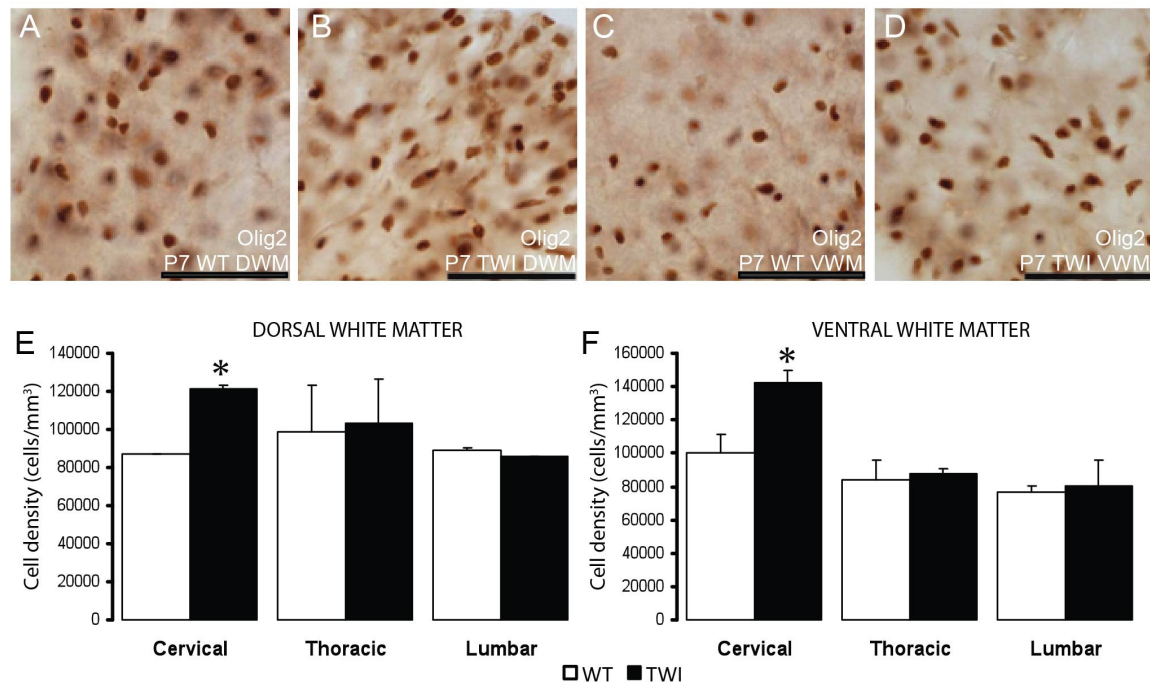


Figure 7. Distribution of Olig2+ OPCs in the P7 TWI spinal cord. A-D) Spinal cords from age-matched TWI and WT were dissected into cervical, thoracic and lumbar segments and cut into 50 μ m sections. OPCs were stained for Olig2. Olig2+ OPCs located in both dorsal (E) and ventral (F) white matter were quantified using stereology. Olig2+ cells density was significantly increased only in the TWI dorsal and ventral white matter of the cervical segment at this age. N=3 animals per genotype. *p<0.05.

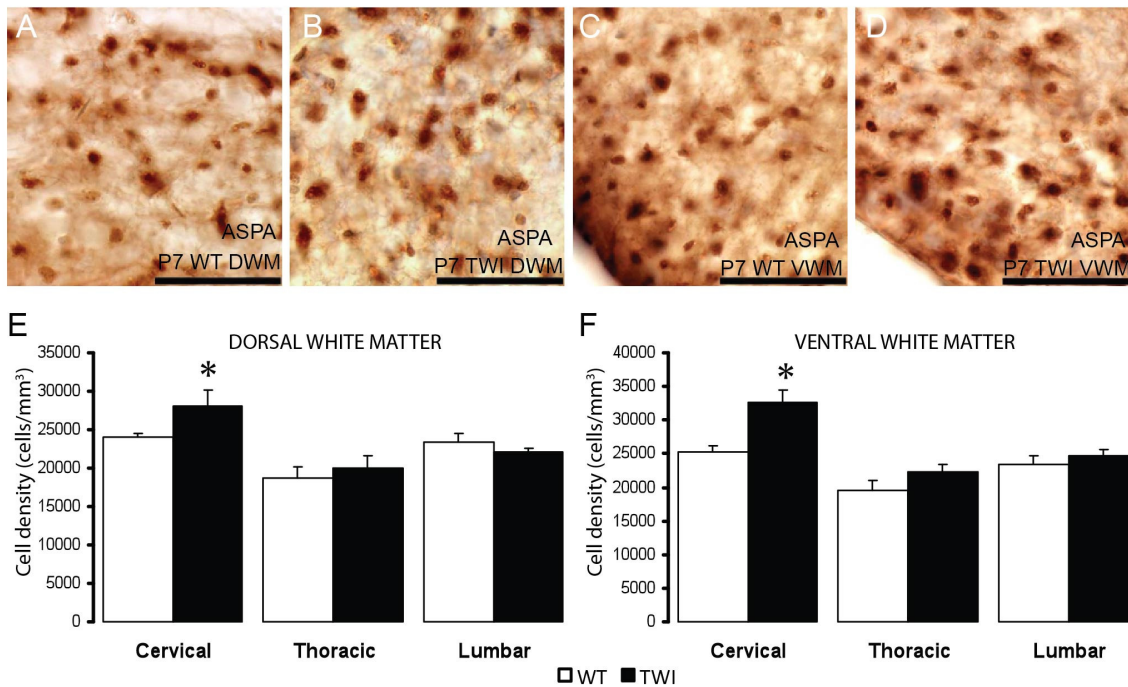


Figure 8. Distribution of ASPA+ OLs in the P7 TWI spinal cord. A-D) Spinal cords from time-matched TWI and WT were dissected into cervical, thoracic and lumbar segments and cut into 50 μ m sections. OLs were stained for ASPA. ASPA+ OLs located in both dorsal (E) and ventral (F) white matter were quantified using stereology. ASPA+ cells density was significantly increased only in the TWI dorsal and ventral white matter of the cervical segment at this age. N=3 animals per genotype. *p<0.05.

5.4 More OPCs and faster differentiation into mature OLs in the cervical region of the young TWI spinal cord. As stated above, at P7 we found an unexpected increase of LacZ⁺ OLs in cervical areas of the TWI spinal cord. This might be caused either by an increased production of OPCs and/or premature differentiation of OPCs into LacZ⁺ cells in this area. To further address these possibilities, we performed immunohistochemical studies to examine the distribution of OPCs and of mature OLs in the P7 TWI spinal cord.

OPCs were identified by immunolabeling against Olig2 (Figure 7A-D). Stereological quantification revealed a ~40% increase of Olig2⁺ OPCs in cervical areas of the TWI spinal cord. However, there was no significant difference in OPC numbers at lower levels of the mutant cord (Figure 7E, F).

Mature OLs were identified by immunolabeling aspartoacylase (ASPA) (Figure 8A-D). Stereological analysis detected a ~20% increase of ASPA⁺ OLs in cervical regions of the TWI spinal cord. ASPA⁺ OLs were similarly abundant in all other regions (Figure 8E, F). These results were complemented with an immunoblotting analysis of the expression levels of various proteins associated with oligodendrogenesis (Figure 9). Our semi-quantitative analysis indicated an increase in expression levels of PDGFR- α (which marks proliferating OPCs), Olig2 and PLP (which marks postmitotic mature OL and myelin) in the cervical segment but not in thoracic or lumbar segments.

Our results revealed an unexpected regulation of oligodendrogenesis in the TWI cervical spinal cord. Even though psychosine accumulation is subtle (about 6 fold) at this early period, rather than a decrease in OLs, we observed an increase in numbers of OPCs and of differentiated OLs. These results pose some questions: does psychosine play a role

in oligodendrogenesis in concentrations near physiological levels? If so, is this effect caused by altered lipid raft-signaling through receptors such as SHH? Are there abnormal responses of oligodendroglial cells at later stages, when the disease is active?

5.5 Increase in dividing Olig2+ OPCs during demyelination in the TWI cord. It is thought that demyelination can be rescued -at least partially- by recruiting OPCs and engaging them in remyelination (Girolamo et al. 2011; Givogri et al. 2006; Hagemeyer et al. 2012; Mi et al. 2009; Suzuki 1995). Based on this, one prediction will be to find increased proliferation of OPCs during demyelination. To evaluate this, we quantitated the number of dividing (BrdU+) Olig2+ OPCs (Durand et al. 1997; Gao and Raff 1997) in the spinal cord of P30 TWI mice.

Our analysis showed that more Olig2+ OPCs were proliferating during the demyelinating stage of the disease (Figure 10A-F). Stereological counting showed ~5 fold increase in proliferating BrdU+/Olig2+ OPCs in the mutant white matter (Figure 10G, H). These results are interesting because the historical view of this disease posed that high levels of psychosine kill OLs and that causes demyelination (Tanaka et al. 1989; Taniike et al. 1999). Our results open the possibility that high levels of psychosine may have different effects on oligodendroglial cells depending on their stage of differentiation. Our data agree well with previous studies done by Taniike and Suzuki (Taniike and Suzuki 1995), who found that there were ~6 times more BrdU+ cells in the P30 TWI spinal cord. However, in their studies, Taniike and Suzuki concluded that less than 10% of the BrdU+ cells were within the oligodendrocyte lineage. In our study instead, we found ~32.2% BrdU+ cells co-labeled with Olig2. This difference is likely

due to the different markers used by us and by Taniike and Suzuki to identify OPCs. In their study, these authors identified proliferative OLs with carbonic anhydrase or the Pi form of glutathione-S-transferase. Unlike Olig2, both markers are mainly expressed by differentiated postmitotic OLs, while Olig2 is well known to label proliferating OPCs as well as postmitotic OLs. Our results suggest an intrinsic resistance of OPCs to psychosine, and rather than dying, they are capable to sustain cell division.

5.6 Analysis of cell death in the spinal cord of the TWI mouse. One interpretation from the previous results is that oligodendroglia cells (OGs) are undergoing differential rates of cell death in the TWI depending on their differentiation stage. For example, the reduction of TWI LacZ⁺ OLs observed at P15 and P30 may be explained by the preferential killing of myelinating OLs while the increase in BrdU⁺Olig2⁺ OPCs may be caused by stimulation to proliferate of quiescent adult OPCs. To investigate these possibilities in more details, we first examined the level of activation of caspase 9 in the TWI spinal cord, which is upstream of the classic pathway for apoptotic cell death. Western blotting for full length and cleaved forms of caspase 9 showed increases of activation of this caspase at each time point in the study (Figure 11).

To determine the level of cell death in TWI spinal cords during disease progression and to answer the question that whether apoptosis is the major cause for the reduction of LacZ⁺ OLs, stereological quantification of double stained TUNEL/glia lineage markers cells was performed.

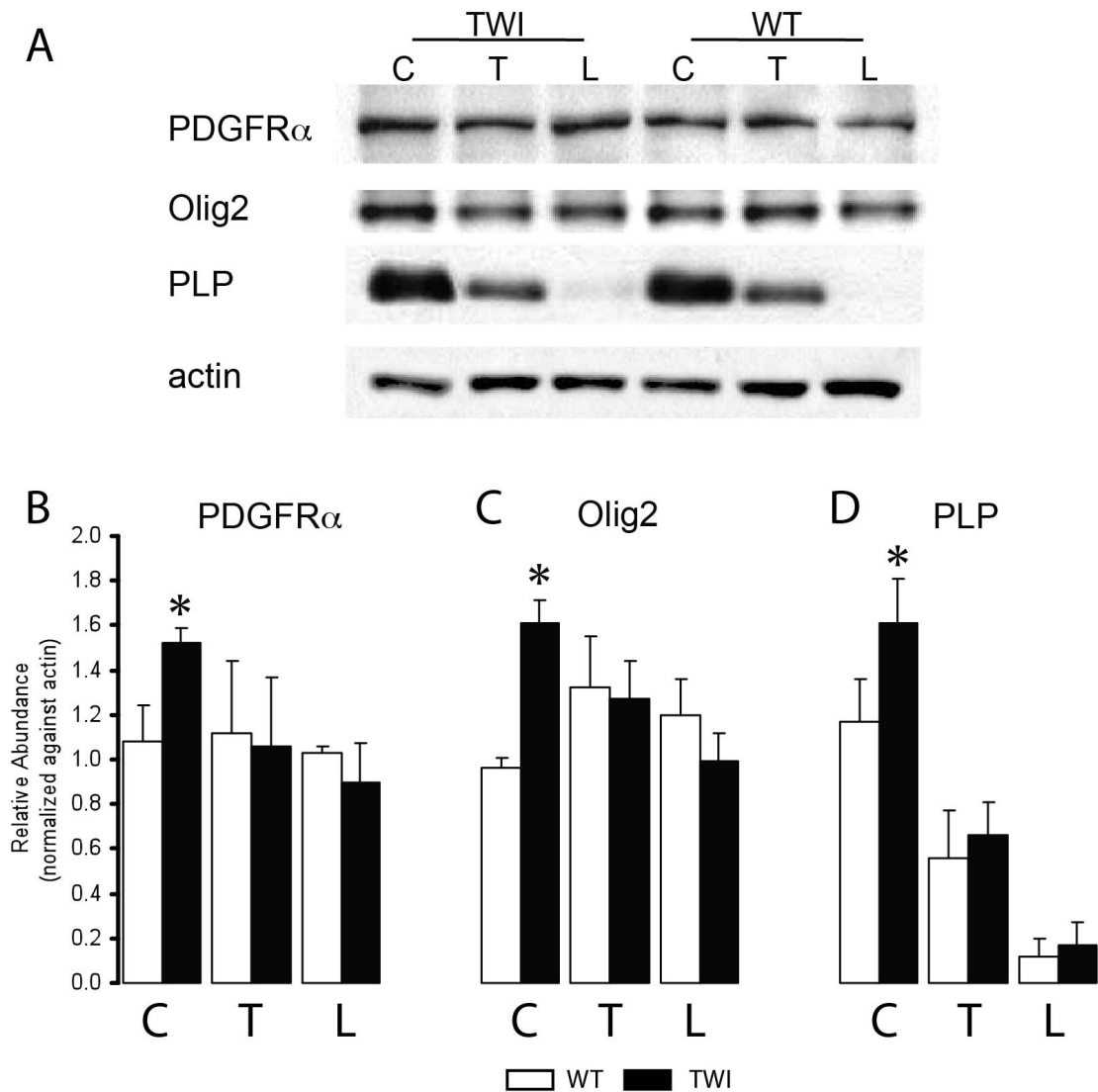


Figure 9 Increase of PDGFR-a, Olig2 and PLP protein levels in cervical segments of P7 TWI cords. A) Spinal cords from P7 TWI and WT were dissected into cervical, thoracic and lumbar segments and whole homogenates were analyzed by semi-quantitative western blotting. B-D) There is a significant increase in the PDGFR-a (B), Olig2 (C) and PLP (D) in cervical cords of the TWI mice. Each tested protein was normalized against actin. N=3 animals per genotype. *p<0.05.

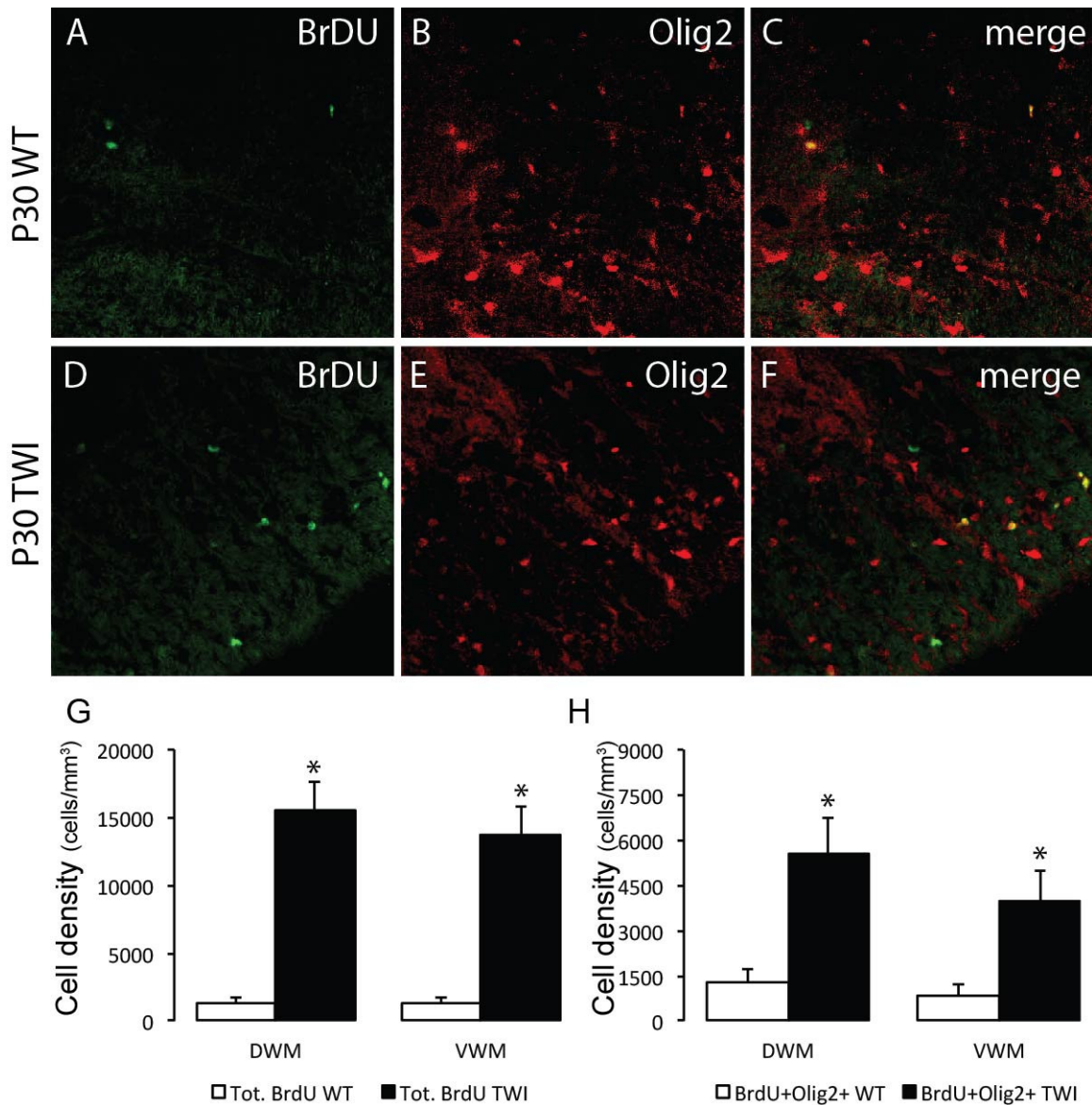


Figure 10 Proliferating OPCs increase in the spinal cord of sick TWI mice. WT and TWI animals were intraperitoneally injected with BrdU at P29 and killed at P30. Lumbar spinal cords were cut into 50 μ m sections and double stained for BrdU and Olig2. A-F) Representative images of ventral white matter stained for BrdU (in green), Olig2 (in red) and merge (in yellow) are shown. G, H) Total BrdU+ and BrdU+/Olig2+ cells were significantly increased in the dorsal and ventral white matter areas (DWM, VWM) in the TWI. N=3 animals per genotype. *p<0.05.

Most if not all of TUNEL+ cells co-localized with the active form of caspase 3 (Figure 12), which was expected based on our previous finding of active caspase 3 and on our past publications (Galbiati et al. 2007b, Smith, 2011 #3). A summary of the quantitative cell death data in the ventral white matter of the lumbar TWI cord is presented in Table I.

Table I Quantitative Profile of Cell Death and correlation with Psychosine storage in the TWI lumbar spinal cord

	DAPI*	TUNEL*	Cell Death (% from DAPI)	Cell Death Fold change (ratio TWI/WT)	Total Psychosine (nmol/mg)	Psychosine Fold change
P8 TWI	4062 ± 229.8	686 ± 145.7	16.9%	2.3	19.0	5
P8 WT	3908 ± 263.2	290 ± 46.6	7.4%		3.9	
P15 TWI	3264 ± 529.1	577 ± 129.6	17.7%	2.5	159.0	55
P15 WT	3045 ± 339.5	218 ± 78.7	7.2%		2.9	
P30 TWI	3034 ± 487.8	168 ± 35.4	5.5%	13.8	455.0	78
P30 WT	2011 ± 196.7	9 ± 10.0	0.4%		5.8	

*: cell numbers per mm², n=3 animals per genotype.

Quantification of TUNEL+ cells after normalization for cell density revealed a quite consistent 2.3-2.5 fold increase of cells dying in the VWM of TWI lumbar segments at P8 and P15 (Table I). Considering the sharp increase of psychosine occurring in this region of the cord (Table I), our results indicate a lack of correlation between the amount of psychosine and the level of cell death in the spinal cord of the TWI mouse during early development.

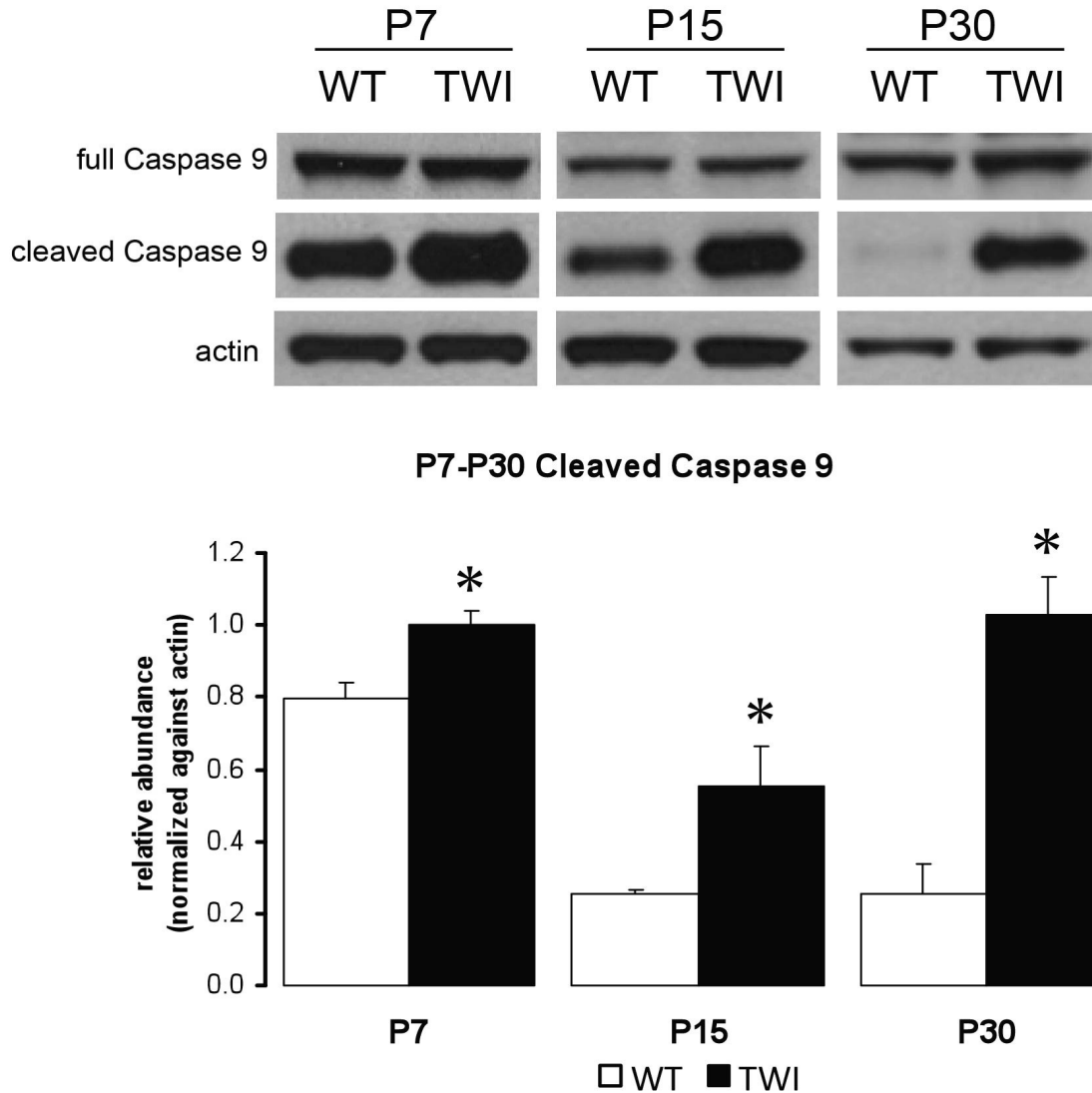


Figure 11 Increased levels of cleaved caspase 9 in the TWI spinal cord. Spinal cords from time-matched TWI and WT were collected and whole homogenates from each segment were analyzed for active-caspase 9 by semi-quantitative western blotting. Caspase 9 was significantly activated at all time points. N=3 animals per genotype. *p<0.05.

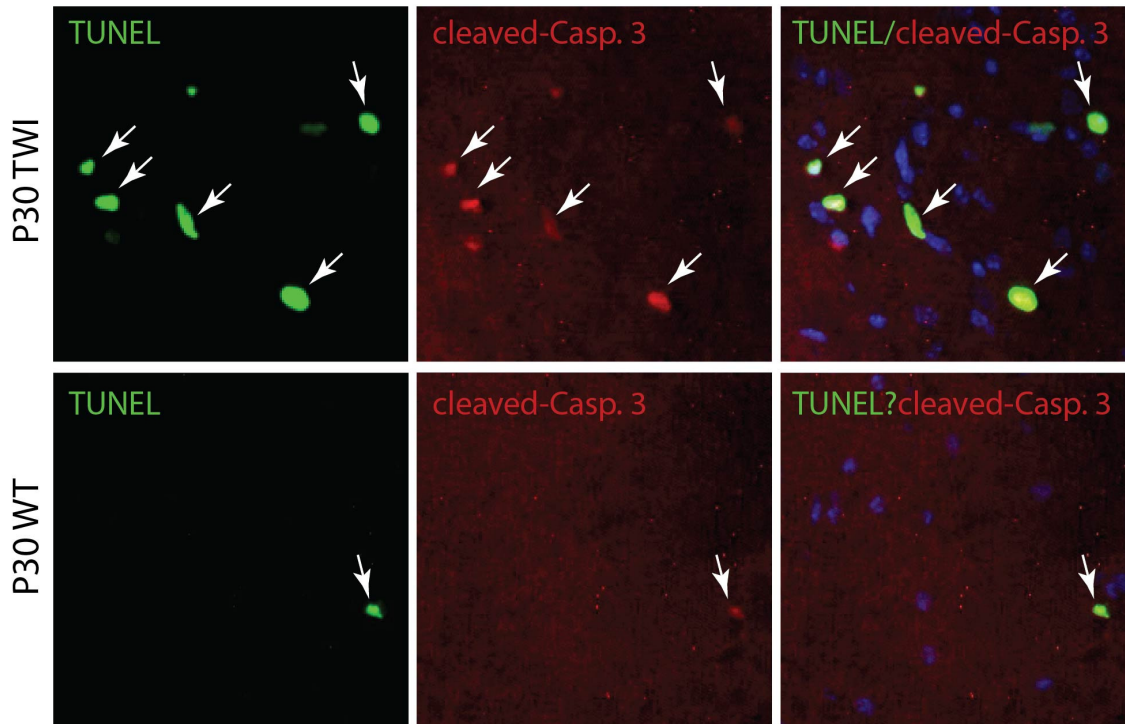


Figure 12 *TUNEL and caspase 3 co-label dying cells in the spinal cord.* Spinal cord sections from age-matched TWI and WT (P30) were cut into 10 μ m sections and stained with the TUNEL assay (in green) in combination with immuno-fluorescence labeling of cleaved caspase 3 (in red). Representative images of ventral white matter are shown. Arrows point to cells co-labeled by both markers.

At P30, while the developmentally regulated apoptosis sharply goes down in WT (only ~0.4% in total cell population), apoptosis is still an active event in TWI during this demyelination stage. The apoptotic cell identifies are further analyzed later on with different cell lineage markers to clarify the role of apoptosis in demyelination. Compared with WT, the total cell population in VWM of TWI spinal cord is significantly increased, which is contributed by the increased gliogenesis (refer to Figure 10) and infiltration of microphages (Figure 16) at P30.

In table II, we show a quantitative analysis of total OGs and myelinating OLs undergoing cell death. Interestingly, ~20% Olig2+ OGs were found to be dying during early postnatal life but less during the sick phase of the disease (Table II). While indeed TUNEL+ OGs were increased in the young TWI tissue (~ 3.1-4.1 fold with respect of WT at P8 and P15), the total numbers of OGs in TWI were kept the same as in the controls in all checked time points. Whereas the proliferation of OPCs can be stimulated by psychosine (Figure 7 and 17), the increase of TUNEL+ OGs could be at least partially contributed by OPCs which cannot compete for axons at early development.

Surprisingly, Olig2+TUNEL+ cells become rare in the P30 TWI cord (Figure 13). It is relevant to note that this happened during a period in the disease when myelin degeneration is established in this mutant and is concomitant with a significant accumulation of psychosine (Table I). To our knowledge, this is the first evidence indicating a process of demyelination in the absence of major death of OLs in the TWI cord. A recent study by Oluich showed that toxin-induced ablation of mature OLs soma would lead to a much delayed demyelination in adult CNS (Oluich et al. 2012). Will earlier increased apoptotic OGs at P8 and P15 contribute to a later demyelination at P30

in TWI? It might be the case if the OL cell bodies are also the major target of the psychosine toxicity instead of their myelin domains. However, it doesn't seem to be favored in our TWI model (refer to Figure 18 and 19). On the other hand, instead of a typical apoptotic cell size shrinkage, morphological characterization of mutant OLs between P33 and P43 revealed an unique swelling pattern that was turned over from myelin sheath, and then moved up along the processes and eventually merged into soma, indicating a dying-back mechanism similarly seen in neuronal degeneration in vivo (LeVine and Torres 1992).

Table II Quantitative Profile of OG and OL Cell Death in the TWI lumbar spinal cord

	Olig2*	TUNEL/ Olig2	Dying OGs (% total)	Dying OGs Fold change (ratio TWI/WT)	LacZ*	TUNEL/ LacZ	Dying OLs (% total)	Dying OLs Fold change (ratio TWI/WT)
P8 TWI	2130 ± 207.4	399 ± 116.8	18.7%	3.1	232 ± 23.7	50 ± 7.5	21.6%	NV
P8 WT	1954 ± 154.7	117 ± 46.3	6.0%		295 ± 57.3	ND	ND	
P15 TWI	1237 ± 226.8	243 ± 47.1	19.6%	4.1	431 ± 69.5	51 ± 18.9	11.8%	NV
P15 WT	1242 ± 187.4	60 ± 45.6	4.8%		659 ± 162.1	ND	ND	
P30 TWI	780 ± 133.2	7 ± 5.1	0.9%	2.3	208 ± 91.8	9 ± 6.4	4.3%	NV
P30 WT	752 ± 86.1	3 ± 3.6	0.4%		272 ± 67.0	ND	ND	

*: cell numbers per mm², n=3 animals per genotype. ND: not detected. NV: not valid.

These findings suggested a lower than expected death of OGs during demyelination stage. To examine the level of cell death in postmitotic myelinating OLs, we measured the density of TUNEL+ OLs labeled by the expression of β -galactosidase (Table II). Surprisingly, dying LacZ+ OLs were abundant in P8 and P15 (21.6% of total LacZ+ OLs at P8 and 11.8% at P15) but much less (4.3% of total LacZ+ OLs) in P30

TWI cords (Figure 14). Here, it has to be noted that immunofluorescent labeling for β -galactosidase is much less sensitive than histochemical labeling for β -galactosidase activities, for example, β -galactosidase+ OLs is only observed as 10% in comparison with Olig2+ OGs while X-gal+ OLs is observed ~ 30% in comparison with Olig2+ OGs at P8 (refer to Figure 4 and 7).

We also examined the temporal distribution of TUNEL+GFAP+ astrocytes, as these cells are greatly activated during the disease. We found increased numbers of dying astrocytes in P8 and P15 cords (table III and Figure 15). Dying astrocytes were less frequent in the P30 cord, which might be a result of the overall reduction of total TUNEL+ cells from P15 to P30. However, TUNEL+ astrocytes would take 25% of the total apoptotic cells at P30 (with reference to table I).

Table III Quantitative Profile of Astroglial Cell Death in the TWI lumbar spinal cord

	GFAP*	TUNEL/ GFAP	Dying AST (% total)	Dying AST Fold change (ratio TWI/WT)
P8 TWI	1378 ± 196. 1	359 ± 39. 2	26.1%	2.5
P8 WT	1402 ± 213. 4	145 ± 6. 7	10.3%	
P15 TWI	1231 ± 222. 1	246 ± 80. 9	20.0%	2.6
P15 WT	1526 ± 290. 7	117 ± 49. 1	7.7%	
P30 TWI	914 ± 126. 7	42 ± 7. 4	4.6%	7.7
P30 WT	814 ± 82. 3	5 ± 7. 2	0.6%	

*: cell numbers per mm², n=3 animals per genotype.

Because globoid cell formation is one major hallmark in KD, we examined whether microglia/macrophages were also undergoing cell death. Activated

microglia/macrophages were identified by labeling with isolectin IB4. IB4 staining showed modest levels in wt spinal cords (Figure 16). In contrast, IB4 immunostaining was dramatically elevated in the TWI cord at P30 (Figure 16). IB4 was strongly found along the edge of the white matter and pia mater, suggesting an active infiltration of macrophages. Unexpectedly, IB4+ cells showed to be TUNEL+, suggesting that an active process of apoptosis in TWI microglia/macrophages at this stage, which account for 65% of total TUNEL+ cells during the sick phase of the disease (Table I and IV).

Table IV Quantitative Profile of Microglia/macrophage Cell Death in the TWI lumbar spinal cord

	IB4*	TUNEL/IB4	Dying microglia/macrophage (% total)	Dying microglia/macrophage Fold change (ratio TWI/WT)
P8 TWI	ND	ND	ND	NV
P8 WT	ND	ND	ND	
P15 TWI	689 ± 188.3	114 ± 13.2	16.5%	NV
P15 WT	ND	ND	ND	
P30 TWI	889 ± 119.2	110 ± 19.0	12.4%	NV
P30 WT	147 ± 16.9	ND	ND	

*: cell numbers per mm², n=3 animals per genotype. ND: not detected. NV: not valid

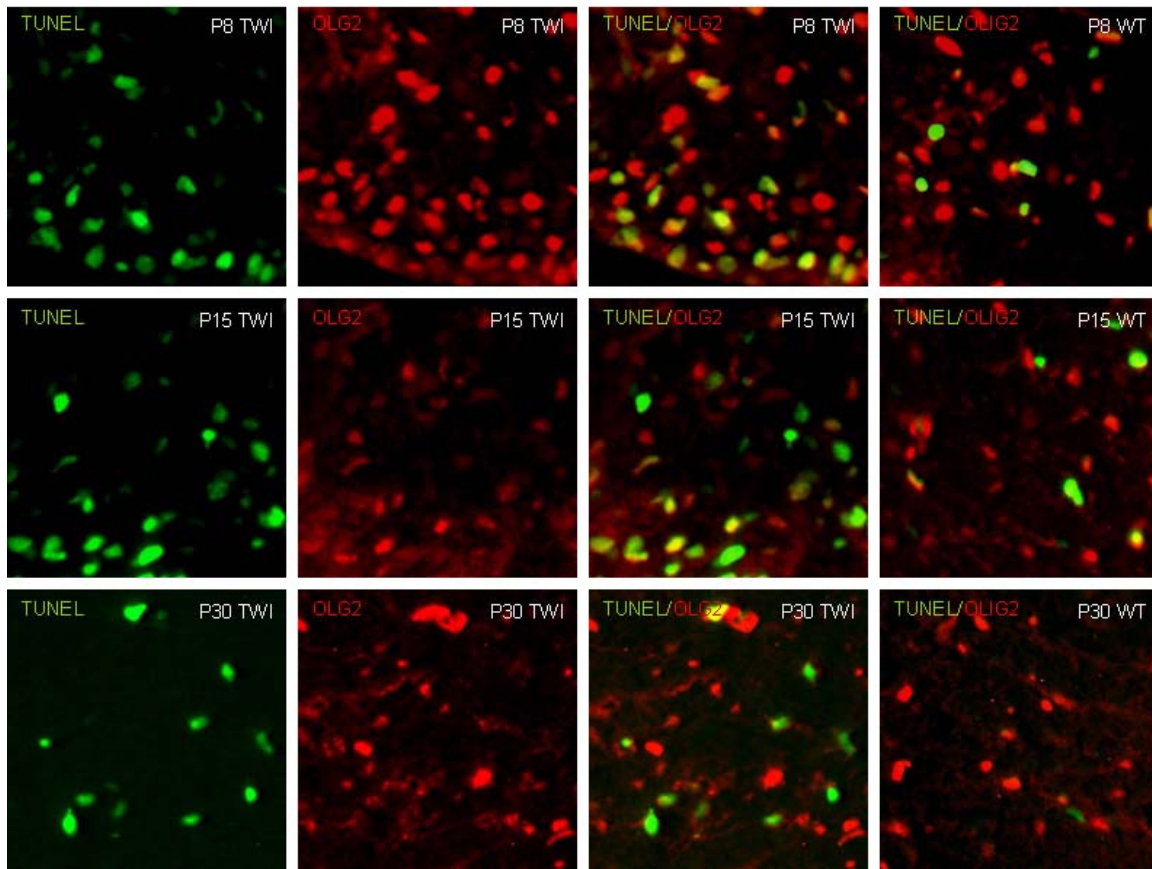


Figure 13. *Olig2+/TUNEL+ cells are found in the TWI spinal cords.* Sections from spinal cords collected from age-matched P7, P15, P30 TWI and WT mice were double stained for TUNEL (green) and Olig2 (red).

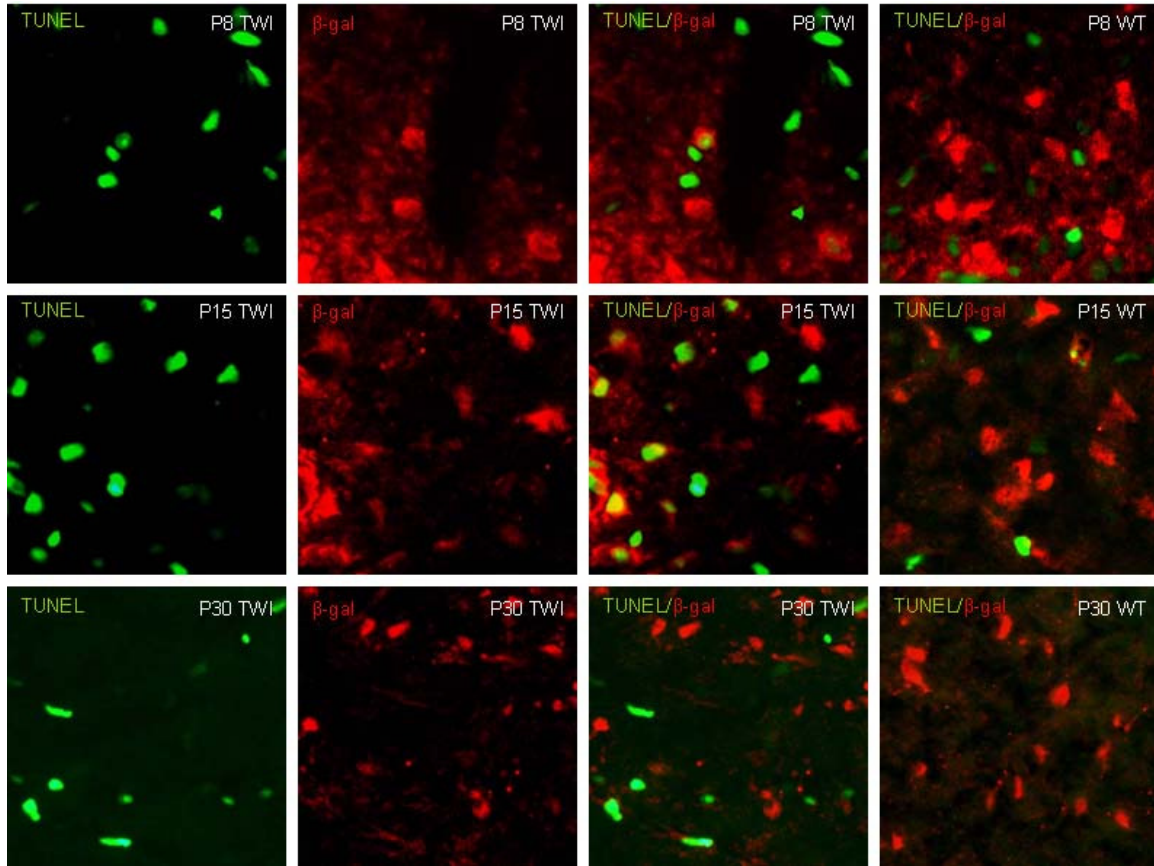


Figure 14. *LacZ*⁺/*TUNEL*⁺ cells are found in the TWI spinal cords. Sections from spinal cords collected from age-matched P7, P15, P30 TWI and WT mice were double stained for TUNEL (green) and LacZ (red). LacZ⁺ cells were rarely labeled by the TUNEL assay in the P30 mutant cord.

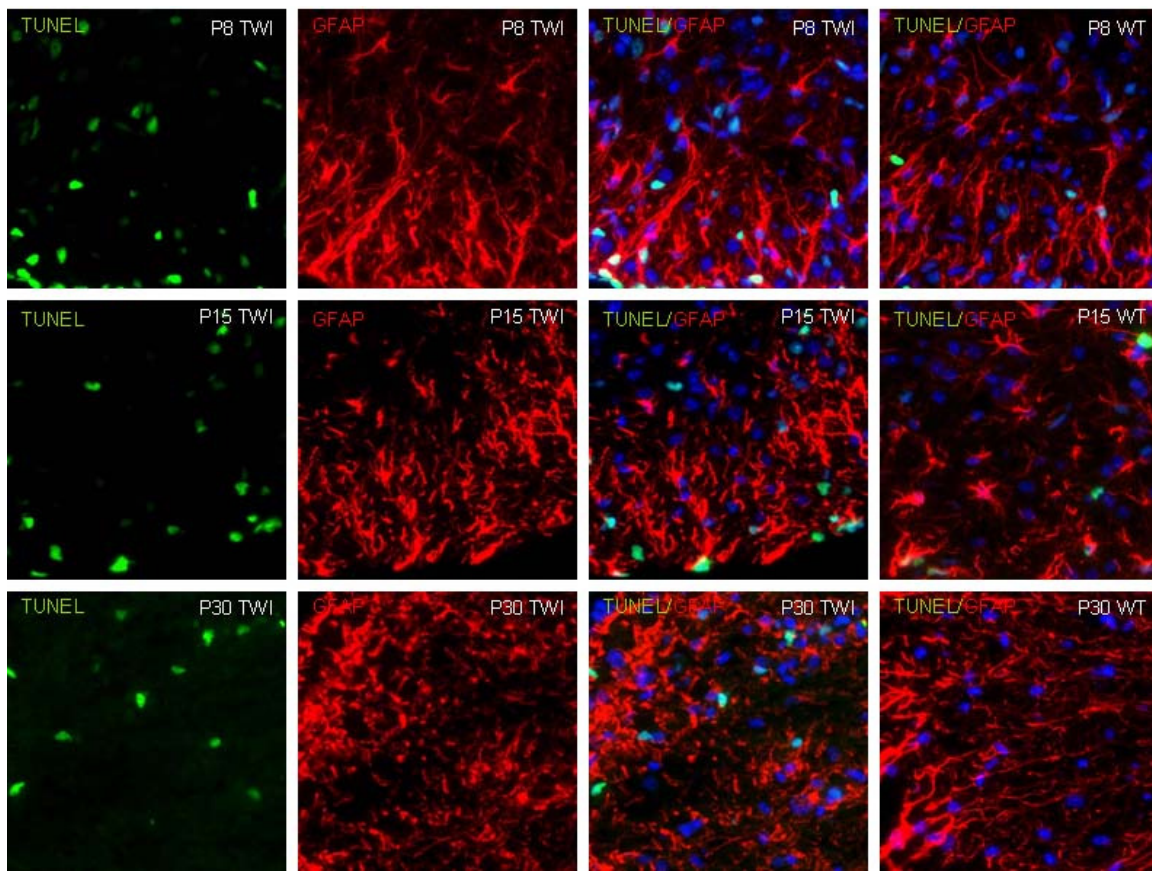


Figure 15. *GFAP⁺/TUNEL⁺ cells are found in the TWI spinal cords.* Sections from spinal cords collected from age-matched P7, P15, P30 TWI and WT mice were double stained for TUNEL (green) and GFAP (red).

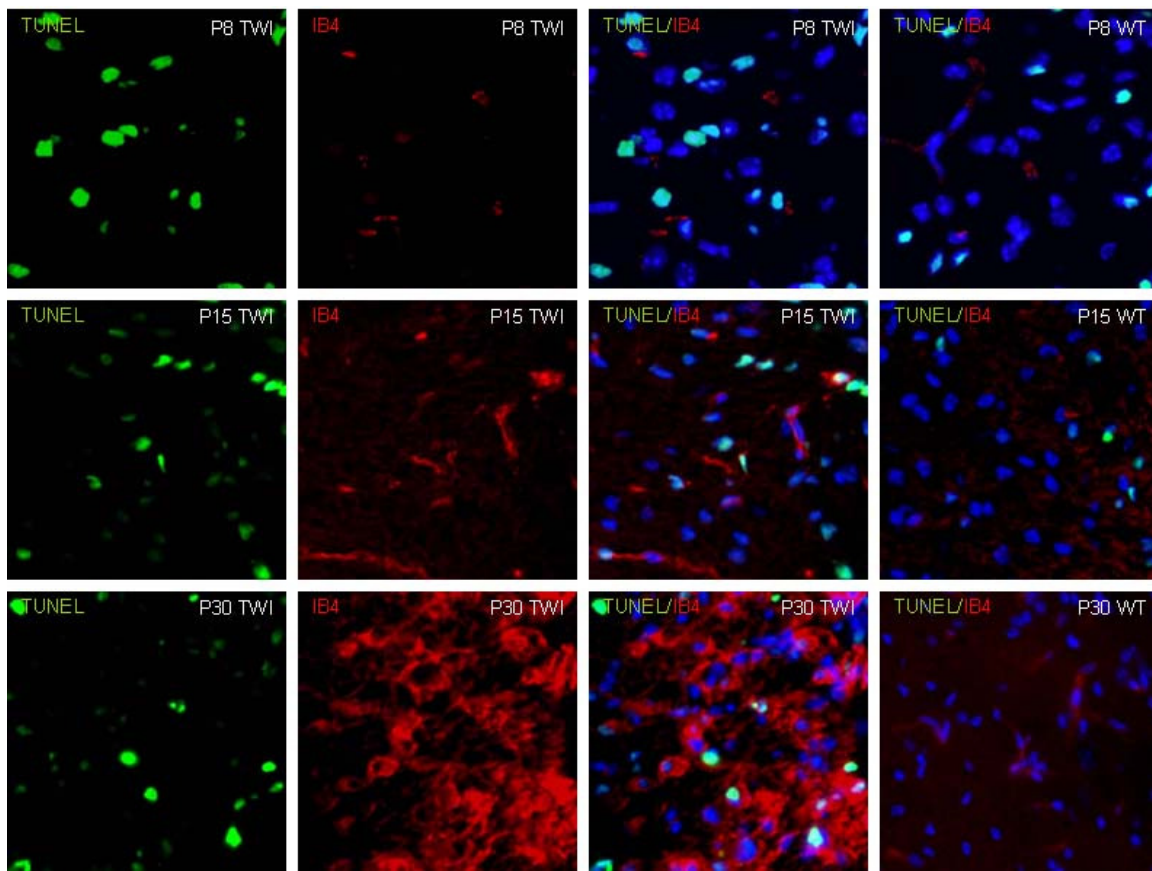


Figure 16. IB4+/TUNEL+ cells are found in the TWI spinal cords. Sections from spinal cords collected from age-matched P7, P15, P30 TWI and WT mice were double stained for TUNEL (green) and IB4 (red). A significant number of TUNEL+ cells were co-labeled by IB4.

5.7 Psychosine appears to have proliferative and anti-survival properties on CG4 cells depending on its concentration. Our in vivo quantitative studies revealed apparent paradoxical effects present in the oligodendrocyte lineage: during early days, there is increased oligodendrogenesis in the TWI cervical spinal cord; however, as disease progresses, a fraction of oligodendroglial cells die. What is changing during this transition? One obvious change is a progressive increase in psychosine. To test if psychosine alone can modulate proliferation vs survival in OLs, CG4 cells were exposed to various concentrations of psychosine. As shown in Figure 17A, psychosine drastically decreases cell survival at concentrations $\geq 1\mu\text{M}$. No CG4 cells survived beyond 72 hours in the presence of $5\mu\text{M}$ psychosine. Surprisingly, CG4 cells survived well when exposed to 100nM psychosine. However, concentrations of psychosine below 50nM promoted the proliferation and survival of CG4 cells in culture (Figure 17B). This effect quickly disappeared above 100nM . These data are interesting and pose the problem that psychosine may exert differential and counteracting effects at any time point in disease. In other words, depending on the stage of differentiation and the amount of psychosine reached, there could be OPC proliferation, demyelination and death of mature OLs, all happening at the same time.

5.8 Psychosine initial damage to OLs seems to involve a retraction of cellular processes. In our previous experiment, we noticed that the most evident effect of large amounts of psychosine on CG4 cells was to induce a retraction of cellular processes. We investigated this in more detail using acutely enriched mouse OLs isolated from primary glial cultures. OLs were shaken off and plated in low density before psychosine was

added. Psychosine was added at 1 and 2 μM and D-sphingosine was used as a lipid control. Cells were incubated for 1 h before mitochondrial activity was evidenced by MTT staining. Figure 18A shows that either vehicle-treated or D-sphingosine-treated OLs showed classic spider-like morphologies, with abundant MTT+ mitochondria within cellular processes. Cells were alive, as evidenced by the MTT assay. Instead, incubation of OLs with increasing amounts of psychosine induced a rapid retraction of cellular processes and an accumulation of mitochondria within the OL cell body (Figure 18A). Of relevance, cell death (measured as loss of MTT reaction) was still very low if any. Longer incubation times led to massive cell death (not-shown). Similar cellular changes were observed when murine OPCs were incubated with psychosine (Figure 18C). However, astrocytes were completely devoid of any noticeable morphological change (Figure 18B).

5.9 Enrichment of psychosine in myelin membranes. The previous results suggested that the first target of psychosine damage might be the cellular process rather than the OL cell body. These data beg for the question whether psychosine has a differential accumulation within the OL cell. To address this, we aimed to determine the relative amount of psychosine concentration in the myelin fraction isolated from the TWI brain and that isolated from enriched TWI OLs. First, we attempted to isolate mature OLs directly from the TWI brain (P30) using a Percoll method but the enrichment in OLs was below our needs for accurate measurement of psychosine. To cope with this limitation, we decided to compare the total amount of psychosine in whole brain homogenates from TWI with enriched myelin membranes isolated from TWI brains. Figure 19 shows

quantitative data indicating an enrichment of psychosine in the myelin fraction during disease progress. A previous experiment performed by Ludovico Cantuti demonstrated that TWI OLs -shaken off two weeks after establishment of primary glia cultures from P2 mutant brains accumulated psychosine to ~10 pmol/mg of protein (Cantuti et al., 2011, Figure 6). These OLs are equivalent to those that could be found in a two-week old brain. Considering the great limitations of this comparison, one could then speculate that for example at P15, psychosine is at least ~8 times concentrated in myelin membranes than in OL cell bodies in the TWI brain. These analyses provide an unexpected scenario where demyelination may be initiated at the myelin domain first, then eventually reaching and killing the OL cell body.

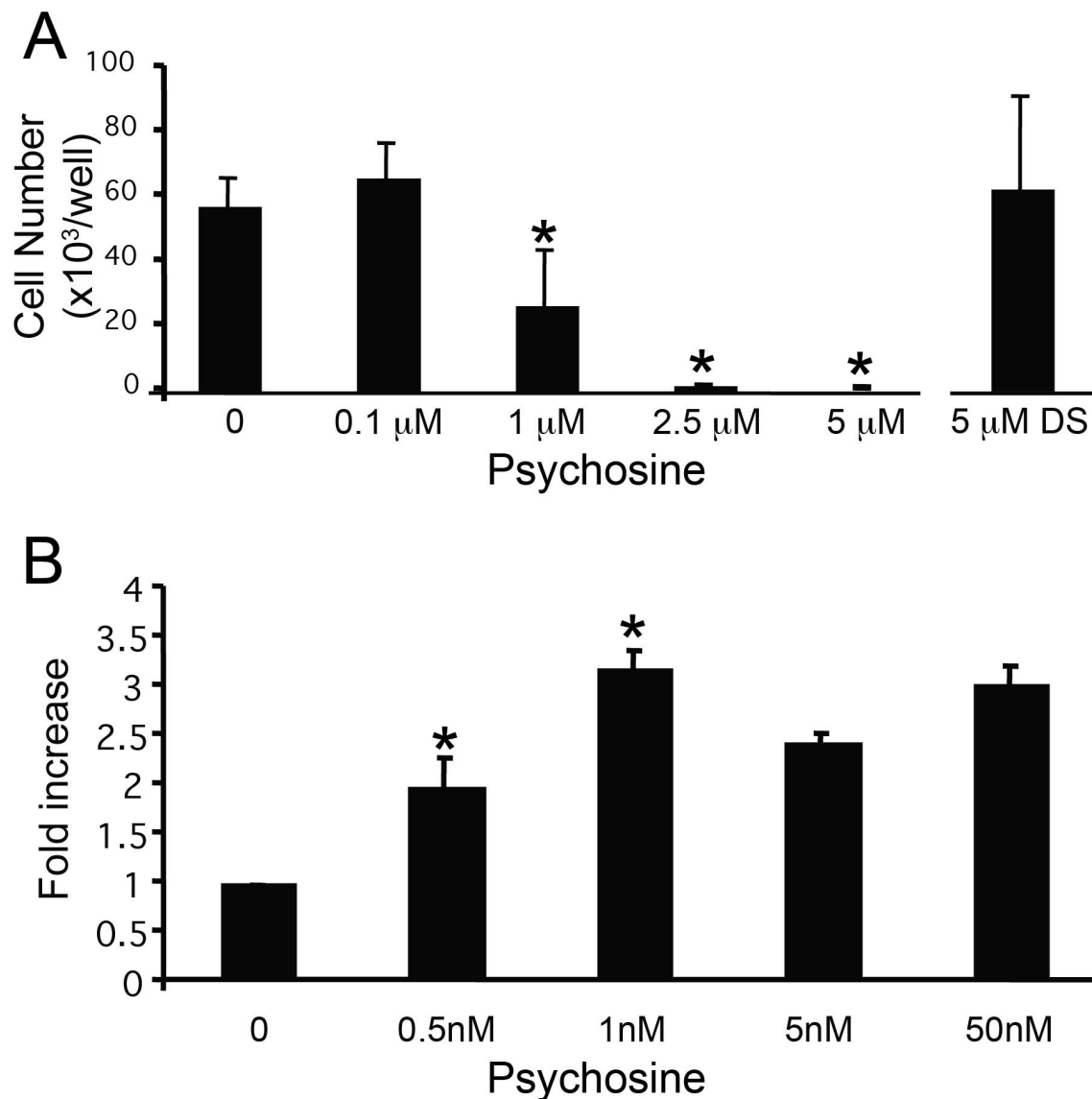


Figure 17. Effects of psychosine on proliferation and survival of CG4 cells. A, B) CG4 cells were plated at a density of 20,000 cells/well and cultured in proliferating media containing increasing concentrations of psychosine for 72 hours. Total number of surviving cells were counted by trypan blue stain. 0=control no psychosine added; DS=D-sphingosine (a control lipid). N=3-4 individual experiments. * $p < 0.05$.

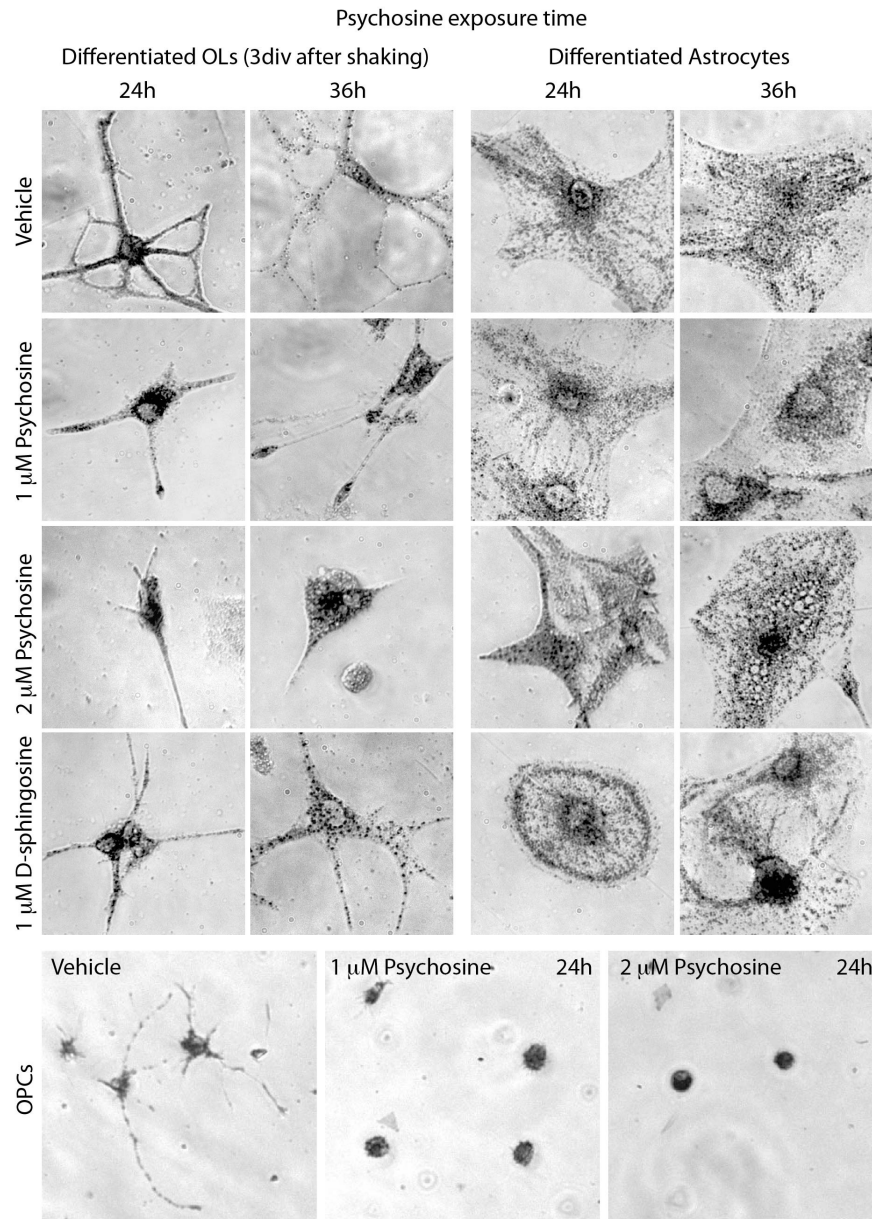


Figure 18. Psychosine promotes cell process retraction in oligodendrocytes. A, B) Mouse primary glial cultures were established from neonatal mouse cortices and differentiated for 2 weeks before shaking off of oligodendrocytes (OLs) and astrocytes. Cells were plated and further differentiated for 3 days before addition of psychosine or D-sphingosine. Survival was evaluated by the MTT staining. Psychosine-treated OLs showed shorter cellular processes already 24 hours after treatment (arrow), which almost completely disappeared by 36 h (arrow). Astrocytes did not show any morphological change. C) OPCs were prepared by shaking glial cultures at 7 days and further maintained in proliferative conditions. Similar process retractions were observed after 24 h of treatment with psychosine.

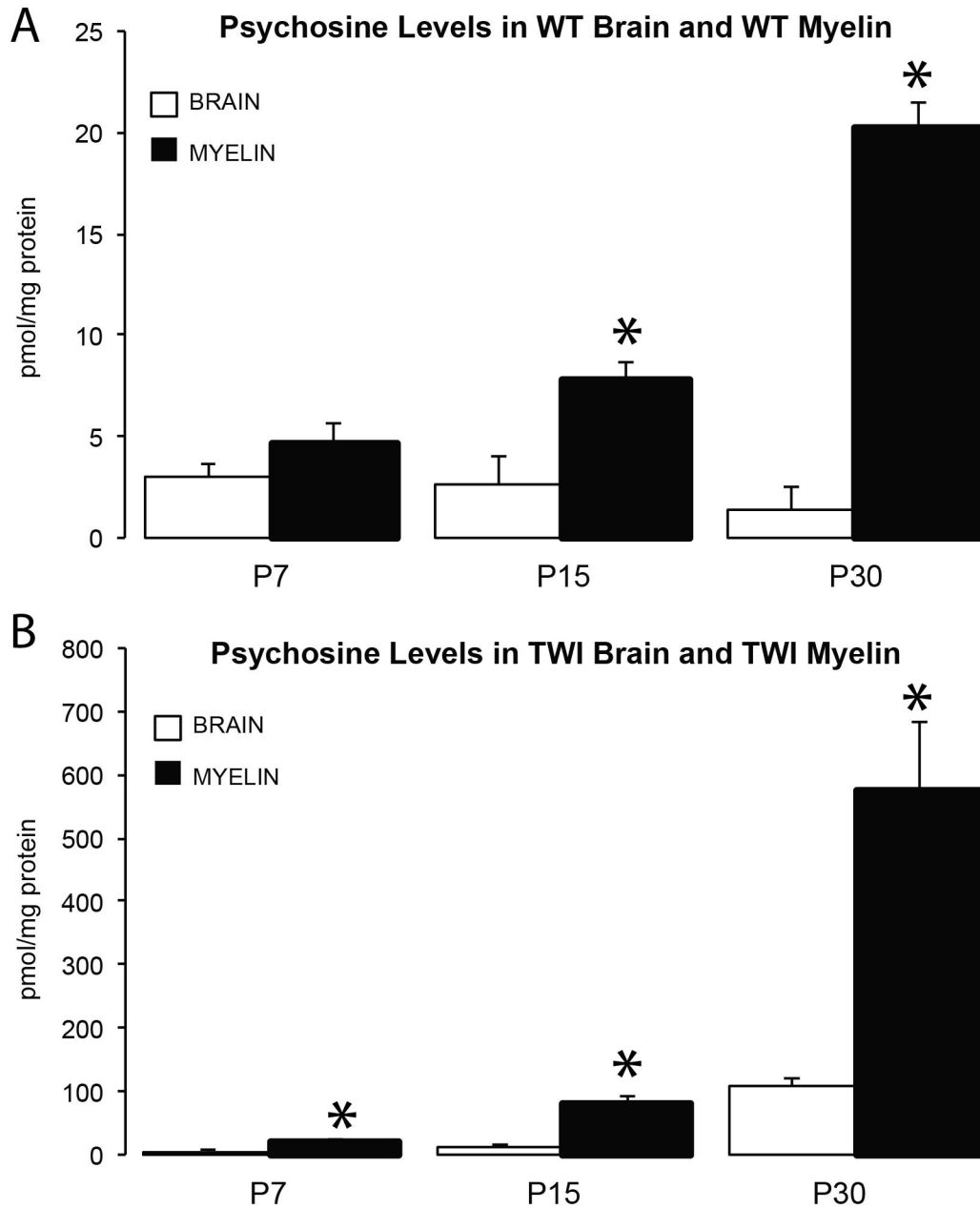


Figure 19. Enrichment of psychosine in myelin. Psychosine was quantified in extracts from total brain and brain myelin from age-matched WT (A) and TWI (B). Psychosine showed significant enrichment in both WT (A) and TWI (B) myelin fractions. N=3 animals per genotype. * $p < 0.05$.

RESULTS PERTINENT TO SPECIFIC AIM 2

5.10 Unexpected psychosine accumulation profile in the nervous system during embryonic development. The previous experiments provided new insights in how oligodendroglial cells respond during the disease and how psychosine may be capable of modulating proliferation vs survival. In the next sections, our interest will focus on investigating for changes in oligodendrogenesis in the embryo and whether or not psychosine may be responsible for these.

We speculated that given the fact that KD is an autosomal recessive genetic disease, the lack of GALC enzyme activity would lead to psychosine accumulation also in the embryonic neural tube development. To test this hypothesis, we quantified psychosine levels in both the brain and spinal cord of E10.5, E12.5 and E15.5 embryos. Interestingly, while psychosine was found in the TWI fetal neural tube at each developmental stage (Figure 20), its progressive accumulation was only seen in the mutant spinal cord. However, psychosine levels were more or less constant at about 10pmol/mg in TWI brain. Unexpectedly, we found that psychosine levels in the WT brains followed a complete different pattern. Psychosine showed highest levels in E10.5 neural tissue (even higher than in the corresponding age-matched TWI samples) and was reduced to trace levels in E15.5 WT tissues (Figure 20). While the reasons for this pattern of psychosine levels in WT are still unclear, these results show that at a developmental time when psychosine should be turned off in the brain (E15.5), TWI embryos have accumulated already ~10 times respect controls.

5.11 Subtle changes in oligodendrogenesis in the embryonic TWI spinal cord. To determine for changes in the generation of OPCs in the TWI spinal cord, OPCs were identified by immunolabeling with anti-Olig2 antibodies and stereological quantification. Figure 21 displays a composite of images showing the localization of Olig2+ OPCs in the cervical regions of the embryonic neural tube at E10.5, E12.5 and E15.5. At first sight, no major differences in distribution or cell density are obvious between the TWI and WT at any embryonic time point (Figure 21). Stereological measurement of the OPC density in cervical regions of the neural tube at each stage showed no significant differences among both groups, although a minor decrease in mutant OPCs in the E10.5 cord (Figure 22). However, a closer look at the E12.5 time point showed higher numbers of Olig2+ OPCs within the mantle layer of the mutant neural tube, in comparison with age matching WT (arrows in Figure 21 and Figure 23A). To examine this observation in more detail, we performed a differential stereological quantification of OPCs in the mantle layer (area where new born OPCs migrate to) and in the pMN (sites where OPCs are born) of the neural tube from E12.5 embryos. Quantitative analysis showed a significant increase in the number of Olig2+ OPCs present in the mantle area of the mutant neural tube at this embryonic stage (Figure 23B). While the number of OPCs in the mutant pMN appears to be higher than in the WT pMN, this difference was not statistically significant (Figure 23B). Furthermore, not only there were more OPCs in the mutant mantle layer but also many appeared to migrate longer distances (Figure 23C). Morphometric measurements showed that the migrated distances of OPCs were significant only in cervical regions of the mutant neural tube but not in lumbar regions (Figure 23C).

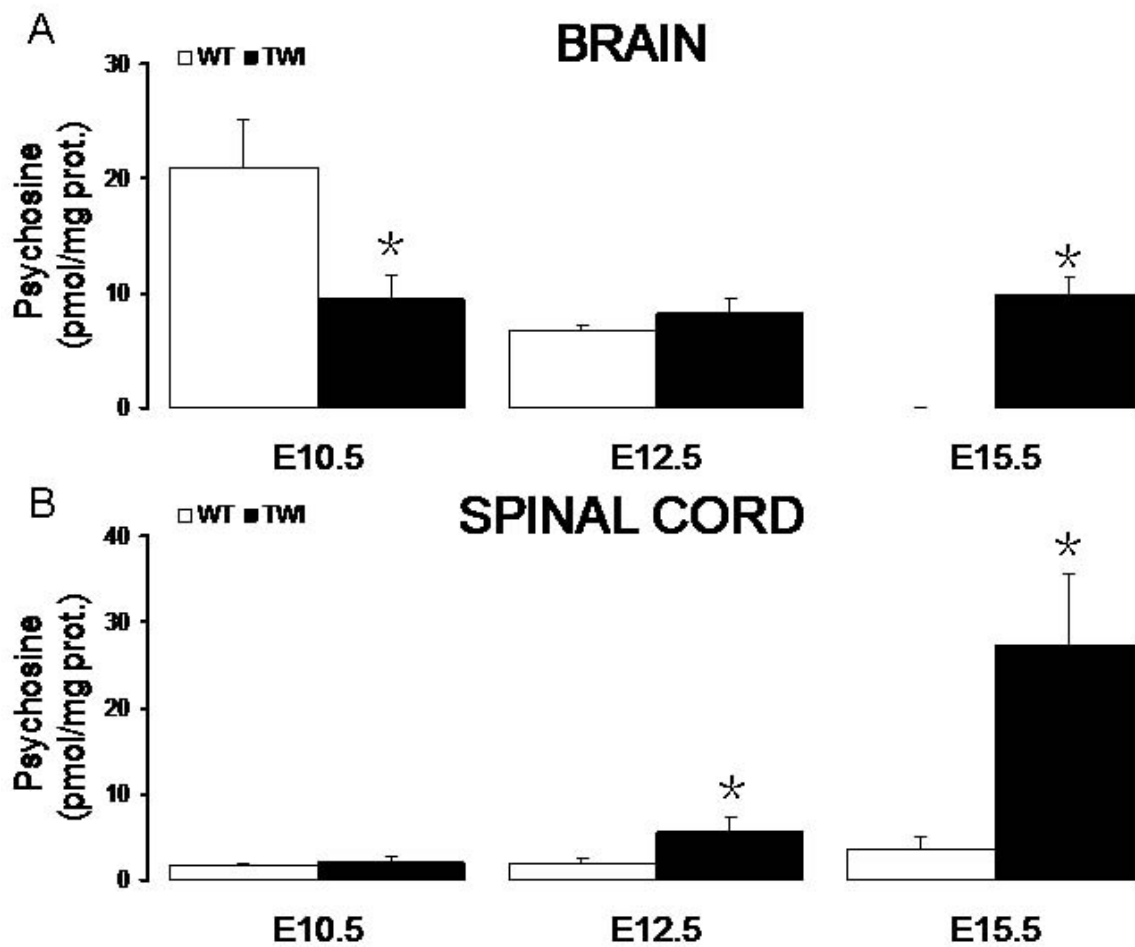


Figure 20. Psychosine is present in the CNS of the mouse embryo. A, B) Psychosine was quantified in the brain (A) and spinal cord (B) from E10.5, E12.5 and E15.5 WT and TWI embryos (n=3 per time point per genotype). N=3 animals per genotype. *p<0.05.

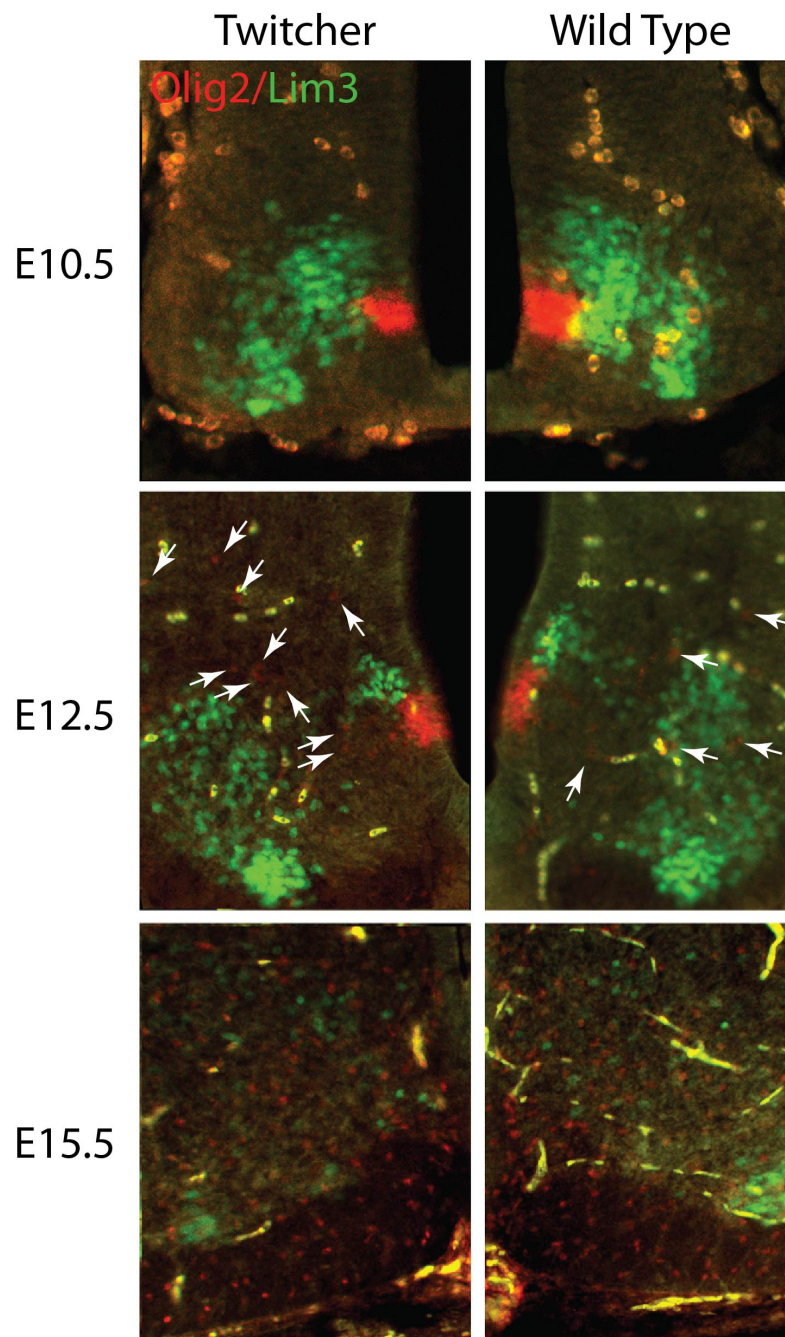


Figure 21. *Subtle changes in oligodendrogenesis in embryonic TWI spinal cords.* Whole-mounted TWI and WT embryos were cross sectioned and stained for Olig2 and Lim3 (to mark motorneurons). No gross differences were seen, except that an apparent increase in Olig2+ cells in the mantle of E12.5 TWI cords (arrows).

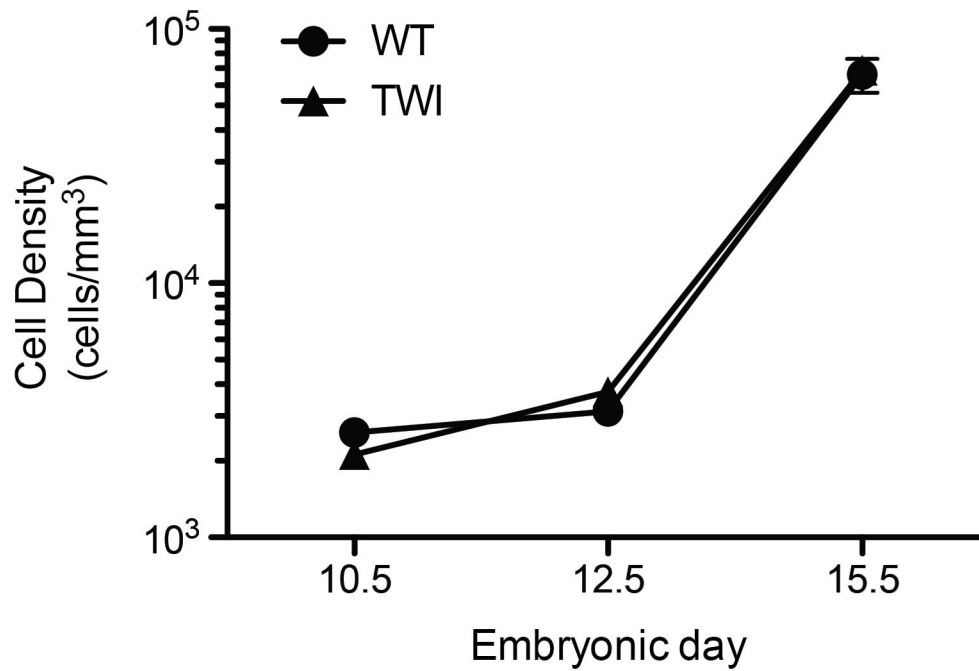


Figure 22. Distribution of Olig2+ OPCs in embryonic mutant spinal cords. Cross sections of E10.5, E12.5 and E15.5 WT and TWI embryos were stained for Olig2. Olig2+ OPCs were quantified using stereology. The graph shows that overall there were no significant differences between WT and TWI embryos. E10.5 TWI cords showed a tendency to have lower Olig2+ OPCs than controls but without significance. N=3 animals per genotype.

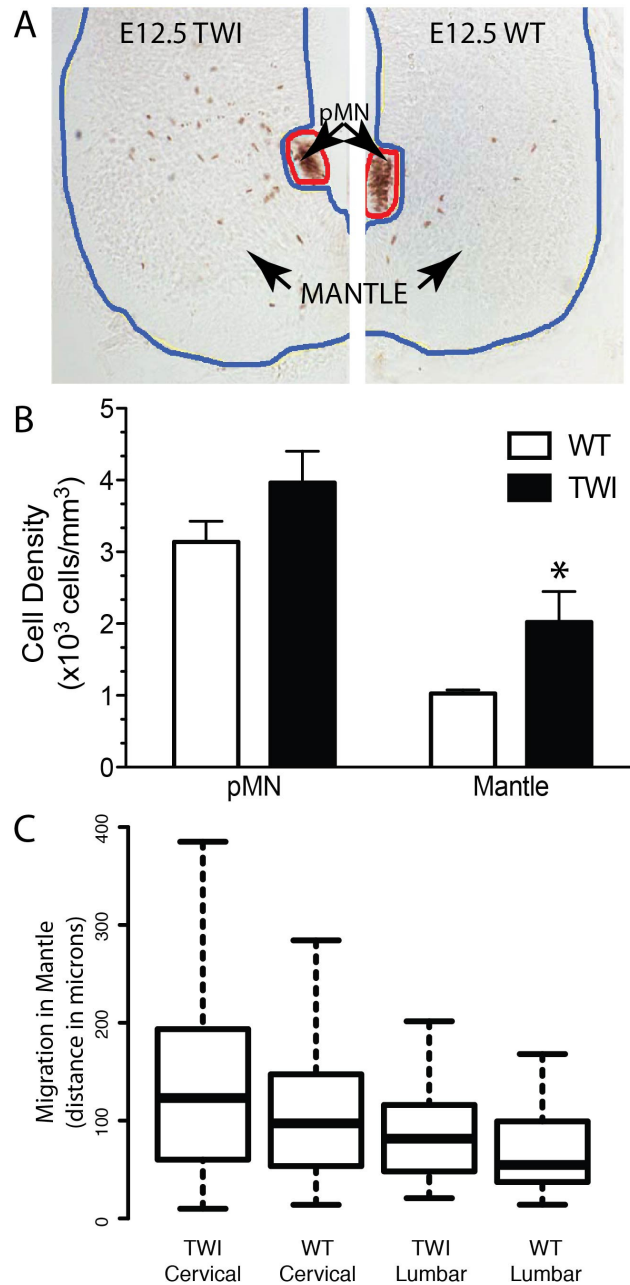


Figure 23. More *Olig2*⁺ cells within the mantle region of the E12.5 TWI cord. Sections of E12.5 WT and TWI embryos were stained for *Olig2*. *Olig2*⁺ cells were stereologically quantified in the mantle and in the pMN site (i.e. the sites where OPCs are born). **A**) Representative images of TWI and WT *Olig2*⁺ distribution. **B**) Density of *Olig2*⁺ cells at the pMN and at the mantle regions were quantified. pMN cell density was higher in the TWI but with no significance. However, more *Olig2*⁺ cells were contained in the mutant mantle region. **C**) Migration of *Olig2*⁺ cells was measured in cervical and lumbar segments. TWI OPCs migrated more in cervical regions of the cords. N=3 animals per genotype. * $p < 0.05$.

Because OPCs are generated from stem cells in response to SHH, we first speculated that the increase in OPCs detected in the E12.5 TWI cord might be caused by abnormal activity of this pathway. To attempt addressing this possibility, we examined the pathway at different levels (Figure 24A). Using immunoblotting semiquantitative analyses, we found that there were not significant differences in the overall levels of the active form of SHH (nSHH) in the TWI cord at any time point in this study (Figure 24B). Furthermore, the relative abundance of the phosphorylated form of SMO, activated upon SHH binding to its receptor complex PTC-SMO, in the mutant cord was also similar to that found in WT tissue (Figure 24C). The levels of PTC, the other components of the receptor complex for SHH, were also similar in both mutant and WT embryos (not-shown). By immunohistochemistry and confocal analysis, we only detected an enlarged SHH domain in the floor plate of the TWI mutant cord at E10.5, in comparison to that observed in the WT cord (Figure 25). This SHH domain widening was not noticeable at later embryonic stages (Figure 25). However, GLI1 was more abundant in the TWI cord than in WT cord at E12.5, suggesting that the transduction of the SHH signal was somehow exacerbated in the mutant cord (Figure 26A, 26B). In fact, when we quantified the abundance of other downstream targets of SHH activity such as PDGFR α and Nkx2.2, which mark newly nascent OPCs, both proteins were significantly increased in the TWI cord at E12.5 (Figure 26A, 26C, 26D), coinciding with the transient increase in distribution of Olig2+ OPCs observed in age matching mutant embryos (Figure 23).

One possible interpretation of these results is that early progenitors have an enhanced response to this pathway, facilitating downstream effectors of the SHH. Because previous studies in the Bongarzone lab showed that psychosine accumulates in

lipid rafts, where it may exert changes in membrane architecture and function, we speculate that psychosine may be facilitating the transduction of SHH signals at the receptor level, without changes in stoichiometry of the system. To examine whether psychosine is capable of enhancing SHH signal, we isolated embryonic neural stem cells from the neural tube from E10.5 WT embryos and exposed to conditions where SHH was added exogenously in the presence of psychosine. Figure 26E shows that under these conditions, expression of Olig2, a direct downstream target of SHH, is slightly increased. This was accompanied by a more significant increase in the expression of PDGFR- α (Figure 26F).

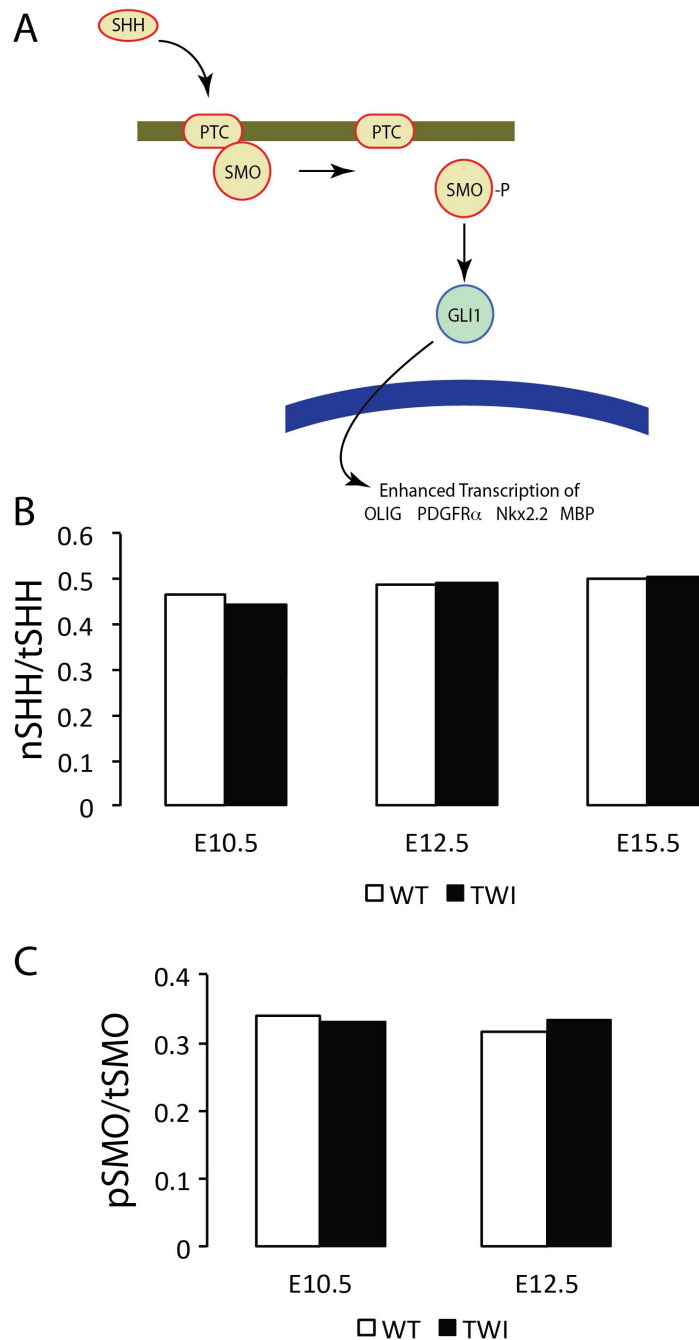


Figure 24. Sonic Hedgehog (SHH) ligand and receptor seem unaffected in TWI embryos. A) Illustration showing the major components of the SHH signaling pathway. B) Semi-quantitative immunoblotting was used for measuring for changes in the abundance of active SHH (nSHH) and phosphorylated SMO (pSMO). After normalization against levels in WT cords, we found no significant differences in expression levels of each of these components of the pathway. N=3 animals per genotype.

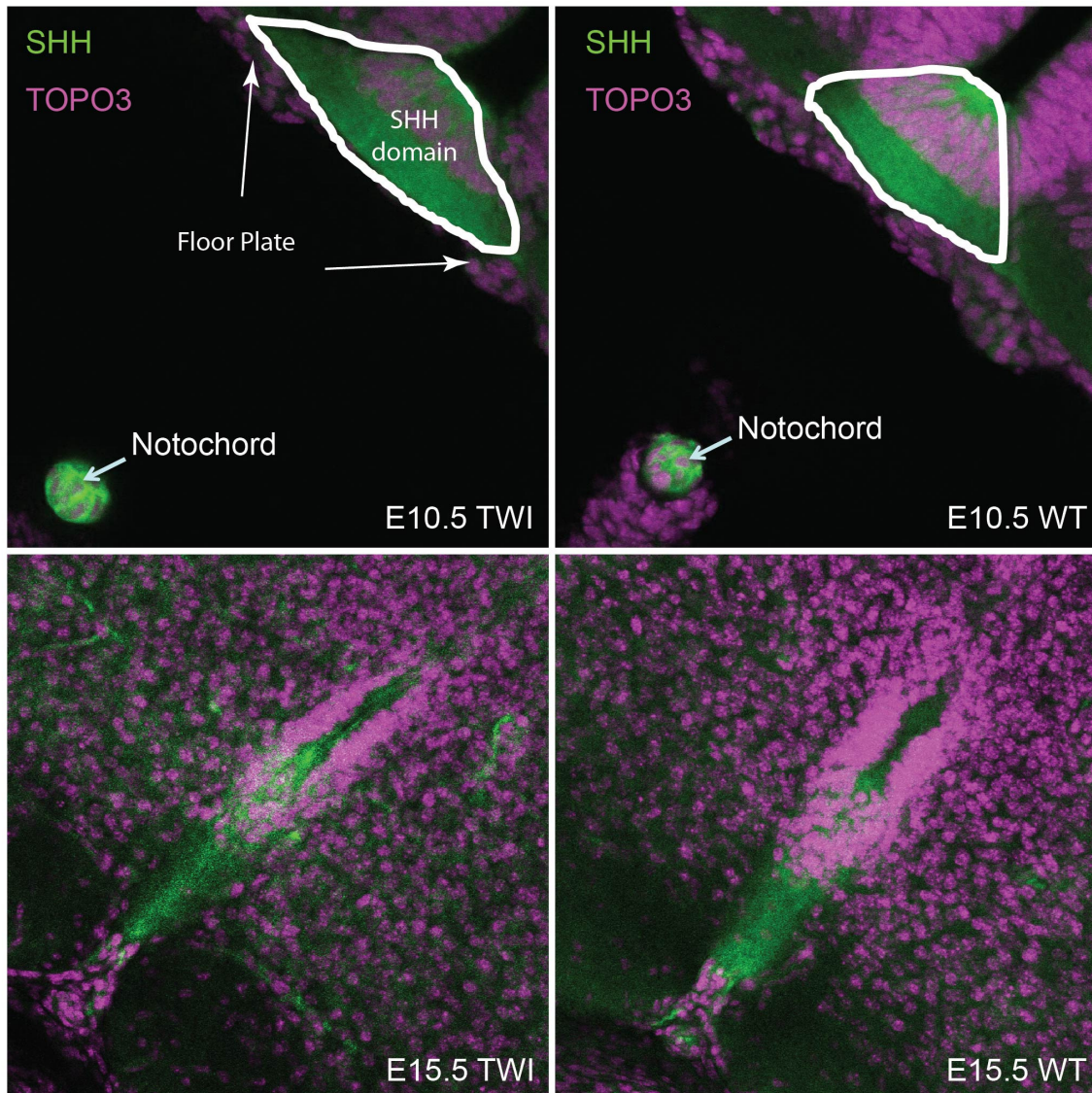


Figure 25. *The floor plate SHH domain is enlarged in TWI cords at E10.5.* Using immuno-fluorescence labeling and confocal microscopy, a visible wider SHH domain was detected in the floor plate of E10.5 TWI embryos.

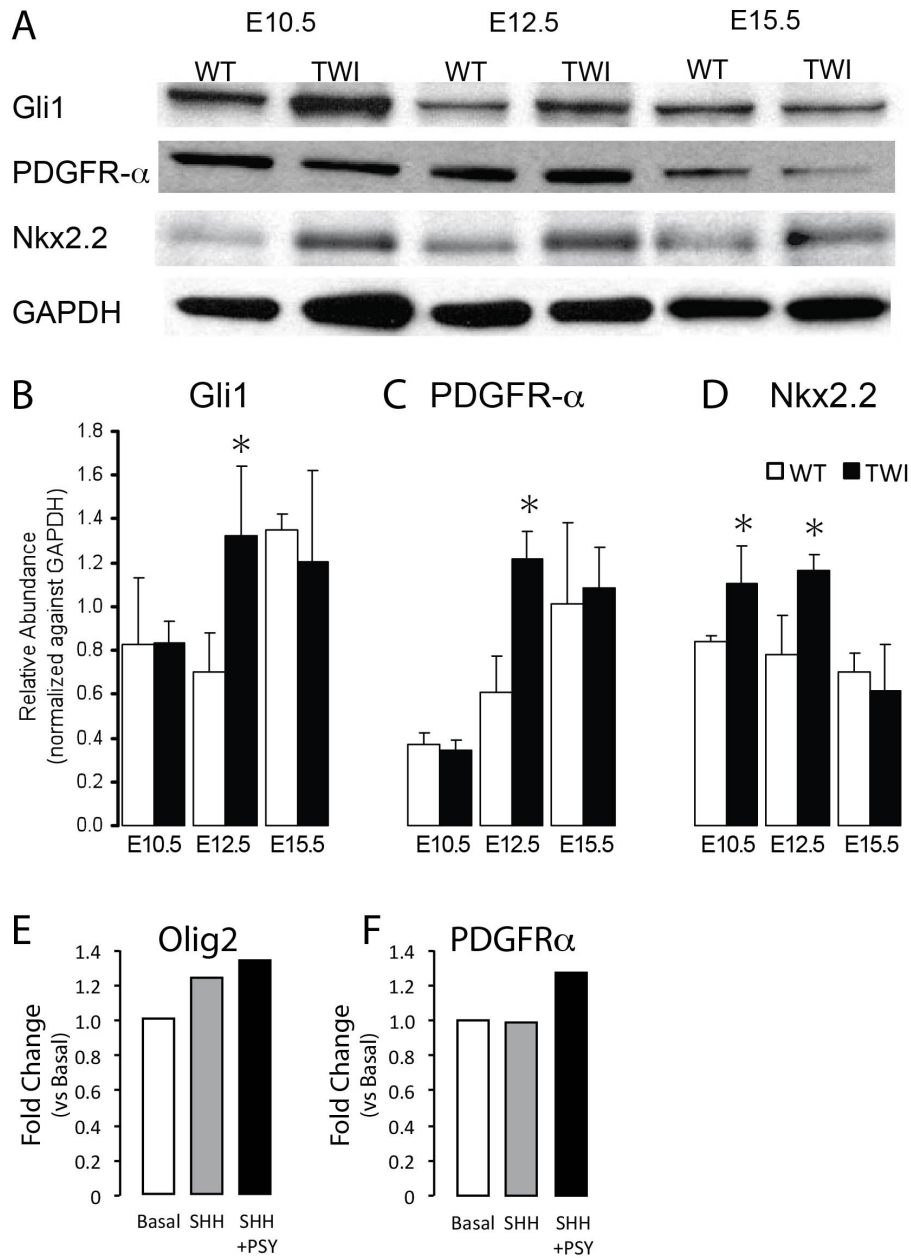


Figure 26. Analysis of SHH effector *Gli1* and downstream target genes *PDGFR- α* and *Nkx2.2*. A) Representative images of western blots for *Gli1*, *PDGFR- α* , *Nkx2.2* and actin. B-D) *Gli1*, *PDGFR- α* and *Nkx2.2* showed significant increases of their relative abundance in the E12.5 TWI spinal cord. N=3 animals per genotype. P<0.05. E-F) Neural stem cells were isolated from E10.5 WT cords and exposed SHH in the presence or absence of 100 nM psychosine. Cells were collected after 3 days and *Olig2* and *PDGFR- α* were semi-quantitated by western blot analysis. Cells stimulated with SHH and SHH with psychosine showed increases in the expression of these two downstream effectors of the SHH pathway. N=2.

CHAPTER 6

DISCUSSION

The work presented in this dissertation provides for the first time an alternative understanding on the pathogenesis of demyelination in KD. We were able to quantify lower-than expected decreases of myelinating OLs during the postnatal life of the TWI mouse, which appear to lack correlation with the sharp increase in psychosine and the diffuse loss of myelin. In addition, we detected temporary changes in embryonic oligodendrogenesis. Considering the overall results of this work within the context of demyelination, we propose that the TWI mouse develops a type of glial-back demyelinating pathology, where myelin is first damaged and OLs die after. In addition, our results provide evidence for a potential role of psychosine in early oligodendrogenesis, likely as a modulator of the SHH pathway during early embryogenesis. In the following sections, we will discuss the possible mechanisms contributing to demyelination and oligodendrogenesis and propose future experimental questions.

Aim 1- To measure for psychosine effects on proliferation, maturation and death of postnatal TWI OLs.

A significant portion of this work was based on the morphometric quantification of OLs during postnatal life in a mouse model of KD. To label myelinating OLs, we crossed the TWI line with the 18.2 MBP-LacZ transgenic. The 18.2 MBP-LacZ parental transgenic line was originally generated by Dr Wrabetz (Wrabetz et al. 1998). This line carries the expression of the LacZ reporter gene under the control of 750bp of the

proximal promoter for the human MBP gene. This transgene efficiently marks OLs in a developmentally regulated manner (Wrabetz et al. 1998). In fact, β -galactosidase expression parallels the transcription of the endogenous MBP gene during postnatal myelinogenesis. Our in vitro studies further demonstrated that the transgene was only activated when oligodendroglia matured into O4+ and O1+ OLs but not in early A2B5+ OPCs. This indicates that in vivo, myelinating OLs will be LacZ-marked. In fact, quantitative studies further confirmed a developmental regulation of the reporter gene in the spinal cord of WT mice, with a peak of LacZ+ OLs (and also of β -galactosidase expression) detected around postnatal day 15, and decreasing by P30, consistent with kinetics described for the mouse myelinogenesis (Shiota et al. 1989; Trapp et al. 1987; Verity and Campagnoni 1988). The value of this transgene line is more limited after forty days of age, particularly in the mouse spinal cord, as it starts to be shut down once myelination is completed (Wrabetz et al. 1998).

The new MBP-LacZ/TWI served to detect for changes in the population of myelinating OL during postnatal life. As expected, LacZ+ OLs were significantly reduced in all regions of spinal cord during demyelination (P30). Interestingly, pre-symptomatic TWI mice (P15) showed a significant reduction of LacZ+OLs along the spinal cord. More intriguing, a small reduction of LacZ+ OLs was detected in the lumbar region of the P7 mutant cord. Because myelin loss in the TWI spinal cord is absent during the first 3 weeks of postnatal life, these results suggest somehow dissociation between the reduction of LacZ+ OLs and demyelination, at least at P15.

The reduction of LacZ+ OLs may be caused by one or more of the following: 1) reduction in OPC numbers; 2) blockage of maturation of OPCs into myelinating OLs; 3)

apoptotic cell death of LacZ⁺ OLs and 4) reduced expression of the reporter gene in mutant OLs.

Immunolabeling with antibodies against Olig2, which marks all stages of the oligodendroglial lineage (Lu et al. 2000; Zhou et al. 2000), showed that overall there were no significant differences in numbers of Olig2⁺ cells in TWI and WT cords at each time point (table II). Semi-quantitative western blotting analysis on the protein levels of Olig2 in TWI also showed no difference from WT at P15 and P30 (data not shown). We only were able to detect a transient increase in the number of Olig2⁺ cells present in the cervical region of the P7 mutant cord, suggesting the presence of a bigger pool of OPCs in this region. All together, counting of Olig2⁺ cells favors the absence of a compromised postnatal oligodendrogenesis in this mutant. Furthermore, our experiment determining the abundance of ASPA⁺ OLs in the young spinal cord suggests that the differentiation properties of the mutant OPCs were also not compromised *in vivo*.

BrdU double labeling analyses showed that the proliferation capacity of Olig2⁺ OPCs was also not compromised in the TWI cord, even in high levels of psychosine. Instead, proliferation of TWI OPCs was ~4 times higher than WT, suggesting that immature mutant OPCs were intrinsically resistant to psychosine and that they may respond to demyelination by increasing their proliferation.

Downregulation of the reporter gene obviously plays a definite role for the identification of myelinating OLs in our model system. Wrabetz and collaborators demonstrated that the MBP-LacZ transgene transcription is sensitive to axonal signals. Using eye enucleation, they observed a 75% reduction of reporter gene expression of OLs in the affected optic nerve, suggesting a supportive role of healthy axons on OLs. This

effect is best exemplified by the complete absence of LacZ⁺ OLs in TWI cords at P40 but not in the WT age-matched cord, (data not shown). However, even a 50% reduction in LacZ expression in OLs will permit their positive identification. This was taken into consideration when performing the stereological counting, and thus, the reductions measured at P15 and P30 are not arising from reporter gene shutdown (unlikely in view of our β -galactosidase and Taqman PCR analyses). However, we did observe a reduction of the level of LacZ staining in individual OLs, especially in P30 cords (which did not compromise their counting), suggesting an abnormal axonal support. Various studies showed evidence of axonal and neuronal degeneration in parallel to demyelination (Galbiati et al. 2007a; Galbiati et al. 2009; Taniike and Suzuki 1994). However, recent studies in the Bongarzone lab identified other axonal defects in the TWI cords, including swelling and breaks in axons (Castelvetri et al. 2011), decreased axonal transport (Cantuti Castelvetri L 2012), dephosphorylation of neurofilaments (Cantuti-Castelvetri et al. 2012) and activation of axonal caspases (Smith et al. 2011). Many of these pathological findings were observed as early as P7, in absence of demyelination. Interestingly, our quantitative analysis showed a significant increase of LacZ⁺ OLs in cervical regions of the P7 cord while a significant reduction was measured in lumbar regions. However, total Olig2⁺ and ASPA⁺ cell numbers were not significantly different, suggesting that LacZ transcription may be reduced in lumbar regions of the TWI cord. With psychosine homogeneously accumulated along the cord, we speculate that an impaired support from mutant axons rather than direct a killing effect from psychosine on LacZ⁺ OLs may be involved in the reduction of these cells in TWI lumbar WM. This is consistent with recent

findings of early axonal damage in the TWI cord (Cantuti-Castelvetri et al. 2012; Castelvetri et al. 2011).

However, an apoptotic depletion of LacZ⁺ OLs may be expected in the TWI cord at later stages. In general, the traditional view of this disease assumes that demyelination is caused by the massive death of OLs. However, definite quantitative proof of this killing was missing. Furthermore, at the moment of carrying out experiments for this dissertation, there was no information about the role of apoptosis in early postnatal days when there is no demyelination in the mutant. Our assessment of apoptosis showed that indeed, significant numbers of Olig2⁺ OGs were apoptotic (TUNEL⁺) in young (P8, P15) mutant cord but unexpectedly, much less in the demyelinating (P30) cord. One possible interpretation is that OPCs respond to a more severe demyelination by contributing with new OPCs and counterbalancing the final numbers of available OPCs. These results seem to support the idea that demyelination at late stages of the disease may not be primarily the consequence from OL apoptosis, but triggered by another mechanism that does not require per se the activation of a cell death program.

One aspect of interest was to find that the increase in cell death observed at P30 (demyelination phase) was primarily contributed by dying IB4⁺ reactive microglial cells. Massive infiltration of immune cells into the nervous system and formation of globoid cells constitute one hallmark of KD (Higashi et al. 1992; Mohri et al. 2006; Oehmichen et al. 1980; Ohno et al. 1993a; Ohno et al. 1993b; Wu et al. 2000). In general, microglia/macrophages are thought to be activated by myelin degeneration and aggravate the symptoms of demyelination by attacking myelin sheath and secreting toxic cytokines to further impair OLs (Merson et al. 2010; Pellegatta et al. 2006; Suzuki 1995; Wu et al.

2001). However, a recent study showed that deficiency of macrophage in TWI would lead to a more severe clinical phenotype, indicating a protective effect of microglia in KD (Kondo et al. 2011).

While the beneficial or harmful role of microglia/macrophage in demyelination may be still under debate, our findings of abundant microglia cell death at the demyelination stage of KD may reveal a new pathological component in KD. If microglia is indeed beneficial during demyelination, its loss may exacerbate the severity of the disease. In fact, during the final days of its life, the TWI mouse shows an extreme level of neurological damage, with a rapid deterioration and death around 45 days of age. Even though there are studies suggesting that morphological defects of demyelination in KD are similar to those seen in autoimmune or toxic demyelination (Suzuki 1995), the roles of the immune response from microglia/macrophage are by far much less understood.

How can we reconcile the loss of myelin, the constant increase in psychosine with a lower-than-expected loss of myelinating OLs? The preferred culprit is obviously psychosine. Psychosine is known to be highly toxic to a wide range of cell types (Dickerman et al. 1981; Sugama et al. 1991; Sugama et al. 1990). In high concentrations, psychosine rapidly kills OLs (Cho et al. 1997; Jatana et al. 2002). Psychosine affects various metabolic pathways including mitochondrial activity (Strasberg 1986), NF- κ B anti-apoptotic pathway and the AP-1 pro-apoptotic pathway (Haq et al. 2003) and caspases (Zaka and Wenger 2004). While these studies support a role for psychosine in the killing of OLs, most of these studies used levels of psychosine (20-50 μ M) larger than those that OLs may face even in vivo during demyelination. In fact, these concentrations of psychosine are far above the minimal to cause death found in our experiments. While

in vitro experiments of psychosine toxicity are a valuable source of information to understand some mechanistic aspects of the disease, their extrapolation to the in vivo situation require a maximum level of caution. The reason for this is that the accumulation of psychosine is a dynamic and continuous process, which depends on multiple variables including the rate of synthesis and catabolism, the transport of psychosine within cellular compartments, the cell type where it is synthesized, the differentiation state of that cell and likely cellular responses to the environment where the cell resides. Many aspects of this process are largely unknown. Just to mention a few: is the synthesis of psychosine “always” occurring at the same rate in “all” OPCs? Is the synthetic rate the same between OPCs and OLs? Is the synthetic rate of psychosine the same in embryonic and postnatal OPCs? Is the synthetic rate of spinal cord OLs the same as in brain OLs? Is psychosine synthesis different in OLs from white versus grey matter? Is psychosine differentially accumulated in different compartments of the OL? We could argue for similar questions on the catabolism of psychosine. To these, we must underline the fact that because OLs differentiate asynchronously, a heterogeneous population of cells at different stages of maturation (and thus, likely with different content of psychosine) co-exists at any given time point after birth. This complicates to an unsuspected level the interpretation of published data as well as the data generated in this dissertation work.

The intricacies of psychosine metabolism cannot be of more importance and we cannot disregard this aspect, simplifying our interpretations by considering only the effects of the deficiency of GALC. In fact, this problem is so complex that is likely to remain still obscure and our conclusions, mere approximations. However, our work and that done previously in our lab may shed some insights, which may lead for future new

avenues of research. The following is one possible interpretation to understand the co-existence of diffuse demyelination and disproportionately low levels of OL cell death. For this theory, we will assume that the synthetic rate of psychosine is the same for all oligodendroglial cells at any stage of their differentiation (in other words, the same synthetic rate in OPCs than in mature OLs). One prediction of this model is that de novo TWI OPCs may start to accumulate psychosine at low levels during their early stages of differentiation. Initially, TWI OPCs may respond to low levels of psychosine by increasing cell division and hence, producing more new TWI OPCs. These new OPCs will contain normal or very low levels of psychosine. However, as some of the OPCs start to differentiate and become intermediate non-myelinating OLs (iOL), psychosine may rise to higher levels. These intermediate OLs are known to have essentially two alternatives: either myelinate or die by apoptosis (Barres and Raff 1994). Those iOL which make contact with axons first (and start myelination) are spared from death, but those that miss the contact and do not myelinate, die consequently to their rising levels of psychosine. This may explain the increase in TUNEL+ Olig2+ cells detected during the first 2 weeks of life in the mutant cord. It seems relevant to underline that even Olig2 is an excellent marker for OPCs and OLs, it is simply impossible to distinguish subpopulations of more or less differentiated OPCs based only on their immunoreactivity to Olig2 antibodies.

In contrast, those iOL spared become postmitotic mature OLs in charge of producing myelin sheaths. These TWI myelinating OLs (mOLs) have a natural intrinsic mode to keep producing psychosine without raising its concentration levels in the cell body: by anterograde transport in vesicles and insertion in nascent myelin membranes.

An average OL cell is thought to maintain a volume of 50,000 to 150,000 μm^3 of myelin membrane. If we consider roughly that the volume of an average OL is $\sim 500 \mu\text{m}^3$, then by transporting psychosine from the cell body to the myelin domain, OLs “dilute” psychosine (from their cell bodies) between 100 to 300 fold by transporting it to myelin. In other words, psychosine may get concentrated in myelin sheaths many fold. We know that psychosine is a sphingolipid that is preferentially targeted to lipid rafts in plasma membranes (White et al. 2009). We also know that psychosine is associated to transport vesicles in the brain (Santos and Bongarzone, unpublished results). As maturation of TWI OLs continues and myelin membrane keeps being formed, our prediction is that psychosine will be progressively transported to myelin and accumulated in lipid rafts within the nascent sheaths (by means of active anterograde vesicular transport). In fact, our measurements revealed that, for example, psychosine is enriched ~ 60 fold in the P30 myelin, which is likely to be an underestimation, because we were unable to accurately measure the psychosine concentration in the cell body of mOLs in vivo. This differential enrichment of psychosine in the myelin compartment may be exacerbated by the inhibitory effects that psychosine exerts on the recycling of membrane domains through the caveolar-endocytic pathway (White et al. 2011). In other words, in the TWI mOL, psychosine follows a one-way dead-end road, where the final residence sites are likely the raft domains in myelin membranes. At this point in the life of the individual myelinating OL, still its cell body may have accumulated relatively low levels of psychosine, insufficient to trigger the death of the cell. Our prediction is that once a threshold of psychosine concentration is reached in the myelin domain, and by an unknown mechanism, the connection between myelin sheath and its oligodendroglial

maintenance cell process is lost, leading to the detachment from the parental OL cell body. This point is when likely activated microglia become an active player in demyelination, engulfing and eating myelin debris, which likely caused the death of TWI microglial cells. Psychosine may then affect myelin normal function/structure and disrupt axonal interactions (Kagitani-Shimono et al. 2008; Malone et al. 1975). The OL cellular process, now devoid of its myelin domain, retracts from the axon and eventually senesces or is completely recycled within the plasma membrane of the OL cell body. In this situation, and with the synthesis of psychosine always at a constant rate, psychosine does not have any other place to be stored than in the remnant of the mOL cell body, what leads to a progressive accumulation in the OL soma. Eventually, the local concentration of psychosine in OLs reaches levels that are too high to avoid activation of apoptosis and the OL dies. This model of psychosine-induced demyelination and OL cell death is depicted in the illustration in figure 27. Evidently, multiple aspects of this theory need to be examined and challenged, but we think it is a good start to understand mechanistically, the process of demyelination in KD.

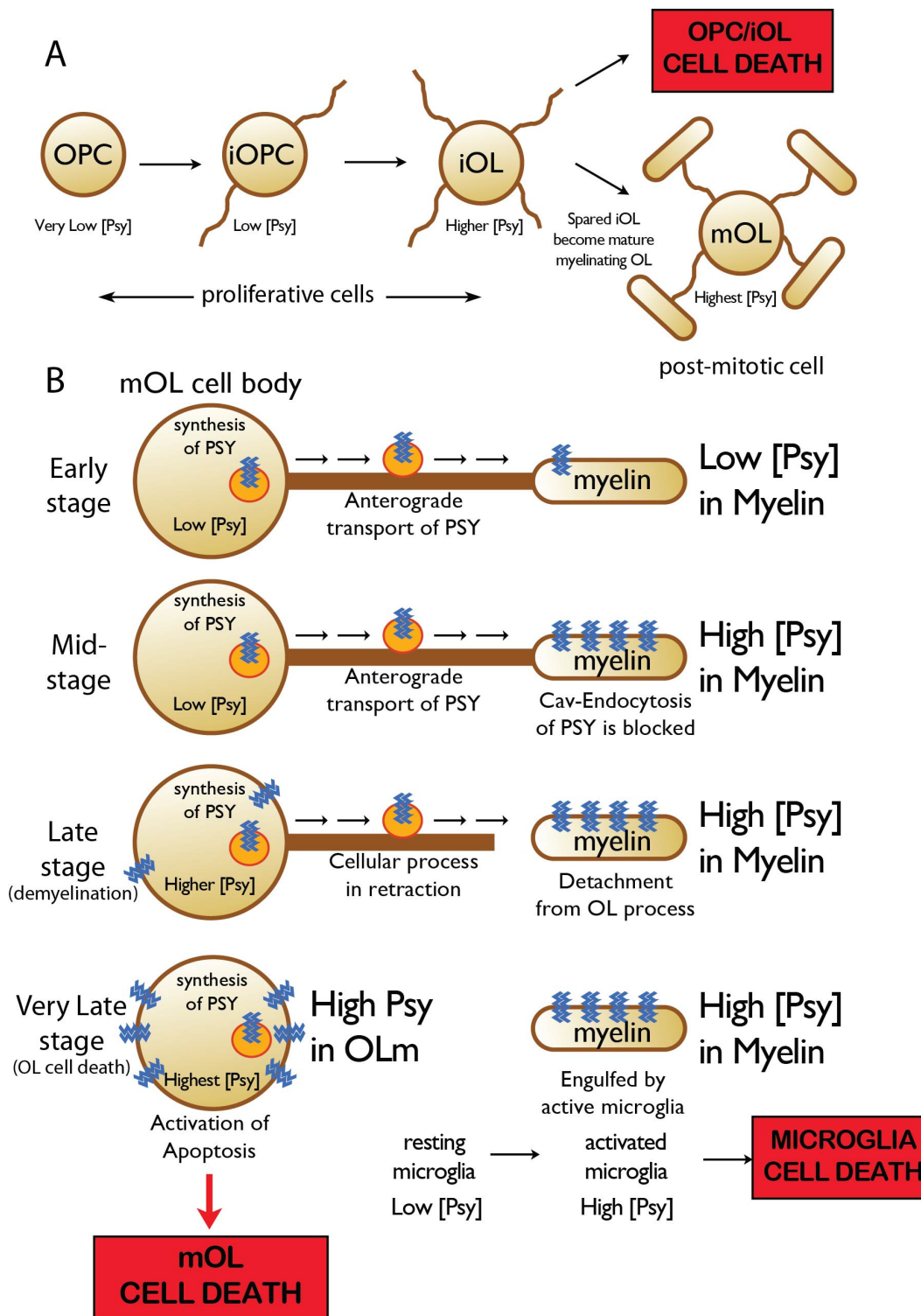


Figure 27. Mechanistic model of demyelination in the TWI spinal cord. For explanation, please see text. OPC: oligodendrocyte progenitor cell; iOPC: intermediate OPC; iOL: intermediate oligodendrocyte; mOL, myelinating OL; [Psy], concentration of psychosine; Cav: caveolar.

Aim 2- To measure for changes in oligodendrogenesis during embryonic development of the TWI mouse.

KD is caused by genetic mutations in GALC gene, which lead to the inactivity of GALC enzyme (Deane et al. 2011; Duffner et al. 2011; Tappino et al. 2010). Thus, affected individuals may develop enzyme deficiency-related alterations since very early in their lives. We have speculated that GALC deficiency-related abnormalities may be even present during the embryonic development of the mutant nervous system. Interestingly, even though the majority of KD human cases are infantile, all of the studies done so far have focused on postnatal changes, leaving out any study on the formation of OLs during embryogenesis in this disease. This seems overall expected because historically, psychosine has been considered just a byproduct during GalCer synthesis without any physiological function in vivo (Suzuki 1998), and thus, there was no need to investigate psychosine effects in physiological or near physiological conditions. However, recent studies in the Bongarzone Lab have shown that psychosine is present in multiple cell types in normal conditions, suggesting that there may be a physiological function for this sphingolipid after all.

Our investigations using CG4 cells, a rat immortalized OPC cell line, provided some insight in this potential function. When CG4 cells were incubated with very low doses of psychosine, cell proliferation was facilitated. However, when cells were exposed to concentrations above 1 μ M of psychosine cell death raised rapidly. Is this revealing a physiological role of psychosine? To address this question, we measured psychosine concentrations in the TWI embryo. The embryo was an obvious choice for our study because if accumulated, psychosine would be at near physiological levels and in the

absence of any compounding effect from demyelination (as this is a postnatal late effect in the disease). We found that psychosine was indeed present in the embryonic CNS. In the TWI, it reached a significant accumulation in E15.5 embryos, while unexpectedly it was significantly below normal levels in the CNS of E10.5 embryos.

Based on our lab's previous findings on the effects of psychosine on lipid rafts, we hypothesized that changes in psychosine concentration will affect raft-mediated signals that control oligodendrogenesis such as that mediated by SHH. SHH is necessary and sufficient for the commitment of neural stem cells into the OL lineage in the ventral neural tube (Marti and Bovolenta 2002; Oh et al. 2005; Orentas et al. 1999; Sussman et al. 2002; Zhu et al. 1999). SHH is a morphogen that acts by promoting ventralization of the neural tube after binding to its receptors PTC and SMO. Upon binding to the receptor complex, SMO is phosphorylated and released intracellularly, where it leads to the activation of gene transcription of downstream target genes by the recruitment of GLI proteins. Downstream targets of SHH include Olig2, PDGFR α , Nkx2.2, MBP, and others. Of relevance, the PTC-SMO complex is associated to rafts in the plasma membrane. Because psychosine's association with rafts, it was reasonable to consider that the SHH signaling pathway may be modified by psychosine. Our experiments showed that mutant embryos do not appear to display significant changes in the level of expression of active SHH, PTC and SMO proteins and overall, the total number of Olig2⁺ OPCs at each developmental day examined were similar between mutants and controls. However, stereological analysis of Olig2⁺ OPCs detected a transient but altered distribution of OPCs in ventral neural tube of E12.5 mutant embryos, with more cells migrating into the mantle area of the cord, and outside of the site of birth of OPCs.

At E10.5, the Olig2⁺ progenitor cells were somehow less in TWI respect WT, but understanding the reason for this might be more difficult because Olig2 is also expressed by motor neuron progenitors (MNP) between E9.5-E10.5, which obscures understanding the situation of OPCs. Though Olig2 gene expression is not sufficient for MNP commitment (Du et al. 2006), knockout of Olig2 greatly eliminates MNP generation and migration in embryos (Sun et al. 2006; Zannino et al. 2012; Zhou and Anderson 2002). At E10.5, whilst the total protein level of SHH is not changed in TWI respect WT, its spatial distribution appears more diffuse in the TWI floor plate. These results suggest that while there is no alteration in the stoichiometry of ligand-receptor (i.e. SHH, PTC and SMO), the regional distribution of SHH activity may be more extended than usual. Whether the higher number of LacZ⁺OPCs detected in the mantle region arise from in situ commitment of neural stem cells within the mantle by means of this enlarged SHH domain or by an increased migration from OPCs generated only within the pMN region remains to be understood.

Unfortunately our expectations for more noticeable changes in oligodendrogenesis in the mutant embryo were not met and only borderline changes were observed. In vitro, psychosine appears to facilitate SHH-mediated increase of Olig2⁺ and PDGF α ⁺ OPCs from spinal cord-derived neural stem cells, suggesting that indeed psychosine may modulate this pathway. However, a number of questions remain unanswered from our embryonic studies: Does psychosine facilitate the SHH pathway by altering the lipid raft architecture in the neural stem cell plasma membrane? Is it possible that psychosine can enhance the SHH activity via a hydrophobic affinity with cholesterol, which is also important for SHH signaling? Could psychosine act as a lipid chaperon for

SHH ligand or its transmembrane receptors PTC/SMO? Given the fact that psychosine can promote the proliferation of CG4 cell at nM concentrations, does psychosine act as small signaling molecule for oligodendrogenesis, in way similar to other sphingosine derivatives such as sphingosine-1-phosphate (Belvitch and Dudek 2012; Maceyka et al. 2012; Walsh et al. 2011)?

We were not able to answer those questions in this dissertation. However, this work should provide the bases for future research on some of the questions posed throughout the discussion of both embryonic and postnatal findings. On the long run, the contribution of this thesis to the field of KD might be inferred as providing insight in the correlation –or lack of it- between demyelination and OL cell death in this severe pediatric disease.

CHAPTER 7

CONCLUSIONS

The studies in this dissertation have provided insights in the processes of demyelination, accumulation of psychosine and OL formation in the TWI mouse, a functional model of Krabbe disease.

1) We found the first significant accumulation of psychosine during the late embryogenesis (E15.5) in the TWI mouse. Psychosine concentration progressively increases in the postnatal life of the mutant with a preferential accumulation in ventral regions of the spinal cord.

2) Embryonic studies suggest a transient increase in the distribution of OPCs outside of the pMN domain at E12.5. It remains to be determined if this effect responds to changes in SHH activity and/or to higher migration capacity of OPCs.

3) During later stages of the disease when psychosine is hundreds times higher in TWI than WT, the proliferative capacity of mutant OPCs is intact, suggesting an intrinsic resistance of proliferative OPCs to psychosine, at least to a certain level. Apoptotic analysis showed that despite demyelination, a lower than expected level of OL death occurs, indicating that demyelination may be triggered by a mechanism that does not require cell death.

4) Most apoptotic cells during demyelination are microglia/macrophages. Even though, the underlying mechanism for their death is still not clear, the tight association of immune cells death with demyelination suggests that the immunoreactions may play an important role in the pathogenesis of demyelination in KD.

5) Our data also suggest a preferential enrichment of psychosine in myelin membranes. It remains to be determined how this plays a decisive role in the process of demyelination.

CHAPTER 8

FUTURE DIRECTIONS

In Suzuki's "psychosine hypothesis", demyelination in mutant CNS was believed as a result of psychosine-induced OL cell death. This hypothesis was proposed based on the assumption that psychosine was mainly produced by OLs as a byproduct of GalCer (a major myelin lipid compound) synthesis. However, our studies have shown with a reasonable level of precision that psychosine accumulation is independent from myelinogenesis and OL cell death is not a required event for demyelination. Since little is known on the GALC histological expression profile, let alone its biological functions besides its known lipid metabolic role, future studies looking into those aspects may help to understand some aspects of KD pathogenesis. The studies of the Bongarzone Lab showing neuronal, immune, and myelin-forming cell defects predict that conditional cell type specific knockout lines of the GALC gene may help to understand different aspects of the pathology in this disease, as well as to clarify GALC function/s in each cell type.

While our studies have suggested a physiological role for psychosine in oligodendrogenesis that may involve changes in raft architecture, this needs to be proved –or disproved by biophysical and biochemical analyses.

Almost nothing is known about the synthesis of psychosine. A systematic analysis on psychosine production is needed to understand the involvement of psychosine in this

disease and in health. Since neuronal pathology is also a very important aspect of this disease, and studies in Bongarzone lab have shown accumulation of psychosine in neurons, it may be relevant to study changes in neurogenic signaling.

Because macrophage infiltration and globoid cell formation are two hallmarks of Krabbe disease, the pathogenic aspects of those immune cells involved in the disease cannot continue to be oversimplified as just a simple inflammatory reaction to demyelination. This dissertation has shown a preferential killing of microglia-macrophages during demyelination. Are those reactive immune cells yet another cause for myelin loss in KD? Do those immune cells attack myelin in KD via mechanisms similar to autoimmune demyelination diseases such as multiple sclerosis? Why do these immune cells die in the disease? Further studies to answer those questions are absolutely needed to correctly interpret their role in this disease.

REFERENCES

- Aberg, D. (2010). "Role of the growth hormone/insulin-like growth factor 1 axis in neurogenesis." Endocr Dev **17**: 63-76.
- Aicardi, J. (1993). "The inherited leukodystrophies: a clinical overview." J Inherit Metab Dis **16**(4): 733-743.
- Andrews, J. M., P. A. Cancilla, J. Grippo and J. H. Menkes (1971). "Globoid cell leukodystrophy (Krabbe's disease): morphological and biochemical studies." Neurology **21**(4): 337-352.
- Baron, W., S. J. Shattil and C. French-Constant (2002). "The oligodendrocyte precursor mitogen PDGF stimulates proliferation by activation of [alpha]v[beta]3 integrins." EMBO J **21**(8): 1957-1966.
- Barres, B. A., I. K. Hart, H. S. Coles, J. F. Burne, J. T. Voyvodic, W. D. Richardson and M. C. Raff (1992). "Cell death and control of cell survival in the oligodendrocyte lineage." Cell **70**(1): 31-46.
- Barres, B. A., M. D. Jacobson, R. Schmid, M. Sendtner and M. C. Raff (1993). "Does oligodendrocyte survival depend on axons?" Curr Biol **3**(8): 489-497.
- Barres, B. A. and M. C. Raff (1994). "Control of oligodendrocyte number in the developing rat optic nerve." Neuron **12**(5): 935-942.
- Baskin, G. B., M. Ratterree, B. B. Davison, K. P. Falkenstein, M. R. Clarke, J. D. England, M. T. Vanier, P. Luzi, M. A. Rafi and D. A. Wenger (1998). "Genetic galactocerebrosidase deficiency (globoid cell leukodystrophy, Krabbe disease) in rhesus monkeys (*Macaca mulatta*)." Lab Anim Sci **48**(5): 476-482.
- Baumann, N. and D. Pham-Dinh (2001). "Biology of oligodendrocyte and myelin in the mammalian central nervous system." Physiol Rev **81**(2): 871-927.
- Belvitch, P. and S. M. Dudek (2012). "Role of FAK in S1P-regulated endothelial permeability." Microvasc Res **83**(1): 22-30.
- Bongarzone, E. R. (2002). "Induction of oligodendrocyte fate during the formation of the vertebrate neural tube." Neurochem Res **27**(11): 1361-1369.
- Bongarzone, E. R., L. M. Foster, S. Byravan, A. N. Verity, C. F. Landry, V. V. Schonmann, S. Amur-Umarjee and A. T. Campagnoni (1996). "Conditionally Immortalized Neural Cell Lines: Potential Models for the Study of Neural Cell Function." Methods **10**(3): 489-500.
- Briscoe, J. and B. G. Novitsch (2008). "Regulatory pathways linking progenitor patterning, cell fates and neurogenesis in the ventral neural tube." Philos Trans R Soc Lond B Biol Sci **363**(1489): 57-70.

- Cai, J., Y. Qi, X. Hu, M. Tan, Z. Liu, J. Zhang, Q. Li, M. Sander and M. Qiu (2005). "Generation of oligodendrocyte precursor cells from mouse dorsal spinal cord independent of Nkx6 regulation and Shh signaling." Neuron **45**(1): 41-53.
- Calver, A. R., A. C. Hall, W.-P. Yu, F. S. Walsh, J. K. Heath, C. Betsholtz and W. D. Richardson (1998a). "Oligodendrocyte Population Dynamics and the Role of PDGF In Vivo." Neuron **20**(5): 869-882.
- Calver, A. R., A. C. Hall, W. P. Yu, F. S. Walsh, J. K. Heath, C. Betsholtz and W. D. Richardson (1998b). "Oligodendrocyte population dynamics and the role of PDGF in vivo." Neuron **20**(5): 869-882.
- Cannizzaro, L. A., Y. Q. Chen, M. A. Rafi and D. A. Wenger (1994). "Regional mapping of the human galactocerebrosidase gene (GALC) to 14q31 by in situ hybridization." Cytogenet Cell Genet **66**(4): 244-245.
- Cantuti Castelvetri L, G. M., Zhu H, Lopez-Rosas A, Morfini G, Pigino G, Cao H, van Breemen R, Brady S, Bongarzone ER (2012). Inhibition of fast axonal transport is a pathogenic mechanism contributing to neuropathology in Krabbe disease. manuscript in submission.
- Cantuti-Castelvetri, L., H. Zhu, M. I. Givogri, R. L. Chidavaenzi, A. Lopez-Rosas and E. R. Bongarzone (2012). "Psychosine induces the dephosphorylation of neurofilaments by deregulation of PP1 and PP2A phosphatases." Neurobiol Dis **46**(2): 325-335.
- Castelvetri, L. C., M. I. Givogri, H. Zhu, B. Smith, A. Lopez-Rosas, X. Qiu, R. van Breemen and E. R. Bongarzone (2011). "Axonopathy is a compounding factor in the pathogenesis of Krabbe disease." Acta Neuropathol **122**(1): 35-48.
- Chen, Y. Q., M. A. Rafi, G. de Gala and D. A. Wenger (1993). "Cloning and expression of cDNA encoding human galactocerebrosidase, the enzyme deficient in globoid cell leukodystrophy." Hum Mol Genet **2**(11): 1841-1845.
- Chirgwin, J. M., A. E. Przybyla, R. J. MacDonald and W. J. Rutter (1979). "Isolation of biologically active ribonucleic acid from sources enriched in ribonuclease." Biochemistry **18**(24): 5294-5299.
- Cho, K. H., M. W. Kim and S. U. Kim (1997). "Tissue culture model of Krabbe's disease: psychosine cytotoxicity in rat oligodendrocyte culture." Dev Neurosci **19**(4): 321-327.
- Chojnacki, A. and S. Weiss (2008). "Production of neurons, astrocytes and oligodendrocytes from mammalian CNS stem cells." Nat Protoc **3**(6): 935-940.
- Crome, L., F. Hanefeld, D. Patrick and J. Wilson (1973). "Late onset globoid cell leucodystrophy." Brain **96**(4): 841-848.
- D'Agostino, A. N., G. P. Sayre and A. B. Hayles (1963). "Krabbe's disease. Globoid cell type of leukodystrophy." Arch Neurol **8**: 82-96.
- De Gasperi, R., M. A. Gama Sosa, E. L. Sartorato, S. Battistini, H. MacFarlane, J. F. Gusella, W. Krivit and E. H. Kolodny (1996). "Molecular heterogeneity of

late-onset forms of globoid-cell leukodystrophy." Am J Hum Genet **59**(6): 1233-1242.

Deane, J. E., S. C. Graham, N. N. Kim, P. E. Stein, R. McNair, M. B. Cachon-Gonzalez, T. M. Cox and R. J. Read (2011). "Insights into Krabbe disease from structures of galactocerebrosidase." Proc Natl Acad Sci U S A **108**(37): 15169-15173.

Dickerman, L. H., T. W. Kurczynski and R. G. Macbride (1981). "The effects of psychosine upon growth of human skin fibroblasts from patients with globoid cell leukodystrophy." J Neurol Sci **50**(2): 181-190.

Dolcetta, D., L. Perani, M. I. Givogri, F. Galbiati, S. Amadio, U. Del Carro, G. Finocchiaro, A. Fanzani, S. Marchesini, L. Naldini, M. G. Roncarolo and E. Bongarzone (2006). "Design and optimization of lentiviral vectors for transfer of GALC expression in Twitcher brain." J Gene Med **8**(8): 962-971.

Du, Z. W., X. J. Li, G. D. Nguyen and S. C. Zhang (2006). "Induced expression of Olig2 is sufficient for oligodendrocyte specification but not for motoneuron specification and astrocyte repression." Mol Cell Neurosci **33**(4): 371-380.

Duchen, L. W., E. M. Eicher, J. M. Jacobs, F. Scaravilli and F. Teixeira (1980). "Hereditary leucodystrophy in the mouse: the new mutant twitcher." Brain **103**(3): 695-710.

Duffner, P. K., A. Barczykowski, K. Jalal, L. Yan, D. M. Kay and R. L. Carter (2011). "Early infantile Krabbe disease: results of the World-Wide Krabbe Registry." Pediatr Neurol **45**(3): 141-148.

Duffner, P. K., A. Barczykowski, D. M. Kay, K. Jalal, L. Yan, A. Abdelhalim, S. Gill, A. L. Gill and R. Carter (2012). "Later onset phenotypes of krabbe disease: results of the world-wide registry." Pediatr Neurol **46**(5): 298-306.

Duffner, P. K., M. Caggana, J. J. Orsini, D. A. Wenger, M. C. Patterson, C. J. Crosley, J. Kurtzberg, G. L. Arnold, M. L. Escolar, D. J. Adams, M. R. Andriola, A. M. Aron, E. Ciafaloni, A. Djukic, R. W. Erbe, P. Galvin-Parton, L. E. Helton, E. H. Kolodny, B. E. Kosofsky, D. F. Kronn, J. M. Kwon, P. A. Levy, J. Miller-Horn, T. P. Naidich, J. E. Pellegrino, J. M. Provenzale, S. J. Rothman and M. P. Wasserstein (2009). "Newborn screening for Krabbe disease: the New York State model." Pediatr Neurol **40**(4): 245-252; discussion 253-245.

Dunn, H. G., B. D. Lake, C. L. Dolman and J. Wilson (1969). "The neuropathy of Krabbe's infantile cerebral sclerosis (globoid cell leucodystrophy)." Brain **92**(2): 329-344.

Durand, B., F. B. Gao and M. Raff (1997). "Accumulation of the cyclin-dependent kinase inhibitor p27/Kip1 and the timing of oligodendrocyte differentiation." EMBO J **16**(2): 306-317.

Eto, Y. and K. Suzuki (1970). "Globoid cell leukodystrophy (Krabbe's disease): isolation of myelin with normal glycolipid composition." J Lipid Res **11**(5): 473-479.

- Farzan, S. F., S. Singh, N. S. Schilling and D. J. Robbins (2008). "The adventures of sonic hedgehog in development and repair. III. Hedgehog processing and biological activity." Am J Physiol Gastrointest Liver Physiol **294**(4): G844-849.
- Feltri, M. L., S. S. Scherer, L. Wrabetz, J. Kamholz and M. E. Shy (1992). "Mitogen-expanded Schwann cells retain the capacity to myelinate regenerating axons after transplantation into rat sciatic nerve." Proc Natl Acad Sci U S A **89**(18): 8827-8831.
- Formichi, P., E. Radi, C. Battisti, A. Pasqui, G. Pompella, P. E. Lazzerini, F. Laghi-Pasini, A. Leonini, A. Di Stefano and A. Federico (2007). "Psychosine-induced apoptosis and cytokine activation in immune peripheral cells of Krabbe patients." J Cell Physiol **212**(3): 737-743.
- Fu, L., K. Inui, T. Nishigaki, N. Tatsumi, H. Tsukamoto, C. Kokubu, T. Muramatsu and S. Okada (1999). "Molecular heterogeneity of Krabbe disease." J Inherit Metab Dis **22**(2): 155-162.
- Galbiati, F., V. Basso, L. Cantuti, M. I. Givogri, A. Lopez-Rosas, N. Perez, C. Vasu, H. Cao, R. van Breemen, A. Mondino and E. R. Bongarzone (2007a). "Autonomic denervation of lymphoid organs leads to epigenetic immune atrophy in a mouse model of Krabbe disease." J Neurosci **27**(50): 13730-13738.
- Galbiati, F., G. Clementi, D. Superchi, M. I. Givogri and E. R. Bongarzone (2007b). "Effects of irradiation on the postnatal development of the brain in a genetic mouse model of globoid cell leukodystrophy." Neurochem Res **32**(2): 377-388.
- Galbiati, F., M. I. Givogri, L. Cantuti, A. L. Rosas, H. Cao, R. van Breemen and E. R. Bongarzone (2009). "Combined hematopoietic and lentiviral gene-transfer therapies in newborn Twitcher mice reveal contemporaneous neurodegeneration and demyelination in Krabbe disease." J Neurosci Res **87**(8): 1748-1759.
- Gao, F. B. and M. Raff (1997). "Cell size control and a cell-intrinsic maturation program in proliferating oligodendrocyte precursor cells." J Cell Biol **138**(6): 1367-1377.
- Gao, W., W. Lin, Y. Chen, G. Gerig, J. K. Smith, V. Jewells and J. H. Gilmore (2009). "Temporal and spatial development of axonal maturation and myelination of white matter in the developing brain." AJNR Am J Neuroradiol **30**(2): 290-296.
- Gard, A. L. and S. E. Pfeiffer (1990). "Two proliferative stages of the oligodendrocyte lineage (A2B5+O4- and O4+GalC-) under different mitogenic control." Neuron **5**(5): 615-625.
- Giri, S., M. Khan, R. Rattan, I. Singh and A. K. Singh (2006). "Krabbe disease: psychosine-mediated activation of phospholipase A2 in oligodendrocyte cell death." J Lipid Res **47**(7): 1478-1492.
- Girolamo, F., G. Ferrara, M. Strippoli, M. Rizzi, M. Errede, M. Trojano, R. Perris, L. Roncali, M. Svelto, T. Mennini and D. Virgintino (2011). "Cerebral cortex

demyelination and oligodendrocyte precursor response to experimental autoimmune encephalomyelitis." Neurobiol Dis **43**(3): 678-689.

Givogri, M. I., F. Galbiati, S. Fasano, S. Amadio, L. Perani, D. Superchi, P. Morana, U. Del Carro, S. Marchesini, R. Brambilla, L. Wrabetz and E. Bongarzone (2006). "Oligodendroglial progenitor cell therapy limits central neurological deficits in mice with metachromatic leukodystrophy." J Neurosci **26**(12): 3109-3119.

Green, D. R. (2005). "Apoptotic pathways: ten minutes to dead." Cell **121**(5): 671-674.

Greenwood, K. and A. M. Butt (2003). "Evidence that perinatal and adult NG2-glia are not conventional oligodendrocyte progenitors and do not depend on axons for their survival." Mol Cell Neurosci **23**(4): 544-558.

Guillemot, F. (2007). "Cell fate specification in the mammalian telencephalon." Prog Neurobiol **83**(1): 37-52.

Hagberg, B., H. Kollberg, P. Sourander and H. O. Akesson (1969). "Infantile globoid cell leucodystrophy (Krabbe's disease). A clinical and genetic study of 32 Swedish cases 1953--1967." Neuropadiatrie **1**(1): 74-88.

Hagemeier, K., W. Bruck and T. Kuhlmann (2012). "Multiple sclerosis - remyelination failure as a cause of disease progression." Histol Histopathol **27**(3): 277-287.

Hall, A., N. A. Giese and W. D. Richardson (1996). "Spinal cord oligodendrocytes develop from ventrally derived progenitor cells that express PDGF alpha-receptors." Development **122**(12): 4085-4094.

Haq, E., M. A. Contreras, S. Giri, I. Singh and A. K. Singh (2006). "Dysfunction of peroxisomes in twitcher mice brain: a possible mechanism of psychosine-induced disease." Biochem Biophys Res Commun **343**(1): 229-238.

Haq, E., S. Giri, I. Singh and A. K. Singh (2003). "Molecular mechanism of psychosine-induced cell death in human oligodendrocyte cell line." J Neurochem **86**(6): 1428-1440.

Harzer, K., R. Knoblich, A. Rolfs, P. Bauer and J. Eggers (2002). "Residual galactosylsphingosine (psychosine) beta-galactosidase activities and associated GALC mutations in late and very late onset Krabbe disease." Clin Chim Acta **317**(1-2): 77-84.

Harzer, K., B. C. Paton, H. Christomanou, M. Chatelut, T. Levade, M. Hiraiwa and J. S. O'Brien (1997). "Saposins (sap) A and C activate the degradation of galactosylceramide in living cells." FEBS Lett **417**(3): 270-274.

Higashi, Y., A. Komiyama and K. Suzuki (1992). "The twitcher mouse: immunocytochemical study of Ia expression in macrophages." J Neuropathol Exp Neurol **51**(1): 47-57.

- Hu, B. Y., Z. W. Du, X. J. Li, M. Ayala and S. C. Zhang (2009). "Human oligodendrocytes from embryonic stem cells: conserved SHH signaling networks and divergent FGF effects." Development **136**(9): 1443-1452.
- Huangfu, D. and K. V. Anderson (2006). "Signaling from Smo to Ci/Gli: conservation and divergence of Hedgehog pathways from Drosophila to vertebrates." Development **133**(1): 3-14.
- Hurle, J. M., M. A. Ros, V. Climent and V. Garcia-Martinez (1996). "Morphology and significance of programmed cell death in the developing limb bud of the vertebrate embryo." Microsc Res Tech **34**(3): 236-246.
- Hyman, B. T. and J. Yuan (2012). "Apoptotic and non-apoptotic roles of caspases in neuronal physiology and pathophysiology." Nat Rev Neurosci **13**(6): 395-406.
- Igisu, H. and K. Suzuki (1984a). "Analysis of galactosylsphingosine (psychosine) in the brain." J Lipid Res **25**(9): 1000-1006.
- Igisu, H. and K. Suzuki (1984b). "Progressive accumulation of toxic metabolite in a genetic leukodystrophy." Science **224**(4650): 753-755.
- Jackman, N., A. Ishii and R. Bansal (2009). "Oligodendrocyte development and myelin biogenesis: parsing out the roles of glycosphingolipids." Physiology (Bethesda) **24**: 290-297.
- Jacobs, J. M., F. Scaravilli and F. T. De Aranda (1982). "The pathogenesis of globoid cell leucodystrophy in peripheral nerve of the mouse mutant twitcher." J Neurol Sci **55**(3): 285-304.
- Jakovcevski, I., R. Filipovic, Z. Mo, S. Rakic and N. Zecevic (2009). "Oligodendrocyte development and the onset of myelination in the human fetal brain." Front Neuroanat **3**: 5.
- Jatana, M., S. Giri and A. K. Singh (2002). "Apoptotic positive cells in Krabbe brain and induction of apoptosis in rat C6 glial cells by psychosine." Neurosci Lett **330**(2): 183-187.
- Kagitani-Shimono, K., I. Mohri, T. Yagi, M. Taniike and K. Suzuki (2008). "Peripheral neuropathy in the twitcher mouse: accumulation of extracellular matrix in the endoneurium and aberrant expression of ion channels." Acta Neuropathol **115**(5): 577-587.
- Kanduc, D., A. Mittelman, R. Serpico, E. Sinigaglia, A. A. Sinha, C. Natale, R. Santacroce, M. G. Di Corcia, A. Lucchese, L. Dini, P. Pani, S. Santacroce, S. Simone, R. Bucci and E. Farber (2002). "Cell death: apoptosis versus necrosis (review)." Int J Oncol **21**(1): 165-170.
- Karpen, H. E., J. T. Bukowski, T. Hughes, J. P. Gratton, W. C. Sessa and M. R. Gailani (2001). "The sonic hedgehog receptor patched associates with caveolin-1 in cholesterol-rich microdomains of the plasma membrane." J Biol Chem **276**(22): 19503-19511.

- Kleijer, W. J., J. L. Keulemans, M. van der Kraan, G. G. Geilen, R. M. van der Helm, M. A. Rafi, P. Luzi, D. A. Wenger, D. J. Halley and O. P. van Diggelen (1997). "Prevalent mutations in the GALC gene of patients with Krabbe disease of Dutch and other European origin." J Inherit Metab Dis **20**(4): 587-594.
- Kobayashi, T., T. Yamanaka, J. M. Jacobs, F. Teixeira and K. Suzuki (1980). "The Twitcher mouse: an enzymatically authentic model of human globoid cell leukodystrophy (Krabbe disease)." Brain Res **202**(2): 479-483.
- Kondo, T. (2001). "[Cell-intrinsic timer regulating oligodendrocyte development]." Tanpakushitsu Kakusan Koso **46**(7): 821-828.
- Kondo, Y., J. M. Adams, M. T. Vanier and I. D. Duncan (2011). "Macrophages counteract demyelination in a mouse model of globoid cell leukodystrophy." J Neurosci **31**(10): 3610-3624.
- Korn-Lubetzki, I., T. Dor-Wollman, D. Soffer, A. Raas-Rothschild, H. Hurvitz and Y. Nevo (2003). "Early peripheral nervous system manifestations of infantile Krabbe disease." Pediatr Neurol **28**(2): 115-118.
- Kornfeld, S. (1986). "Trafficking of lysosomal enzymes in normal and disease states." J Clin Invest **77**(1): 1-6.
- Krabbe, K. (1916). "A new familial form of diffuse brain sclerosis." Brain: 74-114.
- Lee, J. J., S. C. Ekker, D. P. von Kessler, J. A. Porter, B. I. Sun and P. A. Beachy (1994). "Autoproteolysis in hedgehog protein biogenesis." Science **266**(5190): 1528-1537.
- Lee, W. C., D. Kang, E. Causevic, A. R. Herdt, E. A. Eckman and C. B. Eckman (2010). "Molecular characterization of mutations that cause globoid cell leukodystrophy and pharmacological rescue using small molecule chemical chaperones." J Neurosci **30**(16): 5489-5497.
- Lee, W. C., Y. K. Tsoi, C. A. Dickey, M. W. Delucia, D. W. Dickson and C. B. Eckman (2006). "Suppression of galactosylceramidase (GALC) expression in the twitcher mouse model of globoid cell leukodystrophy (GLD) is caused by nonsense-mediated mRNA decay (NMD)." Neurobiol Dis **23**(2): 273-280.
- Leonard, J. R., B. J. Klocke, C. D'Sa, R. A. Flavell and K. A. Roth (2002). "Strain-dependent neurodevelopmental abnormalities in caspase-3-deficient mice." J Neuropathol Exp Neurol **61**(8): 673-677.
- Levine, A. J. and A. H. Brivanlou (2007). "Proposal of a model of mammalian neural induction." Dev Biol **308**(2): 247-256.
- LeVine, S. M. and M. V. Torres (1992). "Morphological features of degenerating oligodendrocytes in twitcher mice." Brain Res **587**(2): 348-352.
- Li, H., Y. He, W. D. Richardson and P. Casaccia (2009). "Two-tier transcriptional control of oligodendrocyte differentiation." Curr Opin Neurobiol **19**(5): 479-485.

- Liem, K. F., Jr., T. M. Jessell and J. Briscoe (2000). "Regulation of the neural patterning activity of sonic hedgehog by secreted BMP inhibitors expressed by notochord and somites." Development **127**(22): 4855-4866.
- Ligon, K. L., S. P. Fancy, R. J. Franklin and D. H. Rowitch (2006). "Olig gene function in CNS development and disease." Glia **54**(1): 1-10.
- Lloyd, J. B. (1996). "Metabolite efflux and influx across the lysosome membrane." Sub-cellular biochemistry **27**: 361-386.
- Lockshin, R. A. and C. M. Williams (1964). "Programmed cell death—II. Endocrine potentiation of the breakdown of the intersegmental muscles of silkmoths." Journal of Insect Physiology **10**(4): 643-649.
- Lu, Q. R., D. Yuk, J. A. Alberta, Z. Zhu, I. Pawlitzky, J. Chan, A. P. McMahon, C. D. Stiles and D. H. Rowitch (2000). "Sonic hedgehog--regulated oligodendrocyte lineage genes encoding bHLH proteins in the mammalian central nervous system." Neuron **25**(2): 317-329.
- Luzi, P., M. A. Rafi and D. A. Wenger (1995). "Structure and organization of the human galactocerebrosidase (GALC) gene." Genomics **26**(2): 407-409.
- Lyon, G., B. Hagberg, P. Evrard, C. Allaire, L. Pavone and M. Vanier (1991). "Symptomatology of late onset Krabbe's leukodystrophy: the European experience." Dev Neurosci **13**(4-5): 240-244.
- Maceyka, M., K. B. Harikumar, S. Milstien and S. Spiegel (2012). "Sphingosine-1-phosphate signaling and its role in disease." Trends Cell Biol **22**(1): 50-60.
- Majno, G. and I. Joris (1995). "Apoptosis, oncosis, and necrosis. An overview of cell death." Am J Pathol **146**(1): 3-15.
- Malone, M. J., M. Szoke and D. A. Davis (1975). "Globid leukodystrophy. II. Ultrastructure and chemical pathology." Arch Neurol **32**(9): 613-617.
- Mao, H., A. M. Diehl and Y. X. Li (2009). "Sonic hedgehog ligand partners with caveolin-1 for intracellular transport." Lab Invest **89**(3): 290-300.
- Marks, H. G., M. T. Scavina, E. H. Kolodny, M. Palmieri and J. Childs (1997). "Krabbe's disease presenting as a peripheral neuropathy." Muscle & Nerve **20**(8): 1024-1028.
- Marti, E. and P. Bovolenta (2002). "Sonic hedgehog in CNS development: one signal, multiple outputs." Trends Neurosci **25**(2): 89-96.
- Merrill, A. (2008). Biochemistry of Lipids, Lipoproteins and Membranes Elsevier, Amsterdam.
- Merson, T. D., M. D. Binder and T. J. Kilpatrick (2010). "Role of cytokines as mediators and regulators of microglial activity in inflammatory demyelination of the CNS." Neuromolecular Med **12**(2): 99-132.
- Mi, S., R. H. Miller, W. Tang, X. Lee, B. Hu, W. Wu, Y. Zhang, C. B. Shields, S. Miklasz, D. Shea, J. Mason, R. J. Franklin, B. Ji, Z. Shao, A. Chedotal, F. Bernard, A. Roulois, J. Xu, V. Jung and B. Pepinsky (2009). "Promotion of central

nervous system remyelination by induced differentiation of oligodendrocyte precursor cells." Ann Neurol **65**(3): 304-315.

Miller, R. H. (2002). "Regulation of oligodendrocyte development in the vertebrate CNS." Prog Neurobiol **67**(6): 451-467.

Miller, R. H., S. David, R. Patel, E. R. Abney and M. C. Raff (1985). "A quantitative immunohistochemical study of macroglial cell development in the rat optic nerve: in vivo evidence for two distinct astrocyte lineages." Dev Biol **111**(1): 35-41.

Miyatake, T. and K. Suzuki (1972). "Globoid cell leukodystrophy: additional deficiency of psychosine galactosidase." Biochem Biophys Res Commun **48**(3): 539-543.

Mohri, I., M. Taniike, H. Taniguchi, T. Kanekiyo, K. Aritake, T. Inui, N. Fukumoto, N. Eguchi, A. Kushi, H. Sasai, Y. Kanaoka, K. Ozono, S. Narumiya, K. Suzuki and Y. Urade (2006). "Prostaglandin D2-mediated microglia/astrocyte interaction enhances astrogliosis and demyelination in twitcher." J Neurosci **26**(16): 4383-4393.

Morimoto, S., B. M. Martin, Y. Yamamoto, K. A. Kretz, J. S. O'Brien and Y. Kishimoto (1989). "Saposin A: second cerebroside activator protein." Proc Natl Acad Sci U S A **86**(9): 3389-3393.

Muller, T., H. E. Meyer, R. Egensperger and K. Marcus (2008). "The amyloid precursor protein intracellular domain (AICD) as modulator of gene expression, apoptosis, and cytoskeletal dynamics-relevance for Alzheimer's disease." Prog Neurobiol **85**(4): 393-406.

Munoz-Pinedo, C. (2012). "Signaling pathways that regulate life and cell death: evolution of apoptosis in the context of self-defense." Adv Exp Med Biol **738**: 124-143.

Nagano, S., T. Yamada, N. Shinnoh, H. Furuya, T. Taniwaki and J. Kira (1998). "Expression and processing of recombinant human galactosylceramidase." Clin Chim Acta **276**(1): 53-61.

Nagara, H., T. Kobayashi and K. Suzuki (1982). "The twitcher mouse: normal pattern of early myelination in the spinal cord." Brain Res **244**(2): 289-294.

Nery, S., H. Wichterle and G. Fishell (2001). "Sonic hedgehog contributes to oligodendrocyte specification in the mammalian forebrain." Development **128**(4): 527-540.

Noble, M., K. Murray, P. Stroobant, M. D. Waterfield and P. Riddle (1988). "Platelet-derived growth factor promotes division and motility and inhibits premature differentiation of the oligodendrocyte/type-2 astrocyte progenitor cell." Nature **333**(6173): 560-562.

Oehmichen, M., H. Wietholter and M. Gencic (1980). "Cytochemical markers for mononuclear phagocytes as demonstrated in reactive microglia and globoid cells." Acta Histochem **66**(2): 243-252.

- Oh, S., X. Huang and C. Chiang (2005). "Specific requirements of sonic hedgehog signaling during oligodendrocyte development." Dev Dyn **234**(3): 489-496.
- Ohno, M., A. Komiyama, P. M. Martin and K. Suzuki (1993a). "MHC class II antigen expression and T-cell infiltration in the demyelinating CNS and PNS of the twitcher mouse." Brain Res **625**(2): 186-196.
- Ohno, M., A. Komiyama, P. M. Martin and K. Suzuki (1993b). "Proliferation of microglia/macrophages in the demyelinating CNS and PNS of twitcher mouse." Brain Res **602**(2): 268-274.
- Oluich, L. J., J. A. Stratton, Y. Lulu Xing, S. W. Ng, H. S. Cate, P. Sah, F. Windels, T. J. Kilpatrick and T. D. Merson (2012). "Targeted ablation of oligodendrocytes induces axonal pathology independent of overt demyelination." J Neurosci **32**(24): 8317-8330.
- Oppenheim, R. W., R. A. Flavell, S. Vinsant, D. Prevet, C. Y. Kuan and P. Rakic (2001). "Programmed cell death of developing mammalian neurons after genetic deletion of caspases." J Neurosci **21**(13): 4752-4760.
- Orentas, D. M., J. E. Hayes, K. L. Dyer and R. H. Miller (1999). "Sonic hedgehog signaling is required during the appearance of spinal cord oligodendrocyte precursors." Development **126**(11): 2419-2429.
- Pellegatta, S., P. Tunici, P. L. Poliani, D. Dolcetta, L. Cajola, C. Colombelli, E. Ciusani, S. Di Donato and G. Finocchiaro (2006). "The therapeutic potential of neural stem/progenitor cells in murine globoid cell leukodystrophy is conditioned by macrophage/microglia activation." Neurobiol Dis **21**(2): 314-323.
- Qi, Y., D. Stapp and M. Qiu (2002). "Origin and molecular specification of oligodendrocytes in the telencephalon." Trends Neurosci **25**(5): 223-225.
- Raff, M., J. Apperly, T. Kondo, Y. Tokumoto and D. Tang (2001). "Timing cell-cycle exit and differentiation in oligodendrocyte development." Novartis Found Symp **237**: 100-107; discussion 107-112, 158-163.
- Raff, M. C., B. Durand and F. B. Gao (1998). "Cell number control and timing in animal development: the oligodendrocyte cell lineage." Int J Dev Biol **42**(3): 263-267.
- Rafi, M. A., P. Luzi, Y. Q. Chen and D. A. Wenger (1995). "A large deletion together with a point mutation in the GALC gene is a common mutant allele in patients with infantile Krabbe disease." Hum Mol Genet **4**(8): 1285-1289.
- Rafi, M. A., P. Luzi, J. Zlotogora and D. A. Wenger (1996). "Two different mutations are responsible for Krabbe disease in the Druze and Moslem Arab populations in Israel." Hum Genet **97**(3): 304-308.
- Sakai, N., K. Inui, N. Fujii, H. Fukushima, J. Nishimoto, I. Yanagihara, Y. Isegawa, A. Iwamatsu and S. Okada (1994). "Krabbe disease: isolation and characterization of a full-length cDNA for human galactocerebrosidase." Biochem Biophys Res Commun **198**(2): 485-491.

Sakai, N., K. Inui, N. Tatsumi, H. Fukushima, T. Nishigaki, M. Taniike, J. Nishimoto, H. Tsukamoto, I. Yanagihara, K. Ozono and S. Okada (1996). "Molecular cloning and expression of cDNA for murine galactocerebrosidase and mutation analysis of the twitcher mouse, a model of Krabbe's disease." J Neurochem **66**(3): 1118-1124.

Saunders, J. W., Jr. (1966). "Death in embryonic systems." Science **154**(3749): 604-612.

Selleri, S., E. Torchiana, D. Pareyson, L. Lulli, B. Bertagnolio, M. Savoiaro, L. Farina, F. Carrara, M. Filocamo, R. Gatti, A. Sghirlanzoni, G. Uziel and G. Finocchiaro (2000). "Deletion of exons 11-17 and novel mutations of the galactocerebrosidase gene in adult- and early-onset patients with Krabbe disease." J Neurol **247**(11): 875-877.

Shimohama, S. (2000). "Apoptosis in Alzheimer's disease--an update." Apoptosis **5**(1): 9-16.

Shinoda, H., T. Kobayashi, M. Katayama, I. Goto and H. Nagara (1987). "Accumulation of galactosylsphingosine (psychosine) in the twitcher mouse: determination by HPLC." J Neurochem **49**(1): 92-99.

Shiota, C., M. Miura and K. Mikoshiba (1989). "Developmental profile and differential localization of mRNAs of myelin proteins (MBP and PLP) in oligodendrocytes in the brain and in culture." Brain Res Dev Brain Res **45**(1): 83-94.

Siddiqi, Z. A., D. B. Sanders and J. M. Massey (2006). "Peripheral neuropathy in Krabbe disease: electrodiagnostic findings." Neurology **67**(2): 263-267.

Singh S, G. J., Robbins DJ (2006) Sonic hedgehog. DOI: 10.1038/mp.a002208.01

Smith, B., F. Galbiati, L. C. Castelvetti, M. I. Givogri, A. Lopez-Rosas and E. R. Bongarzone (2011). "Peripheral neuropathy in the Twitcher mouse involves the activation of axonal caspase 3." ASN Neuro **3**(4).

Strasberg, P. (1986). "Cerebrosides and psychosine disrupt mitochondrial functions." Biochem Cell Biol **64**(5): 485-489.

Sugama, S., Y. Eto, H. Yamamoto and S. U. Kim (1991). "Psychosine cytotoxicity toward rat C6 glioma cells and the protective effects of phorbol ester and dimethylsulfoxide: implications for therapy in Krabbe disease." Brain Dev **13**(2): 104-109.

Sugama, S., S. U. Kim, H. Ida and Y. Eto (1990). "Psychosine cytotoxicity in rat neural cell cultures and protection by phorbol ester and dimethyl sulfoxide." Pediatr Res **28**(5): 473-476.

Sun, T., B. P. Hafner, S. Kaing, M. Kitada, K. L. Ligon, H. R. Widlund, D. I. Yuk, C. D. Stiles and D. H. Rowitch (2006). "Evidence for motoneuron lineage-specific regulation of Olig2 in the vertebrate neural tube." Dev Biol **292**(1): 152-164.

- Sussman, C. R., J. E. Davies and R. H. Miller (2002). "Extracellular and intracellular regulation of oligodendrocyte development: roles of Sonic hedgehog and expression of E proteins." Glia **40**(1): 55-64.
- Suzuki, K. (1985). "Genetic galactosylceramidase deficiency (globoid cell leukodystrophy, Krabbe disease) in different mammalian species." Neurochem Pathol **3**(1): 53-68.
- Suzuki, K. (1995). "The twitcher mouse: a model for Krabbe disease and for experimental therapies." Brain Pathol **5**(3): 249-258.
- Suzuki, K. (1998). "Twenty five years of the "psychosine hypothesis": a personal perspective of its history and present status." Neurochem Res **23**(3): 251-259.
- Suzuki, K. (2003). "Globoid cell leukodystrophy (Krabbe's disease): update." J Child Neurol **18**(9): 595-603.
- Suzuki, K. and Y. Suzuki (1970). "Globoid cell leucodystrophy (Krabbe's disease): deficiency of galactocerebroside beta-galactosidase." Proc Natl Acad Sci U S A **66**(2): 302-309.
- Suzuki, K. and M. Taniike (1995). "Murine model of genetic demyelinating disease: the twitcher mouse." Microsc Res Tech **32**(3): 204-214.
- Suzuki, Y., J. Austin, D. Armstrong, K. Suzuki, J. Schlenker and T. Fletcher (1970). "Studies in globoid leukodystrophy: enzymatic and lipid findings in the canine form." Exp Neurol **29**(1): 65-75.
- Suzuki, Y. and K. Suzuki (1971). "Krabbe's globoid cell leukodystrophy: deficiency of galactocerebroside in serum, leukocytes, and fibroblasts." Science **171**(3966): 73-75.
- Svennerholm, L., M. T. Vanier and J. E. Mansson (1980). "Krabbe disease: a galactosylsphingosine (psychosine) lipidosis." J Lipid Res **21**(1): 53-64.
- Takahashi, H., H. Igisu and K. Suzuki (1983). "The twitcher mouse: an ultrastructural study on the oligodendroglia." Acta Neuropathol **59**(3): 159-166.
- Takahashi, H. and K. Suzuki (1984). "Demyelination in the spinal cord of murine globoid cell leukodystrophy (the twitcher mouse)." Acta Neuropathol **62**(4): 298-308.
- Taketomi, T. and K. Nishimura (1964). "PHYSIOLOGICAL ACTIVITY OF PSYCHOSINE." Jpn J Exp Med **34**: 255-265.
- Tanaka, K., H. Nagara, T. Kobayashi and I. Goto (1989). "The twitcher mouse: accumulation of galactosylsphingosine and pathology of the central nervous system." Brain Res **482**(2): 347-350.
- Taniike, M., I. Mohri, N. Eguchi, D. Irikura, Y. Urade, S. Okada and K. Suzuki (1999). "An apoptotic depletion of oligodendrocytes in the twitcher, a murine model of globoid cell leukodystrophy." J Neuropathol Exp Neurol **58**(6): 644-653.

- Taniike, M. and K. Suzuki (1994). "Spacio-temporal progression of demyelination in twitcher mouse: with clinico-pathological correlation." Acta Neuropathol **88**(3): 228-236.
- Taniike, M. and K. Suzuki (1995). "Proliferative capacity of oligodendrocytes in the demyelinating twitcher spinal cord." J Neurosci Res **40**(3): 325-332.
- Tappino, B., R. Biancheri, M. Mort, S. Regis, F. Corsolini, A. Rossi, M. Stroppiano, S. Lualdi, A. Fiumara, B. Bembi, M. Di Rocco, D. N. Cooper and M. Filocamo (2010). "Identification and characterization of 15 novel GALC gene mutations causing Krabbe disease." Hum Mutat **31**(12): E1894-1914.
- Tekki-Kessarlis, N., R. Woodruff, A. C. Hall, W. Gaffield, S. Kimura, C. D. Stiles, D. H. Rowitch and W. D. Richardson (2001). "Hedgehog-dependent oligodendrocyte lineage specification in the telencephalon." Development **128**(13): 2545-2554.
- Trapp, B. D., T. Moench, M. Pulley, E. Barbosa, G. Tennekoon and J. Griffin (1987). "Spatial segregation of mRNA encoding myelin-specific proteins." Proc Natl Acad Sci U S A **84**(21): 7773-7777.
- Vallstedt, A., J. M. Klos and J. Ericson (2005). "Multiple dorsoventral origins of oligodendrocyte generation in the spinal cord and hindbrain." Neuron **45**(1): 55-67.
- Verity, A. N. and A. T. Campagnoni (1988). "Regional expression of myelin protein genes in the developing mouse brain: in situ hybridization studies." J Neurosci Res **21**(2-4): 238-248.
- Vos, J. P., A. L. Gard and S. E. Pfeiffer (1996). "Regulation of oligodendrocyte cell survival and differentiation by ciliary neurotrophic factor, leukemia inhibitory factor, oncostatin M, and interleukin-6." Perspect Dev Neurobiol **4**(1): 39-52.
- Walsh, K. B., J. R. Teijaro, H. Rosen and M. B. Oldstone (2011). "Quelling the storm: utilization of sphingosine-1-phosphate receptor signaling to ameliorate influenza virus-induced cytokine storm." Immunol Res **51**(1): 15-25.
- Wenger, D. A., M. A. Rafi and P. Luzi (1997). "Molecular genetics of Krabbe disease (globoid cell leukodystrophy): diagnostic and clinical implications." Hum Mutat **10**(4): 268-279.
- Wenger DA, S. K., Suzuki Y, Suzuki K. (2001). In The Metabolic and Molecular Bases of Inherited Disease, McGraw-Hill: New York
- White, A. B., F. Galbiati, M. I. Givogri, A. Lopez Rosas, X. Qiu, R. van Breemen and E. R. Bongarzone (2011). "Persistence of psychosine in brain lipid rafts is a limiting factor in the therapeutic recovery of a mouse model for Krabbe disease." J Neurosci Res **89**(3): 352-364.
- White, A. B., M. I. Givogri, A. Lopez-Rosas, H. Cao, R. van Breemen, G. Thinakaran and E. R. Bongarzone (2009). "Psychosine accumulates in membrane microdomains in the brain of krabbe patients, disrupting the raft architecture." J Neurosci **29**(19): 6068-6077.

- Wrabetz, L., C. Taveggia, M. L. Feltri, A. Quattrini, R. Awatramani, S. S. Scherer, A. Messing and J. Kamholz (1998). "A minimal human MBP promoter-lacZ transgene is appropriately regulated in developing brain and after optic enucleation, but not in shiverer mutant mice." J Neurobiol **34**(1): 10-26.
- Wu, Y. P., J. Matsuda, A. Kubota and K. Suzuki (2000). "Infiltration of hematogenous lineage cells into the demyelinating central nervous system of twitcher mice." J Neuropathol Exp Neurol **59**(7): 628-639.
- Wu, Y. P., E. J. McMahon, J. Matsuda, K. Suzuki and G. K. Matsushima (2001). "Expression of immune-related molecules is downregulated in twitcher mice following bone marrow transplantation." J Neuropathol Exp Neurol **60**(11): 1062-1074.
- Xu, C., N. Sakai, M. Taniike, K. Inui and K. Ozono (2006). "Six novel mutations detected in the GALC gene in 17 Japanese patients with Krabbe disease, and new genotype-phenotype correlation." J Hum Genet **51**(6): 548-554.
- Yunis, E. J. and R. E. Lee (1969). "The ultrastructure of globoid (Krabbe) leukodystrophy." Lab Invest **21**(5): 415-419.
- Zafeiriou, D. I., A. L. Anastasiou, E. M. Michelakaki, P. A. Augoustidou-Savvopoulou, G. S. Katzos and E. E. Kontopoulos (1997). "Early infantile Krabbe disease: deceptively normal magnetic resonance imaging and serial neurophysiological studies." Brain Dev **19**(7): 488-491.
- Zaidi, A. U., C. D'Sa-Eipper, J. Brenner, K. Kuida, T. S. Zheng, R. A. Flavell, P. Rakic and K. A. Roth (2001). "Bcl-X(L)-caspase-9 interactions in the developing nervous system: evidence for multiple death pathways." J Neurosci **21**(1): 169-175.
- Zaka, M. and D. A. Wenger (2004). "Psychosine-induced apoptosis in a mouse oligodendrocyte progenitor cell line is mediated by caspase activation." Neurosci Lett **358**(3): 205-209.
- Zannino, D. A., C. G. Sagerstrom and B. Appel (2012). "olig2-Expressing hindbrain cells are required for migrating facial motor neurons." Dev Dyn **241**(2): 315-326.
- Zhou, Q. and D. J. Anderson (2002). "The bHLH transcription factors OLIG2 and OLIG1 couple neuronal and glial subtype specification." Cell **109**(1): 61-73.
- Zhou, Q., S. Wang and D. J. Anderson (2000). "Identification of a novel family of oligodendrocyte lineage-specific basic helix-loop-helix transcription factors." Neuron **25**(2): 331-343.
- Zhu, G., M. F. Mehler, J. Zhao, S. Yu Yung and J. A. Kessler (1999). "Sonic hedgehog and BMP2 exert opposing actions on proliferation and differentiation of embryonic neural progenitor cells." Dev Biol **215**(1): 118-129.
- Zschoche, A., W. Furst, G. Schwarzmann and K. Sanhoff (1994). "Hydrolysis of lactosylceramide by human galactosylceramidase and GM1-beta-galactosidase in a detergent-free system and its stimulation by sphingolipid activator proteins,

sap-B and sap-C. Activator proteins stimulate lactosylceramide hydrolysis." Eur J Biochem **222**(1): 83-90.

HONGLING ZHU

Anatomy & Cell Biology PhD Program
University of Illinois at Chicago
808 S. Wood St. Rm 578
Chicago, IL 60612

Tel: (312)607-3484
Fax (312)413-0354
hzhu2@uic.edu

Place of Birth: Shaoyang, Hunan Province, People's Republic of China
Citizenship: China

EDUCATION

University of Illinois at Chicago, USA

2006-Current: Ph.D candidate in Anatomy & Cell Biology (Expected year of completion: 2012)

University of Science & Technology of China, China

2000-2004: B.S. in Biology, 2004.

Undergraduate Thesis Topic: *Identification of GPAP, a novel Golgi protein that interacts with PLK1.* (The study was supported by grants from Chinese Natural Science Foundation (39925018), Chinese Academy of Science (KSCX2-2-01), Chinese 973 project (2002CB713700), and National Institutes of Health (DK-56292) to Dr. Xuebiao Yao)

Mentor: Dr. Xuebiao Yao

AWARDS AND SCHOLARSHIP

2011: Graduate College-Student Presenters Award, University of Illinois at Chicago

2009: Graduate Student Council-Travel Award, University of Illinois at Chicago

2001-2003: Outstanding Student Scholarship, University of Science & Technology of China, China

2000: Outstanding Freshman Scholarship, University of Science & Technology of China, China

WORK EXPERIENCE

Graduate Research Assistant

2006-Current: Department of Anatomy & Cell Biology, University of Illinois at Chicago

Principle investigator: Dr. Ernesto R. Bongarzone

Research Topic 1: Study the effect of galactosyl-ceramidase deficiency on postnatal oligodendrogenesis in the Twitcher mouse model of Krabbe disease.

VITA

Research Topic 2: Explore the possible implication of psychosine on SHH signaling pathway for oligodendrogenesis in the Twitcher embryonic neural tube. The studies were funded by contributions from the board of Trustees of the University of Illinois and NIH (RNS065808A) to ERB

Teaching Assistant

2009: Department of Anatomy & Cell Biology, University of Illinois at Chicago
Course: Neuroanatomy for medical and physical therapy students

Project Assistant

2004-2006 Laboratory of Cell Dynamics, University of Science & Technology of China, Hefei National Laboratory for Physical Sciences at the Microscale, China
Project 1: Characterize the cellular localization of Human Yip1A /Yif1 to the Golgi apparatus.

The work was supported by grants from Chinese Natural Science Foundation (39925018, 30121001, 30270654), Chinese Academy of Science (KSCX2-2-01), Chinese 973 project (2002CB713700), and American Cancer Society (RPG-99-173-01) to Dr. Xuebiao Yao

Project 2: Identify and characterize Ezrin-WWOX Interaction and its regulation. The work was supported by grants from Chinese Natural Science Foundation (30070349 and 30270654), Chinese Academy of Science (KSCX2-2-01), Chinese 973 project (2002CB713700), Chinese Minister of Education (20020358051), and National Institutes of Health (DK-56292) to Dr. Xuebiao Yao; NSFC Grant 30500183 for Dr. Xia Ding and 30570926 for Dr. Xinwang Cao.

RESEARCH SKILLS

Molecular cloning; genotyping; virus pseudotyping; RT-PCR; Site-directed mutagenesis; Neuroanatomy; intraventricular microinjections; tissue processing for cryosectioning; immunocytochemistry; immunohistochemistry; histopathology; Expression of protein and fusion constructs; proteins purification; western blot; protein-protein interaction assays: immunoprecipitation; pull-down assay; yeast two hybrid screening; Psychosine extraction; lipid raft assay; enzymology; light/fluorescent/laser confocal; stereology and live-cell imaging microscopy. Cell cultures: embryonic neural stem cell culture; glia cell (astrocyte, oligodendrocyte) primary culture; O2A primary cell culture; cell line cultures (T293, HeLa, CG4, B104 et al).

PUBLICATIONS

1. **Zhu H**, Lopez-Rosas A, Santos M, Qiu X, van Breemen R, Givogri MI Bongarzone ER. Oligodendrogenesis in the developing neural tube of a mouse model for Krabbe disease. (in preparation)

VITA

2. **Zhu H**, Ornaghi F, Lopez-Rosas A, Qiu X, van Breemen R, Wrabetz L, Givogri MI, Bongarzone ER. Galactosyl-ceramidase deficiency influences postnatal oligodendrogenesis in a mouse model of Krabbe disease. (in preparation)
3. Cantuti Castelvetri L, Givogri MI, **Zhu H**, Lopez-Rosas A, Morfini G, Pigino G, Cao H, van Breemen R, Brady S, Bongarzone ER. Inhibition of fast axonal transport is a pathogenic mechanism contributing to neuropathology in Krabbe disease. (manuscript in submission)
4. **Zhu H**, Qiu X, Lopez-Rosas A, van Breemen R, Bongarzone ER. A Detection of the neurotoxin psychosine in samples of peripheral blood: application in diagnostics and follow up of Krabbe disease. 2012 *Arch Pathol Lab Med.* 136(7):709-710
5. Cantuti Castelvetri L, **Zhu H**, Givogri MI, Chidavaenzi R, Lopez-Rosas A, Bongarzone ER. 2012 Dephosphorylation of neurofilaments limits axonal caliber in Krabbe disease. *Neurobiol Dis.* 46(2): 325-335
6. Cantuti Castelvetri L, Givogri MI, **Zhu H**, Smith B, Lopez-Rosas A, Qiu X, van Breemen R, Bongarzone ER. Axonopathy is a compounding factor in the pathogenesis of Krabbe disease. 2011 *Acta Neuropathol.* 122(1):35-48.
7. Givogri MI, Bottai D, **Zhu HL**, Fasano S, Lamorte G, Brambilla R, Vescovi A, Wrabetz L, Bongarzone E. 2008 Multipotential neural precursors transplanted into the metachromatic leukodystrophy brain fail to generate oligodendrocytes but contribute to limit brain dysfunction. *Dev Neurosci* 30: 340-357
8. Jin C¹, Ge L¹, Ding X, Chen Y, **Zhu H**, Ward T, Wu F, Cao X, Wang Q, Yao X, PKA-mediated protein phosphorylation regulates ezrin-WWOX interaction. 2006 *Biochem. Biophys. Res. Commun.* 341: 784-791
9. Jin C, Zhang Y, **Zhu H**, Ahmed K, Fu C, Yao X, 2005. Human Yip1A specifies the localization of Yif1 to the Golgi apparatus, *Biochem. Biophys. Res. Commun.* 334: 16-22

PRESENTATIONS

Zhu HL, Qiu X, Lopez-Rosas A, Rizzo A, Santos M, van Breemen R, Givogri MI, Bongarzone ER. Accumulation of psychosine in the Twitcher embryo and its possible implications on prenatal oligodendrogenesis. 2012 American Society of Neurochemistry Annual Meeting, Baltimore, MD, USA

Zhu HL, Ornaghi F, Lopez-Rosas A, Wrabetz L, Givogri MI, Bongarzone ER. Poster: *Defining the biological role of psychosine in oligodendrogenesis.* 2010 Society for Neuroscience Annual Meeting, San Diego, CA, USA

Zhu HL, Ornaghi F, Lopez-Rosas A, Bongarzone ER, Wrabetz L, Givogri MI. Poster: *Galactosyl-ceramidase deficiency influences Oligodendrogenesis in a*

VITA

mouse model of Krabbe disease. 2009 Society for Neuroscience Annual Meeting. Chicago, IL, USA

Zhu HL, Ornaghi F, Lopez-Rosas A, Bongarzone ER, Wrabetz L, Givogri MI.
Poster: *Characterize oligodendrogenesis affected in a mouse model of Krabbe disease*. 2009 Great Lakes Glia 2009 Meeting. Traverse City, MI, USA

Zhu HL, Prnaghi F, Lopez-Rosas A, Bongarzone ER, Wrabetz L, Givogri MI.
Poster: *Effect of Galactosyl-ceramidase deficiency on oligodendrogenesis*. 2008 Annual Meeting of the Chicago Chapter of the Society for Neuroscience. Chicago, IL, USA

PROFESSIONAL AFFILIATIONS

Society for Neuroscience since 2009

American Society of Neurochemistry since 2008